# Mitigation of Blackout in Kigali Using a Microgrid with Advanced Energy Storage and Solar Photovoltaics

Marvin Karugarama

Thesis submitted to the faculty of the Virginia Polytechnic Institute and State University in partial fulfillment of the requirements for the degree of

Master of Science
In
Electrical Engineering

Kwa-Sur Tam, Chair
Lamine Mili
Virgilio Centeno

December 9th, 2015
Blacksburg, VA

Keywords: Blackout, Microgrid, Resiliency, Solar PV, Energy Storage, Rwanda

# Mitigation of Blackout in Kigali Using a Microgrid with Advanced Energy Storage and Solar Photovoltaics

Marvin K. Karugarama

## Abstract

A blackout is defined as the loss of electric power for a given period in a particular area. With increasing dependence on reliable electric power, the social and economic ramifications of blackouts are dire, negatively impacting the productivity, safety, and security of communities. To reduce blackout occurrence, power system planners incorporate redundancy and advanced controls to the grid to make it more adaptable to disturbances. However, adding redundant transmission lines is not only expensive, it is suboptimal in some contexts. While it is unattainable to have no blackout, it is possible and necessary to implement measures that minimize the likelihood and scale of these outages. This work proposes a solution that uses a microgrid with advanced energy storage and solar PV to mitigate blackouts in Kigali, the capital of Rwanda. A description and steady state analysis of major weaknesses in the Rwandan electric grid is presented. A microgrid application capable of islanding from the system is simulated in the steady state and shown to strengthen the system and decrease the likelihood of blackouts in Kigali. The composition of the microgrid is then designed, simulated, and optimized for technical and financial feasibility using the HOMER model. A microgrid that uses energy storage and solar PV is shown to not only be feasible, but also competitive with current costs of electricity in Rwanda. For comparison, different combinations that include diesel generation are also simulated.

**To my Parents: Tharcisse K. and Teddy B. K.**

# Acknowledgements

First and foremost, I would like to give thanks to the Almighty God who has walked with me throughout this journey and before. Without the constant guidance and protection of the Lord, this work would barely be a dream.

Special thanks to my advisor Dr. KS Tam. Dr. Tam has been more than an academic advisor. During the past year, he was also a moral and spiritual guide. Dr. Tam kindly pushed me to do the best work, patiently guiding me throughout each stage. This thesis would not have been possible without the tenacity with which he oversaw this work. I am especially thankful that Dr. Tam was understanding during the rough patches of this journey.

I would also like to thank Dr. Centeno and Dr. Mili who gladly accepted to serve on the committee that reviews this work. Your time and input is much appreciated.

Thanks to EWSA (now REG Ltd) for providing a model for the Rwandan electric grid, on which this study is based.

I am grateful for all the friends that I have made here at Virginia Tech, especially those who are part of the Power Group. Together, we have navigated the highs and lows of academic pursuits and this journey would not have been manageable without their companionship.

Enough thanks cannot be given to my loving parents who have supported me through all the years and challenged me to be the person I am today. Not once did their faith in me quiver.

Finally, I would like to give thanks for the blessing of my siblings who have always encouraged me and provided moral and spiritual support. I derive great inspiration from their love and companionship, even from thousands of miles away.

# Table of Contents

Abstract ..... ii
Dedication ..... iii
Acknowledgements ..... iv
List of Figures ..... vii
List of Tables ..... viii
Chapter 1 : Introduction ..... 1
1.1 Background and Motivation ..... 1
1.2 Rwandan Context ..... 5
1.3 Goal and Scope of Work ..... 7
1.4 Outline ..... 8
Chapter 2 : Literature Review ..... 9
Chapter 3 : Rwanda's Electric Grid ..... 20
3.1 Description of System Weakness ..... 21
3.2 Identification of Weak Areas ..... 25
3.2.1 Outage on Northern Line ..... 33
3.2.2 Outage on Southern Line ..... 37
3.2.3 Outage on Northern and Southern Lines ..... 39
3.3 Microgrid Solution ..... 40
3.3.1 Outage on Northern Line ..... 44
3.3.2 Outage on Southern Line ..... 47
3.3.3 Outage on Northern and Southern Lines ..... 49
3.3.4 Location and Size of Microgrid ..... 52
Chapter 4 : Design of Microgrid Solution ..... 53
4.1 HOMER Design Tool ..... 53
4.2 Solar PV ..... 55
4.2.1 Solar PV Data ..... 56
4.2.2 PV Technology ..... 68
4.2.3 PV Model ..... 70
4.3 Energy Storage Technologies ..... 73
4.3.1 Conventional Vs. New Technologies ..... 73
4.3.2 Storage Model ..... 77
4.4 Diesel Generator ..... 80
4.5 : Microgrid Design ..... 81

4.5.1 Problem Formulation ..... 81
4.5.2 Diesel Only System ..... 86
4.5.3 Diesel and PV System ..... 89
4.5.4 Diesel with PV and Storage ..... 92
4.5.5 PV and Storage ..... 94
4.5.6 Comparison of System Architectures ..... 96
4.5.7 Sensitivity of Storage and PV System ..... 98
4.5.8 Microgrid Land Requirements ..... 102
Chapter 5 : Conclusions and Future Work ..... 104
References ..... 108
Appendix A.1 Python Code To Create PSSE Case from Text Files ..... 114
Appendix B Microgrid Parameters, Economics, and Control ..... 119
Appendix B.1 Diesel Generators ..... 121
Appendix B.2 Solar PV ..... 123
Appendix B.3 Battery Storage ..... 124

# List of Figures

Figure 2.1 Cycle of Cascading Failures ..... 11
Figure 3.1 Rwanda's Electrical Network ..... 25
Figure 3.2 Map of Rwandan Showing the Main Transmission Network ..... 25
Figure 3.3 Rwanda's Electrical Grid Showing Points of Interest ..... 32
Figure 3.4 Change in Voltage Profile Following Northern Line Outage ..... 36
Figure 3.5 Line Loaded Over 50% Before and After Northern Outage ..... 36
Figure 3.6 Rwanda Electric Grid Showing Microgrid Locations ..... 43
Figure 3.7 Effect of Microgrid on Voltage Profile Following Northern Outage ..... 46
Figure 3.8 Effect of Microgrid on Line Loading Following Northern Outage (> 50% rating) ..... 46
Figure 3.9 Effect of Microgrid on Voltage Profile Following Southern Outage ..... 48
Figure 3.10 Effect of Microgrid on Loading Following Southern Outage (>50% rating) ..... 48
Figure 3.11 Per Unit Voltages in an Islanded Kigali ..... 51
Figure 3.12 Line Loading in Kigali Exceeding 50% of Rating During Islanding ..... 52
Figure 4.1 Relationship between simulation, optimization, and sensitivity analysis [45] ..... 55
Figure 4.2 SolarGIS GHI Validation Sites ..... 59
Figure 4.3 Monthly Average Solar Global Horizontal Irradiance (GHI) ..... 68
Figure 4.4 Trend in Cost of PV from 1995-2020 [53] ..... 70
Figure 4.5 Sample PV Cost Model in Homer ..... 73
Figure 4.6 Daily Load Profile of Airport Microgrid ..... 83
Figure 4.7 Load Profile vs Day and Night ..... 84
Figure 4.8 Problem Formulation and Optimization Consideration ..... 85
Figure 4.9 Diesel Only System ..... 87
Figure 4.10 Diesel and PV System ..... 90
Figure 4.11 Diesel, PV, and Storage System ..... 93
Figure 4.12 PV and Storage Setup ..... 95
Figure 4.13 Sensitivity of Net Present Cost to PV and Battery Prices ..... 100
Figure 4.14 Load vs Battery Energy Content April 12$^{th}$ – April 14$^{th}$ ..... 101
Figure 4.15 Load vs Battery Energy Content March 31$^{st}$ – April 3$^{rd}$ ..... 101
Figure 4.16 "Unoccupied" Land near Kigali International Airport ..... 103

# List of Tables

Table 3.1 Number of Components in System Model ..... 21
Table 3.2 Most Severe Contingencies for Line Overloads ..... 29
Table 3.3 Most Severe Contingencies for Voltage Limit Violations ..... 29
Table 3.4 Generator Summary ..... 31
Table 3.5 Line Overloads Due to Northern Line Outage ..... 34
Table 3.6 Voltage Violations Due to Northern Line Outage ..... 34
Table 3.7 Generation Capacity and Peak Load of Microgrid Locations ..... 44
Table 3.8 Violations Due to Northern Line with Kigali Center MG Disconnected ..... 45
Table 3.9 Violations Due to Northern Line Outage with Airport MG Disconnected ..... 45
Table 3.10 Violations Due to Southern Line Outage with Kigali Center MG Disconnected ..... 47
Table 3.11 Violations Due to Southern Line Outage with Airport MG Disconnected ..... 47
Table 4.1 Cost of Multi-Year Solar Data from SolarGIS ..... 60
Table 4.2 Cost of 12 Continuous Months Solar Data from SolarGIS ..... 60
Table 4.3 Data Validation Bias and Error for MACC-RAD [52] ..... 65
Table 4.4 IrSOLaV Pricing for Solar Radiation Data ..... 66
Table 4.5 Comparison of Solar Data Sources ..... 66
Table 4.6 Optimal System Design for Diesel Only System (Small Generators) ..... 87
Table 4.7 Top Ten Least Cost Diesel Only Systems at 1.4 $/L Diesel ..... 88
Table 4.8 Optimal System Design for Diesel Only Systems (Small and Large Generators) ..... 89
Table 4.9 PV Cost Curve ..... 90
Table 4.10 Optimal System Design for Diesel and PV System ..... 91
Table 4.11 Top Ten Least Cost Diesel & PV System Designs at 1.4 $/L Diesel ..... 92
Table 4.12 Optimal System Design for Diesel, PV, & Storage Systems ..... 93
Table 4.13 Categorized System Designs of Diesel with PV & Storage at 1.4 $/L Diesel ..... 93
Table 4.14 Optimal System Designs for PV and Storage System ..... 96
Table 4.15 Comparison of Optimal Designs (Diesel at 1.2 $/L) ..... 97
Table 4.16 Comparison of Optimal Designs (Diesel at 1.4 $/L) ..... 97
Table 4.17 Sensitivity of PV and Storage System to Solar Irradiation ..... 99
Table 4.18 Area Sizes and Proximity to Airport ..... 103

# Chapter 1 : Introduction

## 1.1 Background and Motivation

Blackouts, which refer to power outages affecting a specific area for a given period of time, are a well-known phenomenon in power systems operation across the world. Small outages happen frequently while large scale blackouts occur rarely, albeit with more devastating impacts. Power systems are thus operated to minimize the frequency, size, and duration of blackouts to maintain reliable power supply to consumers. The causes of blackouts are often linked to equipment failure, extreme weather, or operator misjudgments among other reasons. It is the duty of power system planners and operators to not only design a system that is immune to many of these causes, but one that is also capable of restoring operation during unexpected conditions. When a power system is able to maintain safe operation when a piece of equipment fails or out of service, it is defined as secure [1]. A system is described as resilient if it is able to withstand extreme rare disturbances.

To make the system more secure and resilient, power system planners design redundancy into the system, such that there is a backup in place should a component fail. However, even with redundancy and advanced controls in place, systems are still prone to outages, and in some cases very large ones due to unforeseen circumstances. One of the most recent large scale outages was the Blackout of 2003 that affected vast areas of Northeast and Midwest United States and Ontario, Canada, disconnecting about 61,800 megawatts (MW) and placed 50 million people in the dark [2]. The task force that analyzed this event cited shortage of reactive power support and failure to ensure operation within safe limits as some of the main causes [2]. Similar large scale outages have occurred before in the North East US in 1965, in New York City in 1977, twice on

the West Coast of the United States in 1996 to mention a few. These kinds of wide spread outages have raised more questions about security and resilience and the effectiveness of current practices, prompting further research into making the electric grid less vulnerable.

Following the blackout of 2003 that lasted more than 2 days in some parts, the joint US Canada task force presented various recommendations, many of which centered on policy and regulatory procedures. In fact, the task force recommended first that the congress enact stringent reliability legislation that is enforceable [2]. In deregulated energy markets such as North America's, there are many independent parties involved in the generation and delivery of power which makes policy and regulation of utmost importance to ensure that reliability is prioritized over economic concerns.

Despite many improvements to increase security and resilience, there exists some fundamental weaknesses in the current approach to power system design that are becoming more apparent. Over the last century, the majority of electric grids have relied on placing large generation plants in the most economical locations and using long transmission lines to deliver power to customers. As a result, most electric grids have consisted mainly of fewer large generation stations located far from consumers and an intricate transmission and distribution network. However, entities involved in the generation and distribution of electric power are coming to the realization that this de facto system design is both unsustainable in the long run, and will continue to be vulnerable to failures as more stress is applied to the electric grid. Researchers cite a few reasons for this belief. On one hand, they note that the current and predicted growth in electricity demand cannot be met with construction of traditional large generation and transmission as such projects have long lead times. On the other hand, generation

from fossil fuels is not only predicted to suffer from resource depletion, but it is also faced with opposition from environmentalists who warn of the negative impacts on the environment.

To address these challenges, utilities and larger consumers are adopting a different approach that uses more distributed generation scheme. Distributed generation, in contrast to centralized generation, generally refers to smaller generation units/plants usually connected to the distribution network and located close to consumers. Utilities are constructing distributed generation to meet growing demand and to reduce stress on the transmission network, while consumers are investing in onsite generation to maintain operation during outages. In the United States, the Department of Energy (US DOE) reported in 2007 that about 200 GW (gigawatts) in the form of 12 million distributed generation units had been installed [3]. In Rwanda, the World Bank surveyed over 240 manufacturing firms and reported that about 50 percent owned or shared a generator, but only obtained 3 percent of their electricity from it [4]. The DOE, however, acknowledges that increased distributed generation will change the general topology of electric grids and making it difficult to operate safely using current tools. One of the proposed solutions is the creation of microgrids which combine several distributed generation units with ancillary services into one controllable entity from the point of view of the system operator. Doing so enables millions of distributed generation units to be aggregated into fewer groups known as microgrids, which are easier to manage.

A microgrid can be formally defined as a system comprised of multiple distributed energy resources that are locally controlled, which can operate in parallel to the main grid or separate into an isolated system capable of independent operation [5]. Such a system typically consists of local generation that could be diesel, solar, or wind; an energy storage mechanism such as batteries or pumped hydro; local loads to be supplied; and a control mechanism to

manage the operation of the system. The use of microgrids as a means to increase generation capacity, security, and resilience has garnered attention and support from governments and utilities alike in recent years. Governments, in partnership with utilities, have invested heavily in the study and implementation of microgrids to help strengthen the electric grid especially in light of the most recent blackout in 2003.

The deployment of microgrids in developed regions such as the North America and Europe is increasing, in part due to the perceived versatility of microgrids, a quality which will be needed for the grid of the future. Researchers in electric power systems predict that microgrids necessarily will continue to displace a lot of centrally generated power, especially as cost parity with the grid is achieved. The US Federal Energy Regulatory Commission (FERC), in a 2007 report, contended that distributed generation could increase electric system reliability, provide reactive power support, reduce vulnerability, and make the grid more resilient [3].

Following these developments, and Rwanda's growing energy needs, this study was conducted to show an application of microgrids that can help prevent blackouts in Kigali, the capital of Rwanda. As will be described in the next section, Rwanda is particularly suitable for distributed generation and microgrids. In fact, developing countries with young electric grids such as Rwanda are at advantage with regard to implementing new designs to their grid, precisely because they are developing. While advanced countries are handicapped by the existence of old legacy systems that cannot easily be integrated or adapted to newer designs and technologies, developing grids can implement such designs as the foundation of their grids. Doing so would ensure that the system is largely developed accounting for security and resilience. Rwanda and other developing countries can leverage knowledge from advanced grids to build safer and more efficient grids. It is perhaps helpful at this point to introduce the context

of the study area and point out some of the peculiarities and conditions that distinguish Rwanda.

## 1.2 Rwandan Context

This study is conducted for the particular case of Rwanda, with a focus on the capital Kigali. Research on a specific case study has its benefits and shortcomings. On one hand, it explorers more than a general concept by considering the uniqueness and specifics of a special case which makes for an interesting perspective on a particular problem. On the other hand, by being very specific, it has the potential to limit the application of the work to other settings. Nonetheless, this case study has been adopted to address needs of the electric grid in Rwanda.

Rwanda is located in Central Africa, about one-degree south of the equator. It is notably a landlocked country with a population of about 11.5 million inhabitants on an area of 26,338 square kilometers, making it the most densely populated country in Africa. The capital Kigali is approximately located in the middle of the country (-1.94, 30.05), and has a population of about one million inhabitants making it the largest city in Rwanda. Unfortunately, Rwanda's predominant source of energy, hydropower, is largely generally far north or far south from the capital. To make matters worse, hydro power generation is greatly affected by seasonal changes that impact water levels in the lakes. Besides hydropower, almost all other energy is either imported from the region or generated with imported diesel fuel. As a result, Rwanda is heavily dependent on her neighbors and other foreign countries to fulfill its energy needs, while Kigali is susceptible to outages due to shortage of local generation.

Even more concerning is that despite the steep growth in energy demand, the most promising domestic energy resource, methane gas, presents as many challenges as it does benefits. It has been known for decades that Lake Kivu, which is located in on the western

border with the Democratic Republic of Congo, contains more methane gas than any other lake in the world [6]. However, the estimated 60 billion cubic meters of methane is mixed with 300 billion cubic meters of carbon dioxide (CO2) as reported in a recent article published in the MIT Technology Review [6]. While the methane resource could add up to an estimated 960 MW, several times the current capacity of Rwanda, the potential of a wide scale catastrophe from the CO2 gases trapped under the lake has delayed further extraction. This fear stems from a phenomenon known as a limnic eruption, which occurs when the gas pressure exceeds that of the water above it. Such an eruption would be lethal to life within a radius of tens of kilometers. Previous occurrences of such an event were recorded in the much smaller lake Nyos in Cameroon, where the erupted carbon dioxide killed an estimated 1700 people up to 25 kilometers from the shore. Yet more startling is the fact that Lake Kivu in Rwanda has a thousand times more gas than Lake Nyos, and is surrounded by over 2 million people along its shores. For the time being therefore, as efforts to navigate this challenge are underway, Rwanda is left with few options to increase its energy capacity without becoming more energy dependent.

Another point of interest is the topology of the electric grid in Rwanda. The transmission network in Rwanda is very radial in nature, which means that most areas are supplied by single lines. In fact, as will be shown, the transmission network lacks alternate paths for electricity and notably the service to Kigali. Most of the power is generated in the northern or southern parts of Rwanda and transmitted over a single line to Kigali. This renders Kigali, the heart of the nation's operations, at risk should any one of these lines unexpectedly go out of service. This

vulnerability is the focus of this study, and a proposition to strengthen and secure Kigali is presented.

## 1.3 Goal and Scope of Work

The goal of this study is to show how a microgrid that can be used to mitigate blackouts in Kigali, the capital of Rwanda. As was previously mentioned, no traditional energy resources exist in and around Kigali. The only generation in the Kigali area is from imported diesel generation, some of which is rental power. It is for this reason that an alternative energy resource is explored in the form of solar energy. Located just below the equator, Kigali receives abundant amounts of sunshine all year round. Since solar energy is available only during the day, it is necessary to couple it with energy storage to serve the load at night and create a self-sufficient system.

To this end, this study was conducted to first ascertain some of the major weakness in the Rwandan grid that could negatively impact Kigali. With these weakness, the proposed microgrid solution was simulated to show how it can mitigate these impacts on Kigali. The proposed microgrid solution was then modelled for financial and operational feasibility, and the least cost solutions detailed.

It is important to note that there are various levels at which such a study ought to be carried out. This particular study focused on steady state analysis of the Rwandan system. The "state" refers to a sufficient set of information to determine all the power flows in the system, in this case the voltage magnitudes and angles at the different buses. The implication of steady state analysis is that the study was restricted to analysis of voltages and angles between buses, and the loading of transmission lines, with the frequency of the system assumed to remain constant. As

such, the frequency components of loads and generators are not modelled, in part due to the lack of information, but also due to the exponential increase in scope that would result from completing a dynamic analysis as well. To perform this analysis a base case is obtained, which refers to a predetermined operating point of the system that is feasible and within safety limits. In this sense, we are interested to see whether the system can achieve a new safe operating point following a disturbance by looking at "snapshots' of the grid at a given time.

## 1.4 Outline

This work details the design and simulation of a microgrid in Kigali to reduce the likelihood of blackouts. The paper is organized as follows. Chapter 2 provides a brief literature review of blackouts in general and of the developments in microgrids and their application. Chapter 3 delves into the details of Rwanda's electric grid. In this chapter, the weaknesses of the Rwandan electric grid are explored, and the microgrid implementation to strengthen the system is tested. With the knowledge of the size and location of the microgrid, Chapter 4 details the design and economic analysis of the microgrid and compares the use of various combinations of technologies to find the least cost feasible options. Chapter 5 summarizes the conclusions from this work, and provides suggestions for future work. Finally, a list of references used, and appendices of simulation and design details is given.

# Chapter 2 : Literature Review

Blackouts in electrical grids are not uncommon, especially on small scales. These outages are sometimes considered tolerable if they occur infrequently. This is however changing as many applications are very sensitive to power loss such as medical, military, telecommunication, or even food processing applications. Even then, it is not the small outages that have most worries, but the large scale ones that have dire socio-economic ramifications. In North America, these types of outages are well-documented, the most recent being the blackout of 2003 that took out about 61,800 megawatts (MW) affecting fifty million people, some for days [2]. This blackout, and many before it as was alluded to in the introduction, have raised concern about the ability of the grid to curb occurrence of such outages.

While the report prepared by the US and Canada governments cited the need for stringent regulations [2], it is becoming increasingly clear that drastic measures are needed to address the technical vulnerabilities of the modern grids which are being stretched to their limits in most developed countries. The rapidly increasing electricity demand, and the need for high reliability even during disasters is further pushing governments and power system researchers to devise solutions to blackouts. Even though major power outages are not well-documented or studies in Rwanda, frequent power outages are well-known and reported in news media. In one of the few studies conducted in Rwanda, the World Bank Group surveyed over two hundred and forty firms involved in manufacturing to get a sense of power delivery in the country. These firms reported experiencing four outages per month that lasted an average of about three hours [4]. While this study was completed in 2012 and much has changed since, power outages are still an obstacle for businesses that heavily depend on reliable power. Most of these businesses procure their own on-

site generation to fill the gap left by utility outages. In fact, in the 2012 World Bank Group study, almost fifty percent of firms reported owning or sharing a backup generator [4].

Occurrence of large blackouts usually result from series of cascading failures. In some cases, a single failure in the system can trigger other failures across the network, pushing beyond operational limits. The protection layer in the power system is designed to prevent these kinds of events, while preventing permanent damage to expensive equipment. However, sometimes the indiscriminate actions of protection schemes remove components out of service that make the system even weaker. Figure 2.1 shows the cycle of cascading failures. Due to overloading, faults, or other circumstances, a particular component is taken out of service. In doing so, power is redistributed based on circuit laws. As a result, other components might get overloaded causing

them to be taken out of service by the protection relay signals. The cycle repeats, usually in quick sequence, that operators are not able to manage the situation [7].

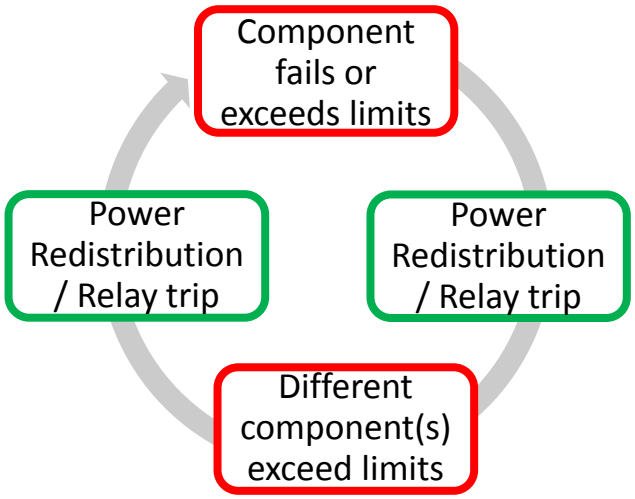


Figure 2.1 Cycle of Cascading Failures

In the 2003 Blackout in the US and Canada, the events started with the outage of a generating Unit in Ohio, whose load was carried by neighboring generators that were already operating near their limits and producing high reactive power. Further trips of generators and a transmission line pushed the system further towards its limits. Because of a failure in the alarm software, this was not noted in time by the operators to take action, and the next failures cascaded into an unrecoverable blackout that left 63 GW of load unserved [8]

In Sweden and Denmark, their 2003 blackout started with the failure of a nuclear power plant that was taken out of service. Interestingly, an outage on a line 300 kilometers away a few minutes later triggered a cascade of failures due to very high power transfer from the north to the

southern regions that overloaded the remaining lines, ultimately leading to voltage collapse with 4700 MW of load lost [8].

In Italy, a tree made contact with a line connecting to Switzerland which caused a fault and tripping of the line. Parallel lines were overloaded and subsequently tripped. This cascaded to more lines, leading to loss of synchronism of the Italian system to the rest of the Europe. Further outages led to 6400 MW of load losing supply [8].

In light of these and other blackouts, several mechanisms are being put in place to curb the occurrence of similar events. In decentralized energy markets in the West, a lot of geared toward is on policy, standards, and regulation. The committee that reported on the 2003 US-Canada blackout reported that regulations ought to be mandatory and clear as some players had circumvented standards and as such left the system vulnerable [2].

It was also noted that events far from each other might cause cascading failures such as the Sweden -Denmark outage. For this reason, studies and recommendations have been made to encourage wide area monitoring systems (WAMS) that report on issues across large areas. WAMS gives operators the ability to view counteracting events that might appear geographically and electrically too far to affect each other [2].

One of the most used methods of curbing blackouts is load shedding, in which power is disconnected to some load in a bid to save the rest of the system. However, even load shedding has been found to be ineffective unless it is preplanned and automatic since cascading events happen too fast for operator action [2, 7]. Automatic actions fall under the control and protection systems which often might cause more problems. With every component taken out of service, the system is weakened and more susceptible to blackouts [7]. To minimize unnecessary tripping of lines, new protection schemes are being developed and implemented including adaptive

protection. Adaptive protection is able to adjust settings in real time based on information from different sensors such that unnecessary trips can be prevented by altering relay settings on the fly [9].

Communication network failures were also blamed for the 2003 US-Canada blackout leading to a call for strengthening and adding redundancy to communication networks as well as putting in place procedures for utilities to act based on failures in neighboring networks [2]. Redundancy in the communication and control networks ensure that failures would not go unnoticed and actions would be taken in time to prevent cascading outages.

In Rwanda, the government has sought means to alleviate energy shortages and blackouts by importing more energy and constructing new generation plants. At the same time, there is a bid to privatize the energy industry that has traditionally been government managed. While generation has been at the forefront of energy developments in Rwanda, attention to the weaknesses in the transmission network are not receiving their due attention. These weaknesses affect the capital Kigali the most since it has the highest load and a poor network serving it. This fact makes it vulnerable to blackouts even though generation might increase. Kigali developed some local generation capacity through a 21 MW plant funded through the World Bank and commissioned in 2010 [10] ushering in the idea of distributed generation, which uses multiple dispersed generation units close to consumers. Distributed generation has taken off in recent years in developed countries with the United States reporting over twelve million units with a capacity over 200 gigawatts (GW).

The concepts of distributed generation and microgrids have necessarily received much attention in recent years as providers strive to meet the ever-growing demand for electricity. Even though distributed generation predates the current centralized structure of most electric

grids, the early days of electricity embraced the idea of locally producing and consuming electricity. This model was the case until the ability to send power over long distances was enabled through alternating current (AC) power [11]. Up until the last decade or so, large remote generation with long transmission lines to deliver it to the loads had been the modus operandi, hereafter referred to as centralized generation. However, even in the most developed nations, involved parties have noted vulnerability of the this electric grid model to natural disasters and unexpected phenomena as reported following the blackout in 2003 that affected a large portion of Eastern United States and parts of Canada [12].

Among the concerned parties were customers that require highly reliable power. These include critical operations such as defense, or medical facilities and telecommunication networks that cannot tolerate power outages. To shield themselves from potential outages, some of these sectors and other industrial players procured and still continue to procure onsite generation and to maintain supply of electricity when the grid is not available [13]. The amount of distributed generation installed was at some point considered too small relative to the main grid, but this view is changing. It was predicted by the Electric Power Research Institute (EPRI) in the early 2000s that about 25% of new generation would be distributed by 2010 [14]. Indeed, the US Department of Energy (US DOE) reported in 2007 that about 12 million DG units had been installed in the US to the tune of two hundred gigawatts (200 GW) [3]. This made distributed generation an issue worthy of careful consideration by utilities, researchers, and policymakers.

With the proliferation of distributed generation in the United States and Europe, there has been concern that the topology of the bulk electric grid could be altered in a way that the operators are not aware of, potentially leading to unforeseen complications. Out of this concern was born the concept of microgrids, which would act as means to mitigate technical barriers to

large scale use of distributed generation as well as allow for effective control and management of these distributed sources. To this end, the United States through the DOE has invested massively in research through organs such as the Consortium for Electric Reliability Technology Solutions (CERTS) that pioneered a microgrid concept and is operating a test bed [15] and the National Renewable Energy Laboratory (NREL), among others. This trend has also been happening in Europe particularly through the MICROGRIDS project comprised of a consortium of research power houses and institutions in many European countries that is tasked with studying the design and implementation of microgrids [16].

At this point, it is important to reiterate that this paper is a case study on Rwanda, whose grid is significantly different from that in the United States or Europe in its size, major concerns, and application. Microgrids being a relatively new field is receiving most attention in developed countries and as such, most of the research and concepts are based on experiences far away and different from Rwanda's. Nonetheless, important lessons can be drawn from these various work, and as will be described, applied to the specific case of Rwanda.

To further discussion, particularly in emerging fields, clear definition of key terms is imperative. The need for clear definitions for distributed generation and microgrids became key to set the stage for comparable research and policy. Attempts to clearly define these two terms however, have been generally unsuccessful owing to the fact that not only is this new research territory, it also means different things in different contexts and countries to the extent that scholars and policymakers alike have not come to a consensus. While there is a close relationship between distributed generation and microgrids, they refer to slightly different implementations of the same idea. In fact, distributed generation can be thought of as a subset of a microgrids, an idea that will hopefully become more apparent. According to Barker and de Mello, distributed

generation is that which is of limited size, about 10 MW or less [17]. Pepermans *et al.* define DG simply as small scale generation, although they agree with the contention that DG is an electric power generation source that is connected directly to the distribution network or on the customer side of the meter [11]. Their definitions and understanding is significantly influenced by Ackerman *et al.* whose definition is more comprehensive [14]. Ackerman *et al.* emphasize that distributed generation is located within the distribution network or connected on the customer side. Other criteria such as size, ownership, and type of generation are considered less definite as they vary from region to region. Sharma and Bartels studying the deregulated energy market in Australia are more precise defining DG as "generation primarily meant as an alternative to electricity generation using large, traditional power stations and the accompanying bulk transmission and distribution system, located in urban or isolated settings,… close to load centers" [18]. The Electric Power Research Institute (EPRI) defines DG as generation of a few kW up to 50 MW, while the International Conference on Large High Voltage Electric Systems (CIGRÉ) considers sizes less than 50-100 MW [14].

It is important to note that the difference in sizing requirements are in part due to the deregulated electricity markets in North America and parts of Europe in which various independent vendors compete in an open market to sell their energy and related services. This is not the case in Rwanda where energy, though recently corporatized, is still managed under one entity and regulated by the government through the Rwanda Utilities Regulatory Authority (RURA) [19]. In the Rwandan context therefore, the size of distributed generation is not of paramount importance, but rather the mode of operation and the location relative to the consumers, two points on which the aforementioned researchers concur. It is generally that

agreed that distributed generation is located close to the load, and more often connected to the distribution network of the grid or on the customer side [11, 14, 18].

Defining microgrids has not been straightforward either, albeit with more consistency. Under the European Commission project, MICROGRIDS, it has been asserted that microgrids comprise of low voltage distribution systems with distributed energy generation such as gen-sets, solar PV; storage capacity such as batteries; loads, all of which can be controlled as part of the main grid or disconnected to form an island [20]. In a separate study also under the MICROGRIDS project, Georgakis *et al.* define microgrids as portions of the grid comprising generation and loads capable of separation from the main grid intentionally [21]. The US DOE in conjunction with CERTS published a white paper on the microgrid concept defining it as an aggregation of loads and microsources operating as a single system [15]. The overarching idea defining a microgrid is that it is comprised of multiple distributed energy resources that are locally controlled, which to the main grid appears as a single entity (load or generator or both) [22, 23].

It is perhaps important to note that microgrids have been demonstrated for off-grid applications to serve remote areas as shown in [24] where an application for rural areas in the UK is proposed, or in Saudi Arabia [25]. This type of microgrid has many applications particularly for remote areas, but is not pertinent to this study.

One of the central questions posed is to what extent microgrids are useful, and at what economic or technical cost. First, the possible benefits will be addressed, and then the challenges will be presented. The benefits range from economical and technical/operational, to environmental. In the economic arena, deferral of building new transmission capacity has been noted as a major economic incentive by the Federal Energy Regulatory Commission (FERC) in

its study of distributed generation following new energy policies [3]. The report also notes that right-of-way for new transmission is increasingly difficult to obtain particularly in congested areas which also happen to need a lot of electricity. In fact, the cost of new transmission is increasing making new transmission even less attractive [26]. Being close to the load centers, microgrids require minimal if any new lines. In Rwanda, this is especially important due to the unfriendly terrain. Rwanda is heavily mountainous, which makes construction of transmission lines technically difficult and economically unfavorable.

Furthermore, by displacing new transmission and reducing the power flowing long distances, energy losses can be reduced. By using microgrids, energy that would be lost is transmission lines is saved, and at the same time, centralized generators do not have to generate more energy simply to compensate for losses [5, 27].

From the technical and operational point of view, FERC reports that microgrids can help improve security, reliability, and quality of power [3]. To improve reliability, the report contends, microgrids can be used to support local voltage levels by supplying reactive power, hence preventing possible outages that are caused by low voltages. Additionally, by reducing stress on the grid, the reliability of electric grid apparatus is improved. Reliability is often quantified in terms of loss of load probability (LOLP) which is the expected value of outage time in a given period, such as 1 day a year (and not a mathematical or statistical probability). This value can be reduced through the ability of microgeneration to black-start (start without external support from the grid) and supplying local load [5]. The LOLP for a certain area can also be further reduced by disconnecting from the grid during disturbances/ outages to prevent propagation of the disturbance and maintain local supply. In fact, this has been a major driver for

microgrid deployment particularly in the defense sector as reported in Department of Defense (DoD) report on microgrids and energy security [23].

The potential benefits of microgrids have been well studied and range from economic savings, to decongestion of the transmission network in addition to improved reliability. Much research has been devoted to the technical implementation of microgrids, particularly control. What has not received enough attention is a method to design microgrids that take a system wide view of security. As was noted, most microgrids are being studied and implemented as a means to supply energy to a small establishment should grid outages occur, and is few cases support the grid. There is a noticeable scarcity of studies that take a system wide view of microgrid applications. This work attempts to provide a concrete example of the use of microgrids in power system planning as a means to prevent wide spread outages in the first place by designing and locating the microgrids such that their operation directly acts to increase security of large portions of the grid.

# Chapter 3 : Rwanda's Electric Grid

Rwanda's electric grid is relatively small, but is experiencing rapid growth as noticed in the last 5 years. For example, the peak load in 2010 was 64 MW and reached 92 MW in 2012, a forty-four percent increase in 2 years [28]. In the same two years, the number of electricity customers also doubled. Current plans and predictions expect the generation capacity to increase from about 120 MW in 2013 to about 500 MW by 2020 [28, 29]. As was noted, majority of the energy in Rwanda is hydropower, although the country is making significant strides to diversify its energy sources. In 2004, one hundred percent of electrical energy was derived from hydropower, but the focus on other sources such as solar and fossil fuels has reduced the dominance of hydropower to about 60% [28, 30].

The electric grid data used in this study is from approximately 2012/2013 and has been slightly modified as will be described. One reason for the modification was to achieve an acceptable initial power flow steady state operation point, which is necessary for the analyses thereafter. The model was also modified to reflect some of the newly generation that was added to the system and was not yet included in the available model. The changes to the system are summarized below.

Generation was increased by adding to the model the recently commissioned Nyabarongo hydro-power plant with a capacity of 28 MW located southwest of Kigali. The corresponding transmission and other equipment was also included. A 3 MW generator was also added to the system about 53 miles (87 km) south of the capital, Kigali. This generator was added to help solve the initial power flow of the system as the raw data received had trouble converging to a feasible solution. As a result of these two increases in generation, the peak load was also

increased uniformly across the grid from about 97 MW to 125 MW to maintain the load to generation ratio.

The system was modelled using PSSE (Power System Simulator for Engineering), a widely used commercial tool for power transmission planning. A summary of the components in the model is given in Table 3.1. The current model consists of transmission and distribution voltage levels from 15 kV to 110 kV. Rwanda's highest voltage network is currently operated at 110 kV with plans in place to expand to 220 kV in the near future.

Table 3.1 Number of Components in System Model

| | |
|---|---|
| Buses | 407 |
| Machines | 48 |
| Loads | 227 |
| Branches | 365 |
| Two-winding transformers | 66 |

## 3.1 Description of System Weakness

The Rwandan electrical transmission system is a generally radial network including at the transmission level as can be seen in Figure 3.1 . In contrast to mesh networks that have multiple parallel transmission lines connecting buses, a radial grid has a tree structure in which an electric customer receives power from one source. Since a single line is used to connect from one bus to the next, the radial topology is cheaper and easier to implement, and as such is common in many developing countries and Rwanda is no exception. In developed countries such as the United

States, the transmission is partially meshed, while the distribution network is mostly radial [31]. While they require more transmission lines and are more expensive, meshed networks generally offer an increased level of reliability because it is possible to reroute power in case a particular line goes out of service.

The weakness is the Rwandan grid can therefore be attributed in part due to its generally radial nature in which the biggest loads, particularly in the capital, receive power from a single line. While there are several methods used to describe or classify the topology of a power system [32, 33], a quantitative distinction between radial and meshed networks is not readily achievable for larger systems. However, the relatively simple topology of the Rwandan grid illustrated in Figure 3.1 and 3.2 lends itself to a visual classification without the necessity for a

comprehensive topology analysis. We therefore proceed from the understanding that the grid is recognizably radial in the subsequent evaluations.

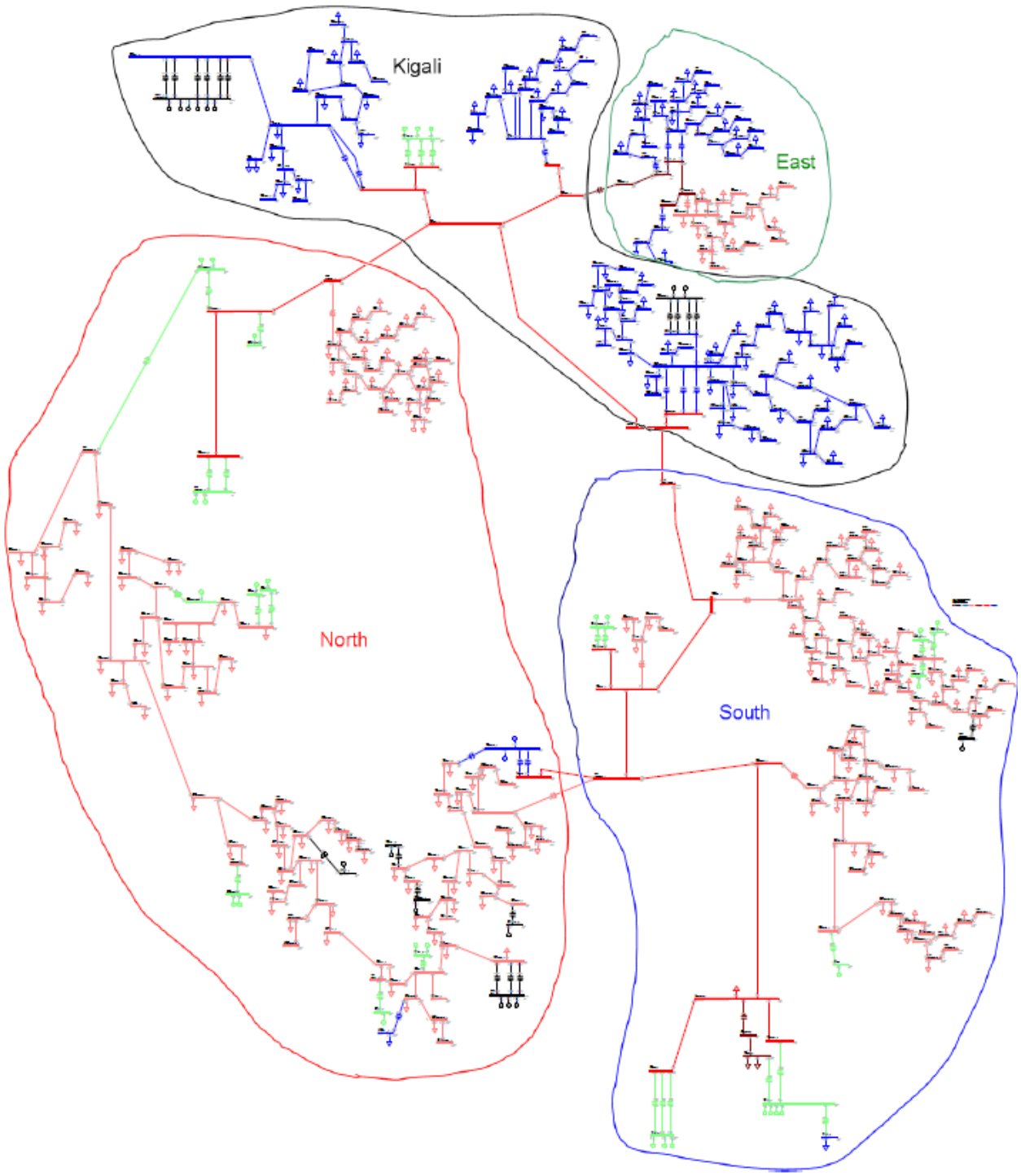
Bus - BASE VOLTAGE (kV)
Branch - IMPEDANCES
Equipment - MW/Mvar
kV: <=0.400 <=6.600 <=15.000 <=30.000 <=70.000 <=110.000
Kigali
East
North
South

Figure 3.1 Rwanda's Electrical Network

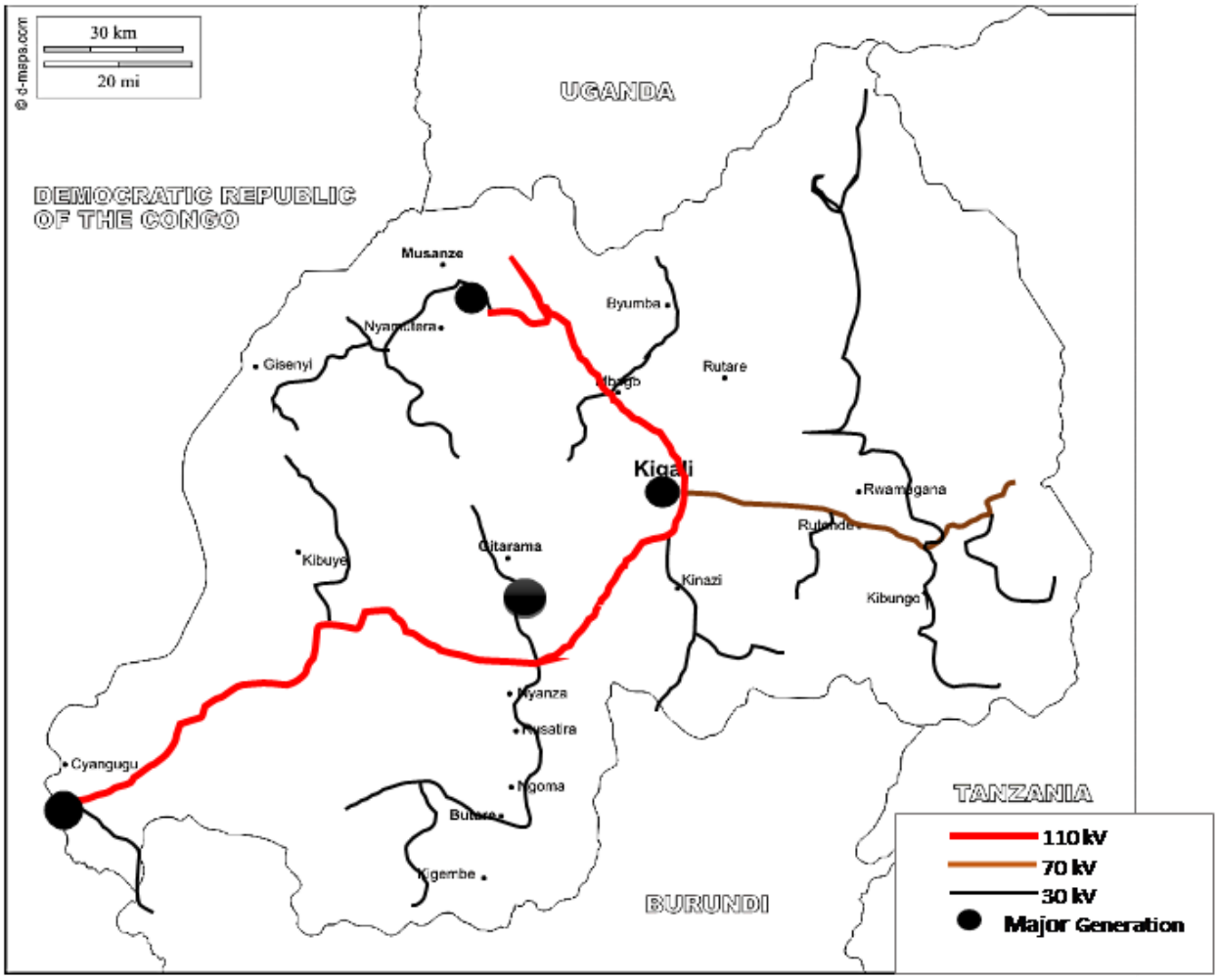


Figure 3.2 Map of Rwandan Showing the Main Transmission Network

## 3.2 Identification of Weak Areas

The identification of areas likely to cause major problems on the grid id done by means of contingency analysis. A contingency is defined as an event that may, but is not certain to occur [34]. In power systems operation, the network must remain within predefined margins

during normal conditions as well as following a contingency. This work focuses on the Rwandan's network ability to operate inside these margins during outages of components. This ability to withstand disturbances is commonly referred to as "security" [1]. While there are multiple stages at which security can be analyzed, namely, static, dynamic, and transient security analysis, this work focuses on the static security. Static security is defined as the ability of the system to return to a steady-state within the specified limits of safety following a contingency [35]. One of the main tools used in static security analysis is the load flow which is used to verify that electrical and thermal constraints are not being violated. The constraints of interest are the voltages at each bus and the power flowing through the lines, which are based on the stability limits of the system and the physical properties of the transmission lines respectively.

The process of contingency analysis involves studying the effect of the removal of a system component on the system, particularly the power flows and the bus voltages. This component can be a generator, transmission line, transformer, and so on. This work however focuses on outages on the transmission network. A can be seen from Figure 3.2, the capital Kigali, which is the main area of interest, is heavily dependent on transmission lines from far north and far south. What follows is a quantitative evaluation of which contingencies lead to the most issues with regard to voltage limit and line loading violations.

As was noted in Table 3.1, the network model used consists of 365 lines. An exhaustive analysis would require that an outage on each line and its effects are simulated using the load flow, and the subsequent analysis would be unnecessarily tedious. The load flow (power flow) is a widely used numerical analysis of the quantity and direction of electric power in a system. Usually, this method is used to compute the voltage magnitude and angle at each bus in the system as these values are sufficient to compute all the power flows in the network. One of the

most popular load flow methods which is also used here, is the Newton-Raphson method named after two of its foremost developers Isaac Newton and Joseph Raphson in the seventeenth century [36]. To reduce the computation and analysis requirement, a more strategic approach was used to screen contingencies and focus only on the most severe ones.

It is true that the most severe contingencies vary by time of day as the load changes [37]. To overcome the need to study the worst contingencies at different times of the day, the system was analyzed at peak load, that is, at the maximum consumption of electricity recorded by the system. In Rwanda, this occurs at around 8pm every day as can be seen in Figure 4.6. At peak load, the system experiences the most stress because the lines are heavily loaded, and the generators are running at high capacity such that the loss of any component could spell serious trouble for the system. Consequently, studying the system at peak load accounts for the worst case scenario, which is the practice in power system planning studies.

The method used to rank contingencies in PSSE is taken from [38]. This method computes a *system performance indices* (PI) which indicate the severity of an outage based on the number of out of limit voltages and line flows that result from it. Two different indices are

specified, one related to voltage violations and the other to line loading violations. The index to quantify problems related to voltage limit violations is given by equation 3-2.

$$PI_V = \sum_{i=1}^{L} w_i \, X_i P_i^2 \qquad 3\text{-}1$$

where

$w_i$ = the weight given to the particular line
$X_i$ = the reactance of branch i
$P_i$ = active power flow on branch i
$L$ = number of monitored branches (all branches in this case)

The performance index for line overloads is given by equation 3-2

$$PI_L = \sum_{i=1}^{L} w_i \left( \frac{P_i}{P_{MAX_i}} \right)^2 \qquad 3\text{-}2$$

where

$P_i$ = active power flow on branch i
$P_{MAX_i}$ = rating of branch i
$L$ = number of monitored branches (all branches in this case)
$w_i$ = weighting factor

Ranking is performed for all branch outages against their rated power carrying capacity, and considering voltage violations outside the range 0.9 per unit to 1.1 per unit which is the provided emergency voltage in the Rwandan system. The ten most severe line outages and the

performance indices for the two criteria are shown in descending order in Tables 3.2 and 3.3 . Buses marked with an asterisk (*) are those which are in Kigali or its electrical proximity.

Table 3.2 Most Severe Contingencies for Line Overloads

| From Bus | To Bus | PI |
|---|---|---|
| 13301* | 13601* | 109.076 |
| 6002* | 13601* | 104.677 |
| 701* | 20401* | 58.068 |
| 701* | 3101* | 50.699 |
| 13201* | 13301* | 47.532 |
| 2302* | 6002* | 45.025 |
| 5702* | 20401* | 43.729 |
| 2302* | 5702* | 43.695 |
| 904* | 1004* | 32.796 |
| 904* | 1103* | 32.571 |

Table 3.3 Most Severe Contingencies for Voltage Limit Violations

| From Bus | To Bus | PI |
|---|---|---|
| 13301* | 13601* | 0.319 |
| 6002* | 13601* | 0.305 |
| 701* | 20401* | 0.167 |
| 701* | 3101* | 0.130 |
| 13201* | 13301* | 0.120 |
| 5702* | 20401* | 0.117 |
| 2302* | 5702* | 0.117 |
| 2302* | 6002* | 0.112 |
| 1202 | 1401 | 0.067 |
| 3706 | 5404 | 0.067 |

The ends of the transmission lines associated with the most severe contingencies are labelled in Figure 3.3. It is evident that these contingencies are predominantly along the highest

* Buses located in Kigali or its electrical proximity

voltage transmission line (110kV) connecting the northern and southern parts of the country to the capital, Kigali. This knowledge implies that, as far as the transmission network is concerned, the main weakness is on the lines feeding Kigali from the north and south. With these key contingencies known, we proceed to analyze the impact of these contingencies on the network. Since the most critical lines are on the same path, two representative portions are tested by disconnecting the lines just before they reach Kigali.

Simulation of these contingencies begins with ascertaining a steady state solution of the system. This means that the system is operating normally, and all states are within the specified limits, that is, no voltage violations or line overloads exist. In addition, all generators are operating at, or close to their specified voltage. Table 3.4 shows a generator summary of the converged steady state solution indicating the power from each generator, as well as the generator voltage.

From this system steady state point, simulated at 8pm which corresponds to peak load, a contingency is applied. The contingencies are understood to be outages on either line feeding Kigali from the north or south. These lines, labelled “northern” and “southern” in Figure 3.3, are disconnected on their last leg before reaching Kigali hence cannot supply power to that capital. The “northern line” is disconnected between buses 13601 and 6002, while the “southern line” is

disconnected between buses 5702 and 2302. The possibility that these lines could both be taken out of service at the same time is also considered, giving three possible contingency scenarios.

Table 3.4 Generator Summary

| Bus # | Bus Name | Base kV | # Mach | MW | MVar | Qmax | Qmin | Sched V(p.u.) | Actual V(p.u.) |
|---|---|---|---|---|---|---|---|---|---|
| 102 | Extra | 0.7 | 1 | 3.1 | 1.1 | 5.0 | -1.5 | 1.000 | 1.000 |
| 201 | Ruzizi I | 6.6 | 4 | 14.3 | 10.7 | 21.7 | -12.4 | 1.020 | 1.020 |
| 202 | Kibuye 11 | 11 | 2 | 2.0 | -1.2 | 1.5 | -1.2 | 1.020 | 1.025 |
| 902 | Ruzizi II | 6.6 | 3 | 17.4 | -0.6 | 27.0 | -19.6 | 1.020 | 1.020 |
| 1001 | Nyabarongo | 6.6 | 2 | 23.8 | 3.4 | 17.4 | -11.2 | 1.020 | 1.020 |
| 1601 | Murunda | 0.4 | 1 | 0.1 | 0.0 | 0.1 | 0.0 | 1.010 | 1.039 |
| 2001 | Gihira | 6.6 | 2 | 1.5 | -0.7 | 1.3 | -0.8 | 1.020 | 1.020 |
| 2901 | Kp 1 | 0.4 | 3 | 2.6 | -1.7 | 2.2 | -1.7 | 1.020 | 1.025 |
| 3001 | Cyimbiri | 0.4 | 1 | 0.3 | -0.1 | 0.2 | -0.1 | 1.030 | 1.049 |
| 3503 | Aggreko I | 0.4 | 2 | 7.0 | 2.9 | 4.9 | -3.3 | 1.020 | 1.020 |
| 3802 | Nkora | 0.4 | 1 | 0.7 | -0.2 | 0.5 | -0.2 | 1.010 | 1.049 |
| 3906 | Ntaruka | 6.6 | 2 | 5.0 | 0.1 | 4.6 | -1.4 | 1.020 | 1.020 |
| 3907 | Ntaruka_sp | 6.6 | 1 | 2.7 | 1.1 | 2.0 | 0.2 | 1.020 | 1.020 |
| 4002 | Keya | 3.3 | 1 | 2.0 | -0.7 | 1.4 | -0.7 | 1.010 | 1.020 |
| 4506 | Rugezi | 0.7 | 1 | 0.9 | -0.8 | 2.6 | -1.6 | 1.020 | 1.020 |
| 4706 | Rugezi | 0.7 | 1 | 0.9 | -0.8 | 2.6 | -1.6 | 1.020 | 1.020 |
| 4805 | Gatuna | 30 | 1 | 1.2 | 0.0 | 0.2 | 0.0 | 1.000 | 1.040 |
| 5802 | Jabana II | 6.6 | 3 | 15.6 | 3.2 | 15.3 | -9.9 | 1.000 | 1.000 |
| 10601 | Jabana I | 0.4 | 6 | 5.8 | -2.6 | 4.9 | -2.6 | 1.000 | 1.012 |
| 11501 | Mukungwa_I | 6.6 | 2 | 1.2 | -1.2 | 1.5 | -1.2 | 1.000 | 1.002 |
| 12501 | Giciye | 0.4 | 1 | 0.6 | -0.3 | 0.6 | -0.3 | 1.000 | 1.005 |
| 13201 | Mukungwa_H | 6.6 | 2 | 7.5 | 4.9 | 7.9 | -4.7 | 1.020 | 1.020 |
| 13501 | Mukungwa_II | 6.6 | 1 | 5.8 | 1.6 | 4.9 | -3.4 | 1.020 | 1.020 |
| 20501 | Rukarara | 0.7 | 1 | 2.9 | -1.0 | 1.9 | -1.5 | 1.020 | 1.020 |
| 20701 | Rukarara | 0.7 | 1 | 2.5 | -1.0 | 2.0 | -1.3 | 1.020 | 1.020 |
| 20801 | Rukarara | 0.7 | 1 | 2.3 | -1.0 | 2.0 | -1.3 | 1.020 | 1.020 |
| 22001 | Mazimeru | 0.4 | 1 | 0.3 | 0.9 | 5.0 | -3.0 | 1.000 | 1.000 |
| | | | Total | 130.1 | 16.0 | 141.2 | -86.2 | | |

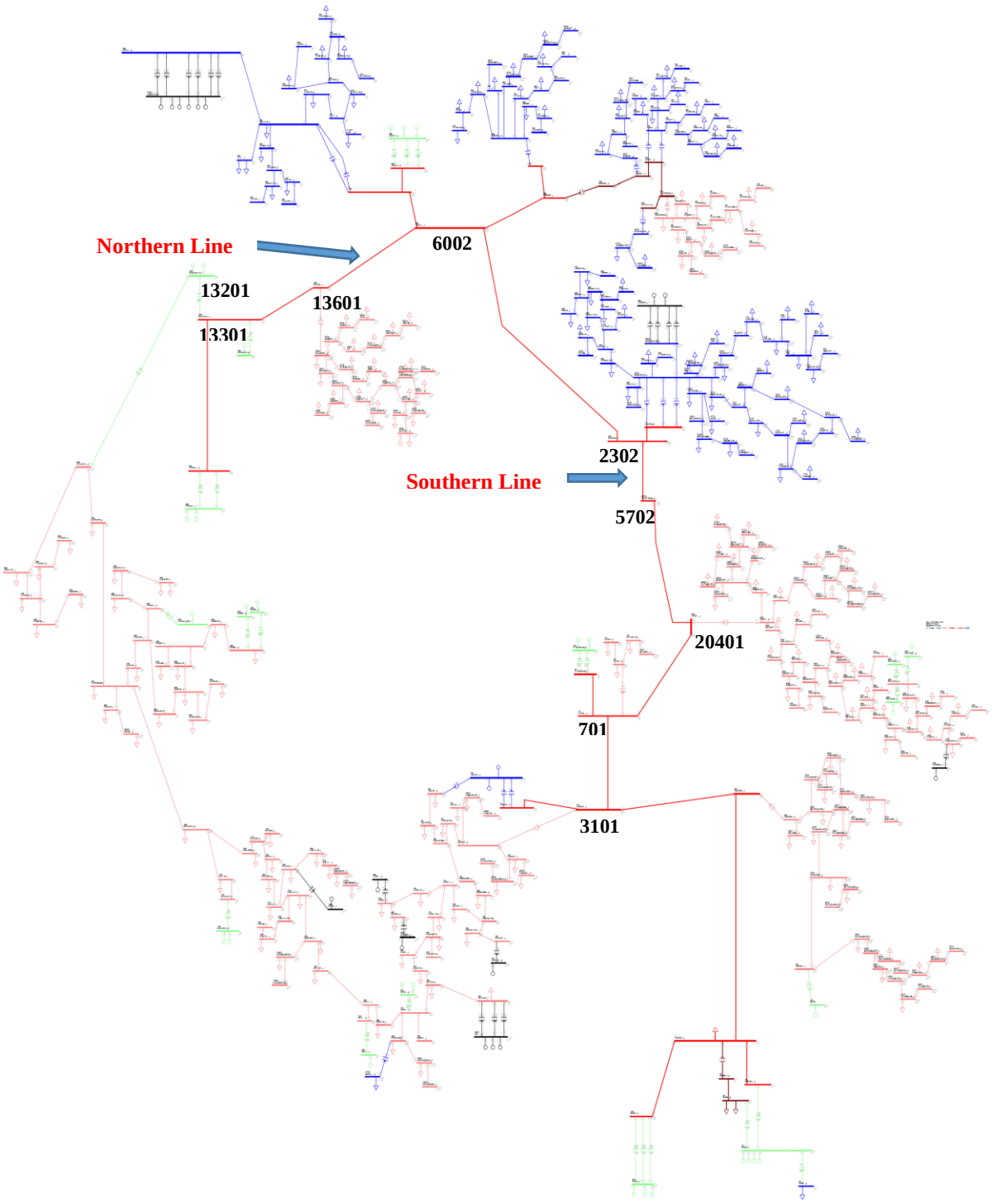


Figure 3.3 Rwanda's Electrical Grid Showing Points of Interest

### 3.2.1 Outage on Northern Line

The first contingency considered is an outage on the “northern line”. As mentioned before, we are interested in knowing whether post-contingency, lines are carrying an acceptable amount of power and that the voltage at each bus is within the pre-defined stability limits. A stricter voltage threshold is used between 0.93 per-unit and 1.08 per-unit, while the power flow threshold is predefined for each line by the power system designers. The results of simulating

this contingency are shown in Table 3.5 which shows the lines that exceed their loading, and Table 3.6 which shows the buses whose voltages are outside the limits.

Table 3.5 Line Overloads Due to Northern Line Outage

| From # | Name | To # | Name | Current Rating (MVA) | Current Flow (MVA) | % of Rating |
|---|---|---|---|---|---|---|
| 202 | Kibuye | 602 | Kibuye | 5 | 10.9 | 6.8 |
| 801 | Nyabarongo | 1001 | Nyabarongo | 20 | 25 | 124.9 |
| 801 | Nyabarongo | 1001 | Nyabarongo | 20 | 25 | 124.9 |
| 803 | Kibuye Tee | 903 | Rubengera | 11 | 16.2 | 147.6 |
| 903 | Rubengera | 1003 | Rubengera | 11 | 16.3 | 148.0 |
| 1003 | Rubengera | 1102 | Murunda Te | 11 | 16.3 | 148.3 |
| 1102 | Murunda Te | 1202 | Kayove | 11 | 16.4 | 149.2 |
| 1202 | Kayove | 1401 | Nkora T | 11 | 16.5 | 149.8 |
| 1401 | Nkora T | 1701 | Nkora T Mp | 11 | 16.7 | 151.6 |
| 1701 | Nkora T MP | 2601 | Gashashi T | 11 | 16.7 | 152.2 |
| 1901 | Gihira | 2201 | KP1 Pilot | 11 | 16.8 | 152.5 |
| 2201 | KP1 Pilot | 2401 | Kigufi MP | 11 | 17.3 | 156.8 |
| 2401 | Kigufi MP | 2501 | Kigufi | 11 | 16.8 | 153.0 |
| 2501 | Kigufi | 2601 | Gashashi T | 11 | 16.8 | 152.8 |
| 3606 | Mukungwa | 3706 | Camp Bmp2 | 11 | 18 | 163.8 |
| 3606 | Mukungwa | 13201 | Mukungwa H | 10 | 19.5 | 194.8 |
| 3702 | Nkora | 3802 | Nkora | 0.8 | 0.9 | 107.8 |
| 3706 | Camp Bmp2 | 5404 | Camp Belge | 11 | 17.8 | 161.6 |

Table 3.6 Voltage Violations Due to Northern Line Outage

| Bus # | Name | Base kV | Initial Voltage | Contingency Voltage |
|---|---|---|---|---|
| **Low Voltage Violations** | | | | |
| 903 | Rubengera | 30 | 1.02916 | 0.9068 |
| 1003 | Rubengera | 30 | 1.03298 | 0.8511 |
| 1102 | Murunda Te | 30 | 1.03787 | 0.8197 |
| 1202 | Kayove | 30 | 1.03894 | 0.8156 |
| 1302 | Murunda Mp | 30 | 1.03819 | 0.8203 |
| 1401 | Nkora T | 30 | 1.04554 | 0.8218 |
| 1501 | Murunda | 30 | 1.03854 | 0.8211 |
| 1601 | Murunda | 0.4 | 1.03854 | 0.8211 |
| 1701 | Nkora T Mp | 30 | 1.04564 | 0.8341 |
| 1801 | Nkora Mp | 30 | 1.04722 | 0.8257 |
| 2001 | Gihira | 6.6 | 1.02 | 0.9088 |
| 2201 | KP1 Pilot | 30 | 1.04811 | 0.9114 |
| 2301 | KP1 Pilot | 30 | 1.0508 | 0.9187 |
| 2401 | Kigufi Mp | 30 | 1.04726 | 0.9017 |
| 2501 | Kigufi | 30 | 1.04704 | 0.8931 |
| 2601 | Gashashi T | 30 | 1.04616 | 0.8580 |
| 2701 | Gashashi H | 30 | 1.04617 | 0.8581 |
| 2901 | KP 1 | 0.4 | 1.02485 | 0.8969 |
| 3001 | Cyimbiri | 0.4 | 1.04944 | 0.8309 |
| 3702 | Nkora | 30 | 1.04907 | 0.8299 |
| 3802 | Nkora | 0.4 | 1.04903 | 0.8302 |
| 3902 | Cyimbiri | 30 | 1.04945 | 0.8307 |
| 4002 | Keya | 3.3 | 1.02002 | 0.9127 |
| 4402 | Poids Lour | 30 | 1.04339 | 0.9276 |
| 4702 | Goma | 15 | 1.02286 | 0.9093 |
| 4802 | Karukogo M | 30 | 1.04313 | 0.9273 |
| 4902 | Karukogo | 30 | 1.04314 | 0.9273 |
| 12101 | Mudende T | 30 | 1.03707 | 0.9296 |
| 12401 | Keya MP | 30 | 1.04039 | 0.9287 |
| 12501 | Giciye | 0.4 | 1.00538 | 0.9246 |
| 12801 | Mudende Mp | 30 | 1.03649 | 0.9290 |
| 12901 | Cyanzarwe | 30 | 1.03652 | 0.9290 |
| 3403 | Amahoro | 15 | 0.94607 | 0.9286 |
| 5602 | Mushikiri | 15 | 0.9405 | 0.9229 |
| 1903 | Karenge | 15 | 0.94336 | 0.9265 |
| **High Voltage Violations** | | | | |
| Bus # | Bus Name | Base kV | Initial Voltage | Contingency Voltage |
| 4605 | Mulindi | 30 | 1.03134 | 1.0837 |
| 4805 | Gatuna | 30 | 1.03962 | 1.0916 |

The resultant voltage profile and line loading following an outage on the northern line are visualized in figures 3.4 and 3.5 .

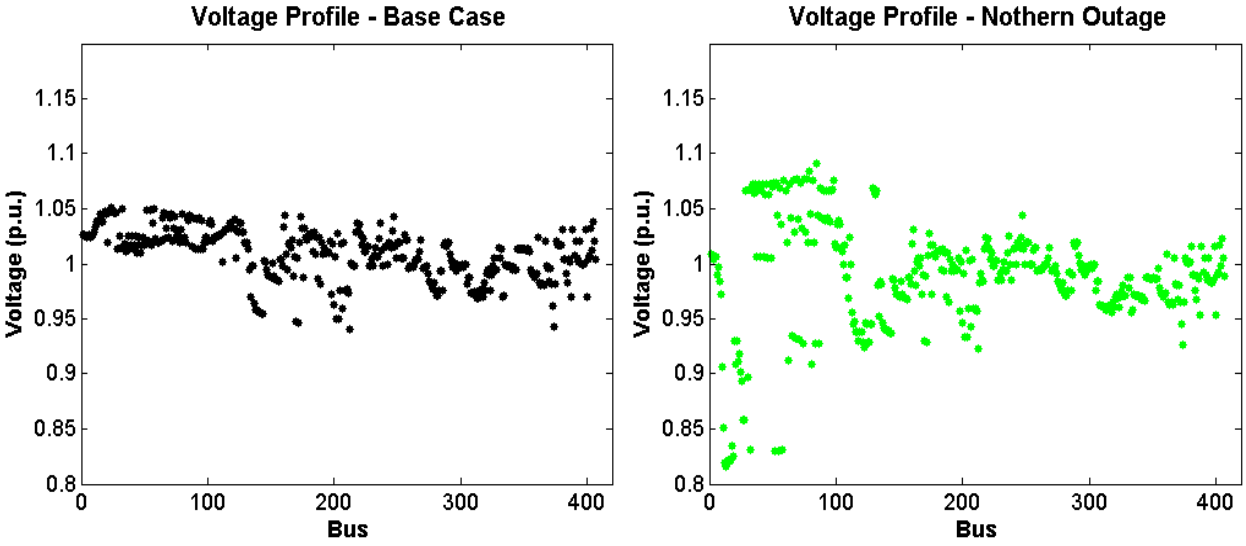


Figure 3.4 Change in Voltage Profile Following Northern Line Outage

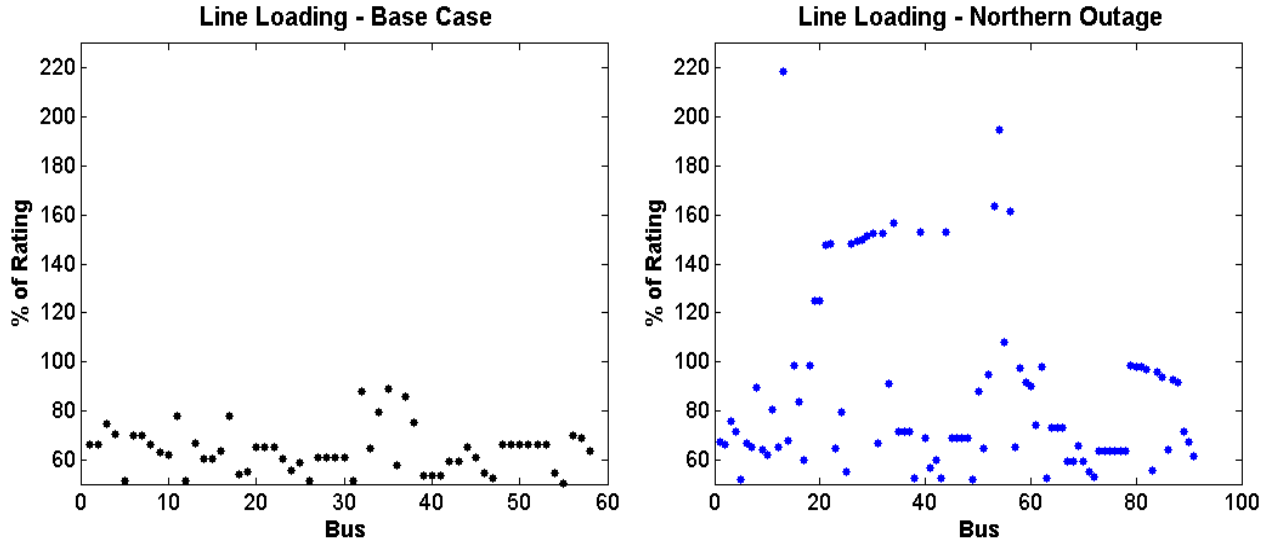


Figure 3.5 Line Loaded Over 50% Before and After Northern Outage

Even though the resultant state of the system is successfully computed, several violations are present as shown in the tables 3.5 and 3.6 above. With this many violations, it is unlikely

that the system would be able to operate. Voltages outside their limits could lead to widespread instability, failures, and damage of equipment while overloads could permanently damage equipment also leading to instability [39]. Normally, procedures are in place to prevent the system from reaching such an operating point and may require that parts of the system get shut down in a coordinated way to save the system from damage, at the cost of cutting off supply to some customers. This type of forced blackout is all too common in Rwanda and has been widely reported about in news media as recently as this year, even though scientific publications on this issue are not available. Some example news stories can be read here [40]

### 3.2.2 Outage on Southern Line

The other contingency of interest is an outage on the line serving the capital from the south labelled as “southern line” in Figure 3.3. Unlike in the previous contingency where a post contingency solutions was obtained, this outage causes the power flow not to converge, that is, a solution cannot be achieved to establish the state of the system. While this is often an indication that is something might be amiss, it does not necessarily imply that this is a worse condition than the previous contingency, even though this might be the case. What is more certain, however, is that corrective actions need to be taken such that a solution can be achieved, otherwise there cannot be a quantitative understanding of the condition of the system.

To be more confident that indeed this contingency leads to divergence of the power flow, several steps were taken to try and arrive at a solution. Up to this point, the preferred algorithm has been the Newton-Raphson (NR) method. However, this method, though powerful and efficient, is known to diverge if the system is ill-conditioned, that is, its Jacobian is sensitive to small changes [41]. The NR is also intolerant of poor initial estimates. The different methods

used to solve the system for this contingency include the Gauss-Seidel method and decoupled load flow [42], with no success in convergence. On the other hand, application of the DC load flow under certain assumptions does produce an estimated result due to its non-iterative approach, but showed large power flow mismatches, indicating that the solution is unreliable. In fact, this particular case does not lend itself to the assumptions of the DC power flow, specifically, the assumption of a near-flat voltage profile (close to 1.0 per unit), or high reactance/resistance (X/R) ratio. At base case for example, the system's voltage profile which certainly is not flat, and neither is X/R ratio high for the lines in the system, negating the results from the DC load flow. It is only in rare cases that a system that has a solution cannot be solved if different methods are employed.

The divergence of the load flow is often difficult to investigate, but we do know that the system was solved prior to the contingency, implying that generation was adequate to meet the load. There are a few reasons that might explain this inability to converge or to diverge. Mathematically, it is possible that the solution might go outside the solution space and not return. From the power system viewpoint, there could be insufficient power to serve the load hence Kirchhoff's Current and Voltage Laws that govern the flow of energy in an electric system cannot possibly satisfied. It is a safe assumption that this is not the case since no generation was taken or load added to the system, but rather transfer capability in the form of a transmission line was removed from the system. Alternatively, the divergence might result from the system being at an infeasible operating point caused by insufficient reactive power, but this cannot be

ascertained. There are some indices that can be used to quantify how far off the case is from a solution such as shown in [43], but this is beyond the scope of this work.

The main tool used for power flow studies is PSS/E (Power System Simulator for Engineering) which has the ability to use a non-divergent methodology for cases that are difficult to solve. In this method, when updating the voltage magnitudes and angles after each iteration, the magnitude and angle vectors are monitored for divergence, and the factor by which they are being updated is halved if divergence is detected. The process is repeated until either no indication of divergence is measured or the factor is approaching zero without steering the voltage vector from divergence. Using this method did not solve the power flow for the southern line outage either. It is therefore assumed that this contingency, though not quantifiable, is likely to negatively impact the operation of the system, possibly leading to instability.

### 3.2.3 Outage on Northern and Southern Lines

A simultaneous outage on the northern and southern lines effectively divides the system into two separate entities. Kigali and the east of the country are separated from the north and south networks which are only loosely connected. This separation again points to the radial nature of the transmission grid and its inherent weakness such that two outages completely separate the system into two. During this condition, Kigali and the east would have an energy deficit of 17 megawatts at peak load and certainly power outages would necessarily occur. On the other half of the system there is enough generation to supply the load. With the compete

bisection of the system, this outage however introduces a whole new set of problems, the extent of which are beyond the scope of this work.

## 3.3 Microgrid Solution

In this section, a solution to the severe repercussions of the main outage events is proposed. The solution proposed here is the creation of a microgrid(s) in Kigali that can disconnect from the main grid and operate autonomously (island mode) during contingencies. The expectation is this microgrid(s) can be appropriately located and sized such that it counteracts the failures that arise from outages on the transmission system, this improving system security. Security is understood as the ability of the power system to maintain operation within specified limits following a contingency.

In this study, security is considered at two levels. The primary area to secure is the capital Kigali and the secondary objective is to secure the rest of the system where possible using the same microgrid. Microgrids are commonly seen as a way to maintain uninterrupted power to a specific area or operation such as a military base, an academic institution, factory, and so on. In a way, the microgrid solution is inward looking, seeking to shield itself from outages or instability issues arising at the main grid. In this application, the goal is two ways – the microgrid seeks the ability to island from the grid and support itself during contingencies while also supporting the main grid.

Microgrid locations were chosen in Kigali to test their impact on steady-state security of the system. Locations were chosen on their physical and geographical proximity to Kigali. They were also chosen to be on the distribution side such that they have a single point of contact with the transmission network such that they can be isolated by a single action of a high speed switch.

This single point is commonly referred to as the point of common coupling (PCC). Three microgrid locations were initially considered, one in the city center, here after referred to as the Kigali Center MG; one in the airport area (Airport MG), and one just outside the city center (MG

3) as shown in Figure 3.6. Each microgrid was assigned a single PCC as shown. The composition of each microgrid, load and generation, is summarized in Table 3.7.

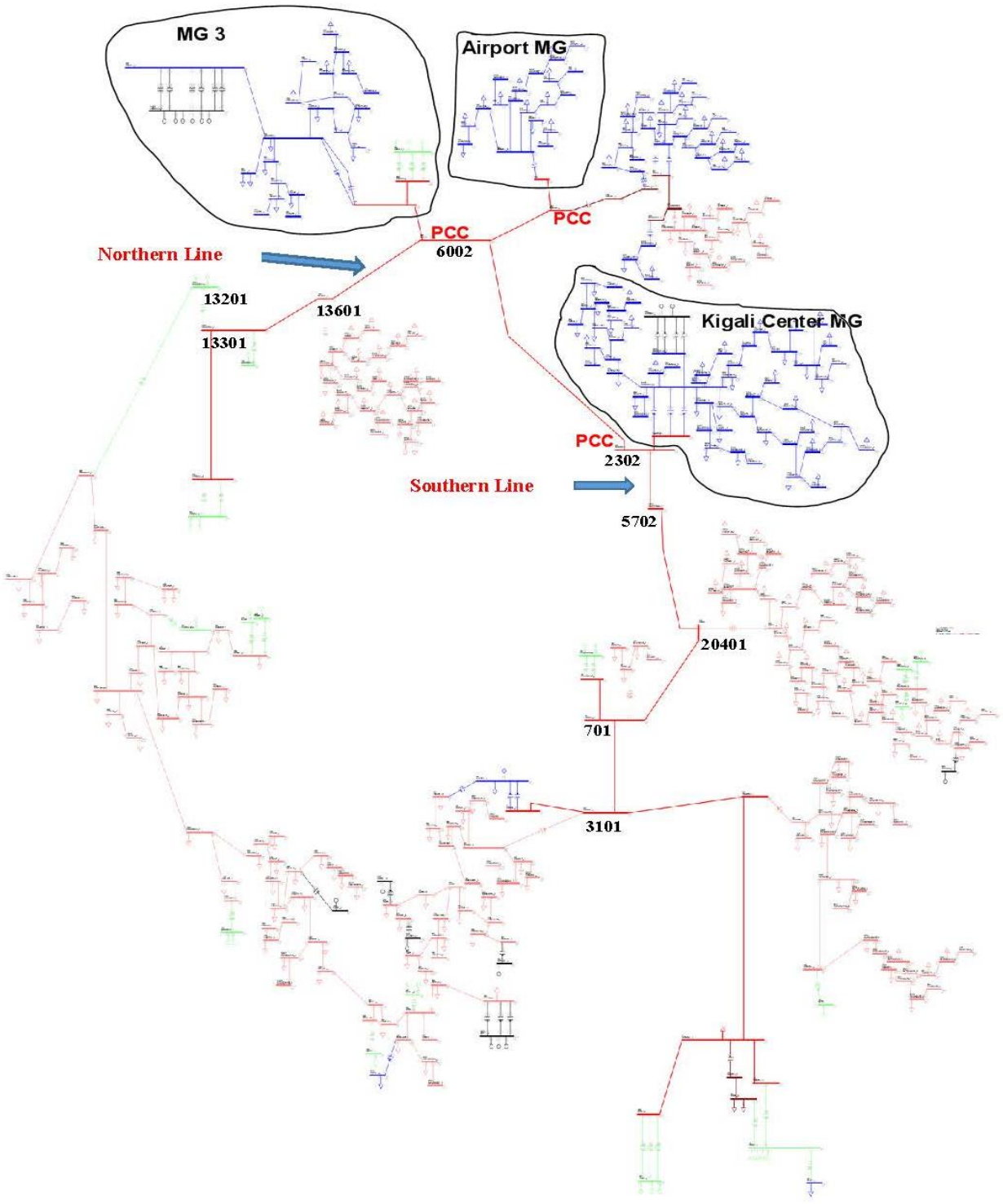


Figure 3.6 Rwanda Electric Grid Showing Microgrid Locations

Table 3.7 Generation Capacity and Peak Load of Microgrid Locations

| Microgrid | Peak Load | | Generation Capacity | |
|---|---|---|---|---|
| | MW | MVAR | MW | MVAR |
| Kigali Center | 24.2 | 9.7 | 10.0 | 4.9 |
| Airport | 12.3 | 2.7 | 0.0 | 0.0 |
| MG 3 | 10.3 | 4.0 | 28.2 | 20.2 |

The microgrid labelled “MG 3” makes a good candidate for a microgrid that could island because it has more than enough capacity to support its own load. This is the common way in which microgrids are viewed. For this purpose, however, disconnecting this microgrid is detrimental to the Kigali and whole system in general because it has excess capacity and removing it would result in a net generation loss. For this reason, this microgrid was not considered a good choice, while the other two, which when islanded result in a net load reduction for the system, were simulated. In a sense, disconnecting either one of these two microgrids, Kigali Center and Airport, a form of load shedding is being implemented, except these microgrids are not really losing power. These two microgrids were then tested with the most severe contingencies previously discussed to quantify any positive impact they might have on the security of the system. The preceding simulations are performed with the assumption that a particular microgrid is in place, and can be disconnected as needed. The microgrid composition is detailed in chapter 4.

### 3.3.1 Outage on Northern Line

The worst contingencies were again simulated starting with an outage on the line between buses 6002 and 13601, this time with either microgrid disconnected. The results were checked for voltage and flow violations. First the northern line contingency was imposed and the Kigali

Center MG disconnected. This resulted in significant reduction in number and severity of flow violations, and voltage violations were entirely eliminated. Table 3.8 shows the persistent flow violations when the northern line is disconnected and Kigali Center MG is removed. Similarly, removing the Airport MG for the Northern line outage eliminated voltage violations and mitigated flow violations. Only a few violations were present with much less severity as shown in Table 3.9.

Table 3.8 Violations Due to Northern Line with Kigali Center MG Disconnected

| From # | Name | To # | Name | Current Rating (MVA) | Current Flow (MVA) | % of Rating |
|---|---|---|---|---|---|---|
| 202 | Kibuye | 602 | Kibuye | 5 | 6.8 | 136.3 |
| 1901 | Gihira | 2201 | KP1 Pilot | 11 | 12.2 | 107 |
| 2201 | KP1Pilot | 2401 | Kigufi MP | 11 | 11.6 | 101.8 |
| 3606 | Mukungwa | 3706 | Camp Bmp2 | 11 | 14.7 | 125.4 |
| 3606 | Mukungwa | 13201 | Mukungwa | 10 | 14.8 | 148.2 |
| 3706 | Camp Bmp2 | 5404 | Camp Belge | 11 | 14.2 | 123.4 |

Table 3.9 Violations Due to Northern Line Outage with Airport MG Disconnected

| From # | Name | To # | Name | Current Rating (MVA) | Current Flow (MVA) | % of Rating |
|---|---|---|---|---|---|---|
| 202 | Kibuye | 602 | Kibuye | 5 | 7 | 139.6 |
| 2201 | KP1 Pilot | 2401 | Kigufi MP | 11 | 11.7 | 102.7 |
| 3702 | Nkora | 3802 | Nkora | 0.8 | 0.9 | 107.9 |

A visual comparison of the voltage profile following an outage on the northern line with or without the microgrid is shown in Figure 3.7. The line loading is shown in Figure 3.8.

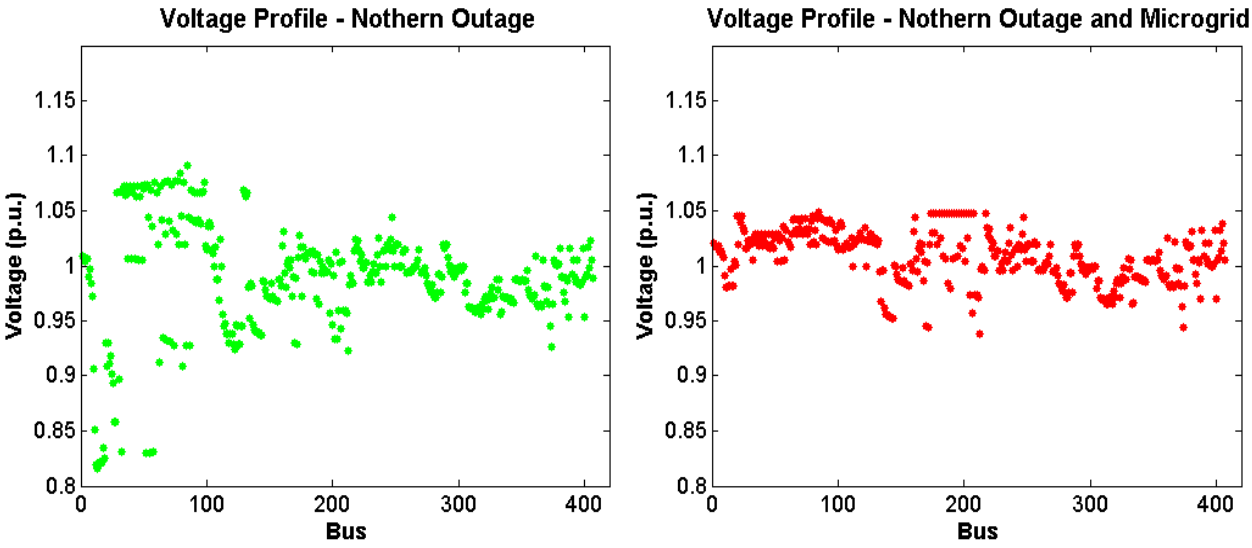


Figure 3.7 Effect of Microgrid on Voltage Profile Following Northern Outage

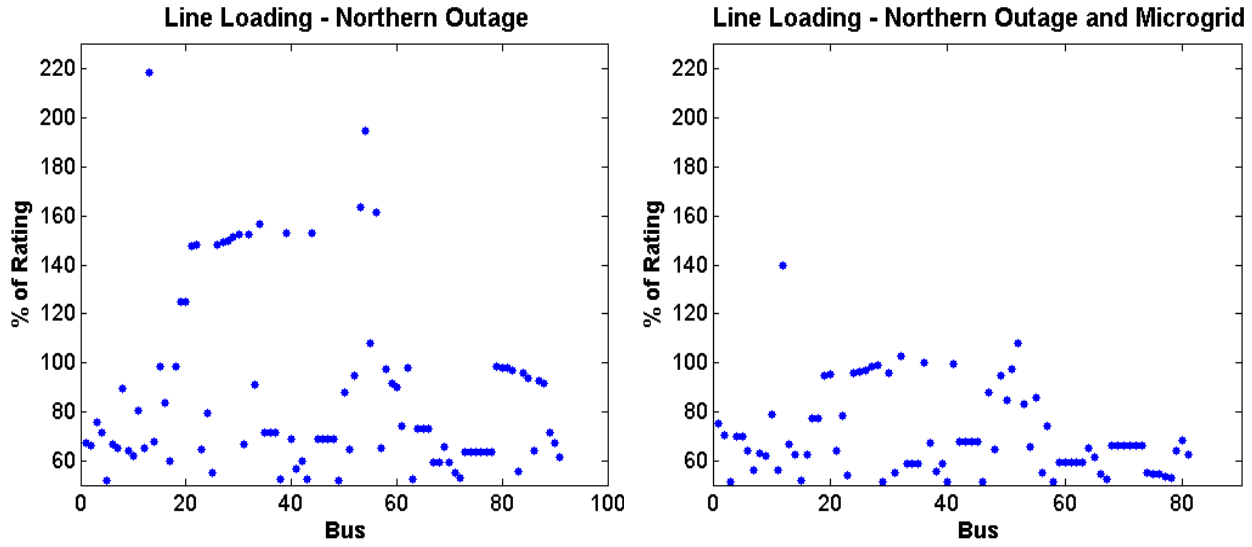


Figure 3.8 Effect of Microgrid on Line Loading Following Northern Outage (> 50% rating)

### 3.3.2 Outage on Southern Line

The procedure in the precious step is repeated, this time taking the Southern line out of service and simultaneously disconnecting the proposed microgrids. The results are shown in tables 3.10 and 3.11. A visual comparison showing the effect of the microgrid of the base case voltages and line loading following the southern outage is shown in Figure 3.9 and Figure 3.10. Since a load flow solution could not be ascertained for an outage on the southern line, voltages and line loading is compared to base case.

Table 3.10 Violations Due to Southern Line Outage with Kigali Center MG Disconnected

| From # | Name | To # | Name | Current Rating (MVA) | Current Flow (MVA) | % of Rating |
|---|---|---|---|---|---|---|
| 202 | Kibuye | 602 | Kibuye | 5 | 7 | 139.9 |
| 2201 | KP1 pilot | 2401 | Kigufi MP | 11 | 11.8 | 103.5 |
| 2401 | Kigufi MP | 2501 | Kigufi | 11 | 11.5 | 100.7 |
| 2501 | Kigufi | 2601 | Gashashi T | 11 | 11.4 | 100.6 |
| 3606 | Mukungwa | 13201 | Mukungwa H | 10 | 10.6 | 106.1 |
| 3702 | Nkora | 3802 | Nkora | 0.8 | 0.9 | 107.9 |

Table 3.11 Violations Due to Southern Line Outage with Airport MG Disconnected

| From # | Name | To # | Name | Current Rating (MVA) | Current Flow (MVA) | % of Rating |
|---|---|---|---|---|---|---|
| 202 | Kibuye | 602 | Kibuye | 5 | 5.1 | 102.8 |

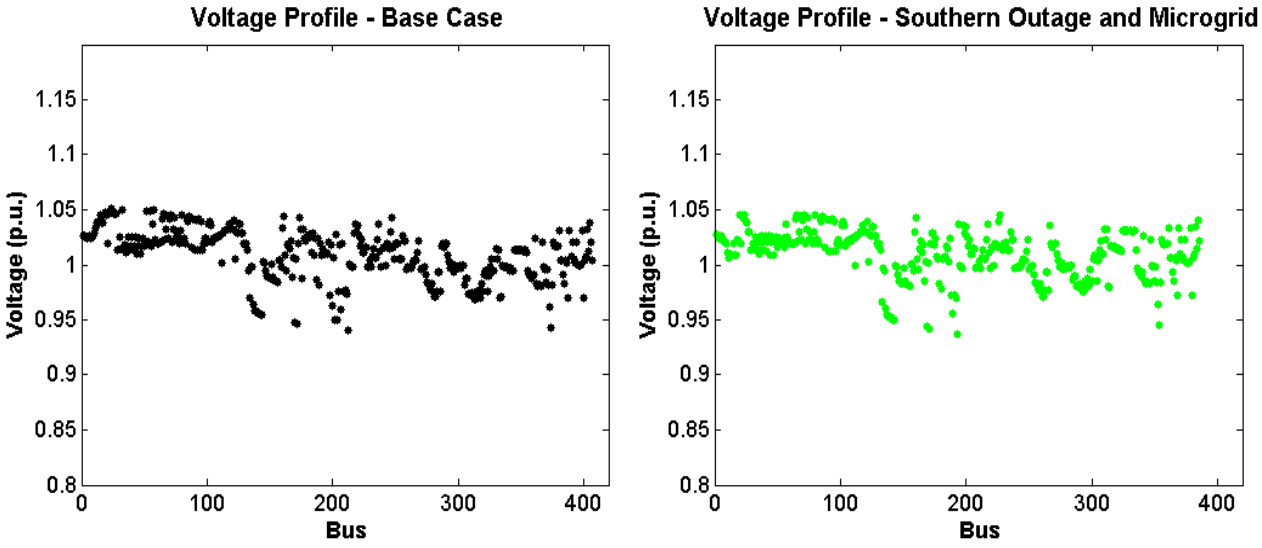


Figure 3.9 Effect of Microgrid on Voltage Profile Following Southern Outage

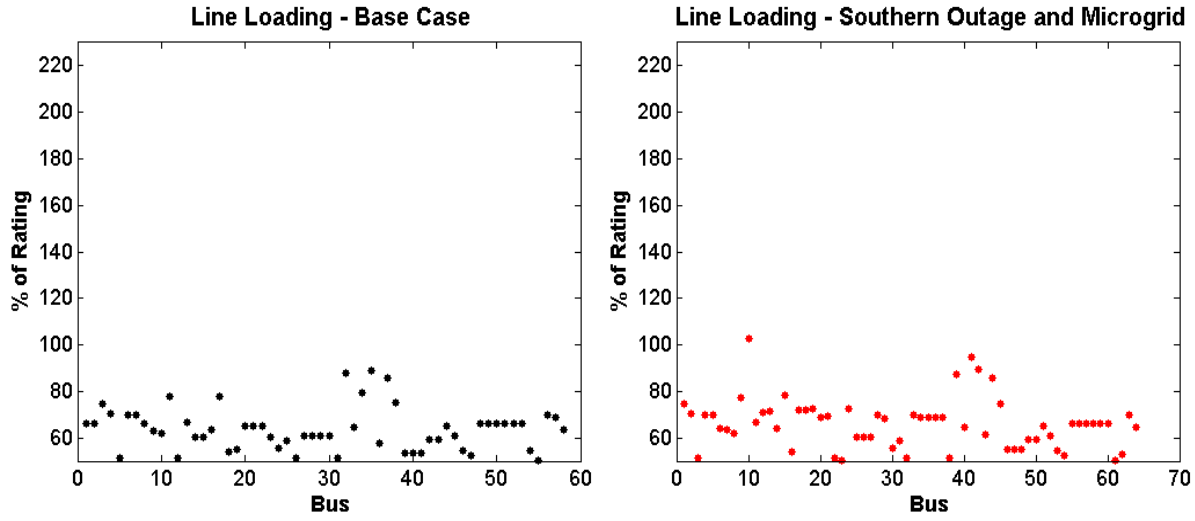


Figure 3.10 Effect of Microgrid on Loading Following Southern Outage (>50% rating)

There are some issues that warrant addressing from the two previous subsections. Even though islanding a microgrid greatly improved the systems condition, there are still remaining violations related to line ratings. It is the author's opinion that these violations are within the

ability of the system operators to mitigate, and will have much less impact on Kigali and the system in general. During contingencies, operators are tasked with taking measures to return the system within safe limits, and can thus conceivably contain these violations because they are fewer and smaller in magnitude compared to the state prior to disconnecting the microgrid. In addition, these outages are far from Kigali such that as a worst case measure, some load can be shed in those areas to ensure that line loading limits are respected. The only lines closely linked to Kigali are the line from bus 3606 to 13201 and bus 3606 to 3706, both of which have an emergency rating of 14 MVA, putting them within operational limits for a certain length of time stipulated in emergency ratings.

### 3.3.3 Outage on Northern and Southern Lines

It was noted previously that an outage on both the northern and southern lines at the same time would effectively separate the system into two separate entities. This would leave Kigali and the eastern part connected to each other, but separate from the northern and southern networks. Under the current setup, Kigali and the East would have a power deficit of about 17 MW assuming this event occurred during peak loading. If the Airport MG was disconnected to operate in island mode, the remainder portion of Kigali and the east would still have a power deficit of about 5 MW necessitating load shedding in Kigali.

Such a scenario with both lines out would be considered an extreme event. To mitigate its impact, extreme measures would be required. Since this work is focused on minimizing the impact on Kigali, the proposed solution requires simultaneously isolating Kigali while leveraging the microgrid. This solution means that Kigali would separate from the east by activating the switch at the PCC between the two networks while the airport microgrid would island as well.

Naturally, the east would lose power, but Kigali can continue to operate until the outages are fixed. To test this solution, a simulation was performed that initiates outages on the northern and southern lines. The switch connecting the east to the Kigali is opened, and the Airport MG is disconnected. The rest of Kigali is shown to be self-sufficient and capable of supplying its load without violating line or voltage limits as illustrated in figures 3.11 and 3.12.

These results indicate that it can be possible for Kigali to remain powered in the unlikely event that the two main transmission lines serving Kigali were simultaneously out of service. Preliminary analysis shows that a microgrid capable of serving a particular load in the capital could ensure Kigali is safe from the most severe outages on the Rwandan grid. This analysis

serves as an encouraging starting point to motivate further investigation into the characteristics and performance of such a system.

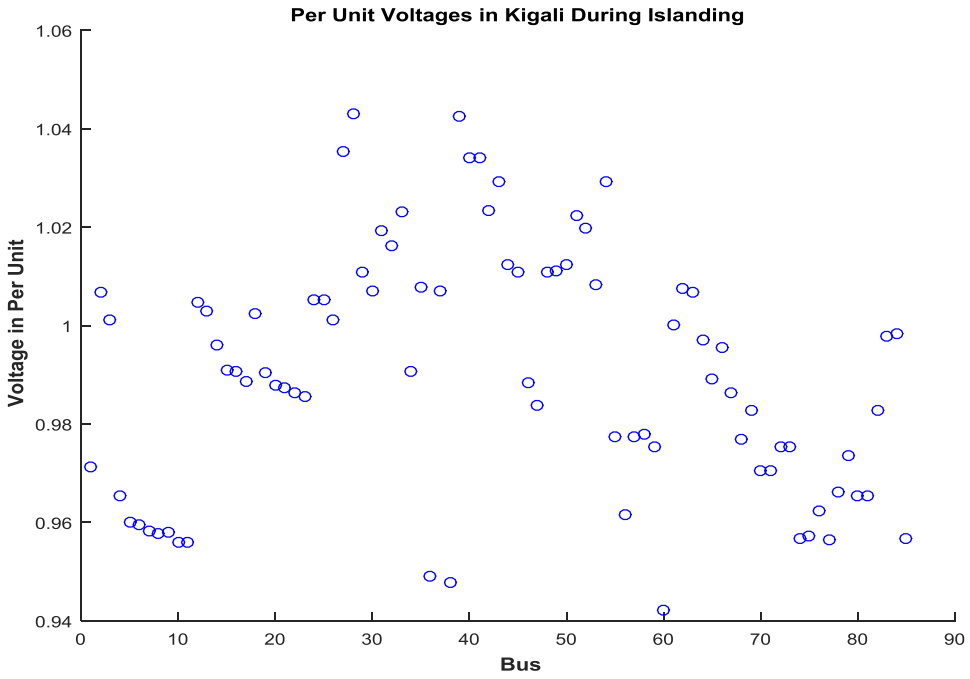


Figure 3.11 Per Unit Voltages in an Islanded Kigali

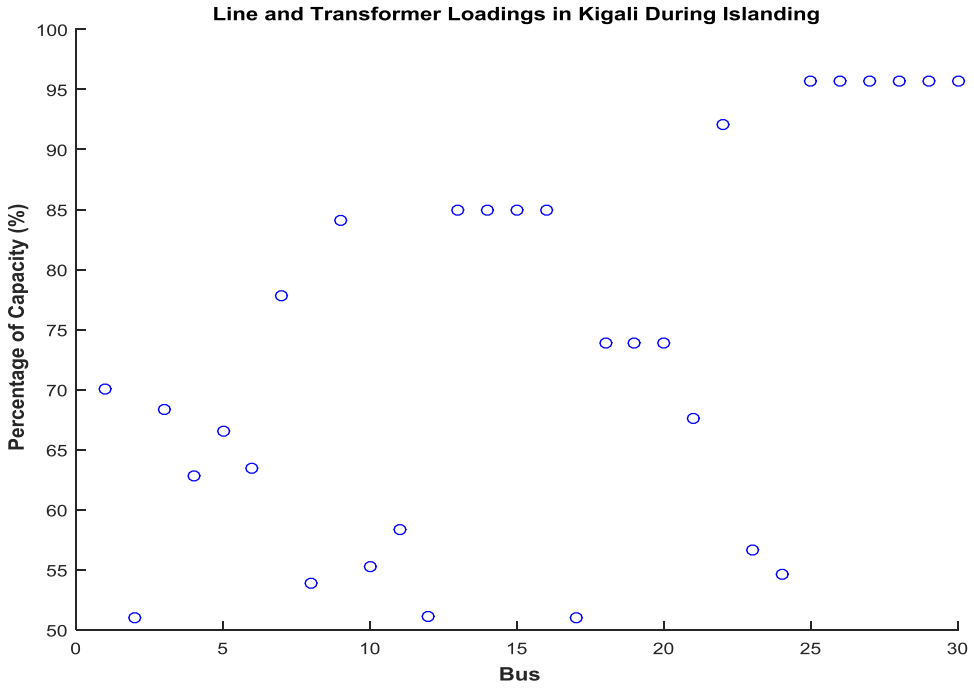


Figure 3.12 Line Loading in Kigali Exceeding 50% of Rating During Islanding

### 3.3.4 Location and Size of Microgrid

In previous sections, it was shown that utilizing a microgrid that disconnects from the grid during outages on the northern and southern lines, line loading violations are greatly minimized and pushed further away from Kigali while voltage violations are eliminated. As was noted earlier, during the simulation the, the microgrid was simply removed from the system. However, the contents of the microgrid were not assessed. What follows is an assessment of what makes up this microgrid. Of the two microgrids simulated, the Airport MG was chosen, based on its additional advantage of shielding the only international airport, a matter of national security. This microgrid contains no prior generation, but a load of 12.5 MW. This load forms the basis for the microgrid design, explicitly explained in the following chapter.

# Chapter 4 : Design of Microgrid Solution

This chapter focuses on the design and analysis of what makes up the microgrid, the different components considered, and the optimization of the system. The size and location of the microgrid were established in the previous chapter. The microgrid is located approximately in the neighborhood of Kigali International Airport, the largest and main airport serving Rwanda, and connected to the low voltage side of the PCC connecting that area to the transmission network as shown in Figure 3.6. The coordinates for the airport is at approximately -1.96, 30.13 and the peak load for this area is 12.5 MW. This location was chosen for its positive impact on the security and resilience of the electric grid, and also for its strategic importance. This chapter expounds on the design aspects for this particular microgrid, and gives consideration to technical and economic aspects. Note that all monetary values are represented in US dollars unless stated otherwise.

## 4.1 HOMER Design Tool

Various tools are available to perform microgrid design as will be shown in subsequent sections. However, the main tool used in this study was HOMER software (Hybrid Optimization of Multiple Energy Resources). As the name suggests, HOMER is an optimization tool used to design and analyze power systems with multiple energy sources. This software was developed by the National Renewable Energy Laboratory (NREL) which is a division the United States Department of Energy, and was later commercialized through Homer Energy LLC. HOMER is

currently a commercially available tool used widely in the design and optimization of microgrids particularly in North America.

Perhaps HOMER's attractiveness is its ability to evaluate a multitude of equipment and resource options over a varying range of constraints effectively and efficiently [44]. In addition, HOMER is capable of evaluating system at a temporal resolution of up to one minute, even though this study was conducted at hourly intervals since it is a high level planning study that does not require such detail. The task at this stage was to ascertain that the physical system deployed is capable of providing electricity as needed throughout the year, particularly at peak loading. To test this, HOMER models electrical system's physical behavior to ascertain its feasibility, then computes the cost of that particular system over its lifetime. This allows for comparison between different feasible systems and the components that comprise them.

The approach of HOMER is quite robust and done in three stages to provide a comprehensive assessment of the system and the technical and financial implications of design choices. The three stages are simulation, optimization, and sensitivity analysis [45]. Here, a configuration or architecture represents one combination of components and their quantity that make up a system.

During simulation, HOMER assesses the performance of the system at every hour of the year to determine its technical viability and lifetime cost. Once technically feasible configurations are obtained, an optimization is performed to find the least-cost option. Finally, a sensitivity analysis is performed to evaluate how uncertainty in the inputs and assumptions made impact the output. This is particularly useful when considering inputs that are variable or uncertain such as solar radiation, price of fuel, or the lifetime of some components. The fact that

each optimization results from multiple simulations, and each sensitivity analysis is obtained from several simulations can be as in illustrated in Figure 4.1 [45].

The HOMER model was also adopted in this study for its versatility in simulating various components and energy sources commonly used in microgrids. The components of interest to this study include solar photovoltaics (PV), diesel generators, bi-directional inverters, and energy storage. The energy resources considered are solar irradiation for PV and diesel for gen-sets. In addition, HOMER accepts various forms of loads such as electric, thermal, and so on. This versatility makes HOMER a suitable choice for microgrid modelling because it is a comprehensive modelling tool for microgrids and as such, design can easily be extended to incorporate more configurations within the same framework.

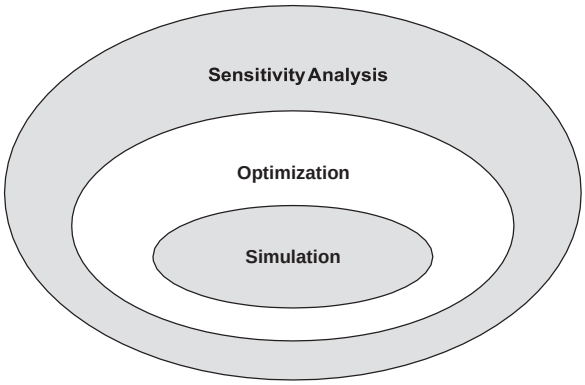


Figure 4.1 Relationship between simulation, optimization, and sensitivity analysis [45]

## 4.2 Solar PV

This study aims first and foremost at designing a microgrid that uses solar energy as the primary energy source. Essential to employing PV is knowledge of the different facets involved in estimating the amount of energy obtainable from solar radiation. In this section, the process of

obtaining solar resource data is explained, the general trends in Solar PV technology are explored, and the HOMER radiation and PV models are presented.

### 4.2.1 Solar PV Data

The solar data of interest is amount of solar energy that is accessible from the sun by means of photovoltaics. Particularly, we are interested in solar irradiance, which is defined as the rate at which radiant energy arrives at a surface area during a specific time interval and has the units of watts per square meter ($W/m^2$), watt being the unit of energy [46]. For one hour intervals, the unit of watt-hours per square meter ($Wh/m^2$) is used, which is the prevalent unit used in the business side of solar energy to represent the energy received from the sun on one square meter of area over the course of an hour.

There are various sources of solar irradiation data that are available for commercial or academic use. The solar radiation data gives a direct indication of the solar energy potential of a specific geographical location, and is essential to modeling the system's performance. A comparison is made on different sources for this data to determine which is suitable for this study. The different services vary in cost and quality, and depending on the needs of the user, several considerations need to be made. What follows is a description and comparison of some of the major solar data vendors.

#### 4.2.1.1 SolarGIS

SolarGIS is an online portal that delivers different solar solutions including solar radiation data. The portal is operated by *GeoModel Solar* which offers multiple types of data such as maps, time-series data, and forecasts. As previously mentioned, this data is based on

models developed by the company to translate acquired satellite images into solar radiation information.

SolarGIS models use data obtained from the following satellites and databases:

- Meteosat and GOES (Geostationary Operational Environmental Satellite System) for cloud and snow indices (operated by the European Organization for the Exploitation of Meteorological Satellites - EUMETSAT)
- GFS database for water vapor (Global Forecast System operated by NOAA)
- MACC database (Monitoring Atmospheric Composition and Climate) for atmospheric optical depth
- SRTM-3 (Shuttle Radar Topography Mission) for the digital elevation model

The SolarGIS database covers the continent of Africa from the year 1994 to present. According to the vendor, satellite data used has a spatial resolution of 3km near the equator in 15 minute and 30 minute steps which is sufficient for this particular study. The spatial resolution is further enhanced using models developed by SolarGIS and various measurements to obtain up to 90m resolution.

SolarGIS provides uncertainties for their data which useful to establish the level of accuracy of results obtained using this data. Uncertainties of data according to the vendor are $\pm 4\%$ for Global Horizontal Irradiation (GHI) and $\pm 8\%$ for Direct Normal Irradiance (DNI) in about 80% of their values and a bit higher for 90% of values. However, this is true only for yearly averages, and not necessarily daily and hourly values. It is important to note that Rwanda is probably among the areas that show higher inaccuracy. This is because, according to the vendor, error prone areas were found to be close to water, at high latitudes, had high changing aerosols, or lacked accurate ground measurements. Since ground measurements in Central

African were not used by SolarGIS in their model validation, it is probable that the data here is not as accurate as other regions with high accuracy ground sensors.

However, and independent 2011 study by the Institute of Environmental Sciences at the University of Geneva compared various commercial vendors and concluded that SolarGIS data showed more consistency and accuracy with respect to accurate ground measurements [47]. Since over one hundred ground sensors globally were used by SolarGIS to validate their model (both GHI and DNI), including several in West and South Africa, it is a reasonable assumption

that the model extends well to parts of central Africa. Figure 4.2 shows the location of high accuracy sensors used by SolarGIS for model validation.

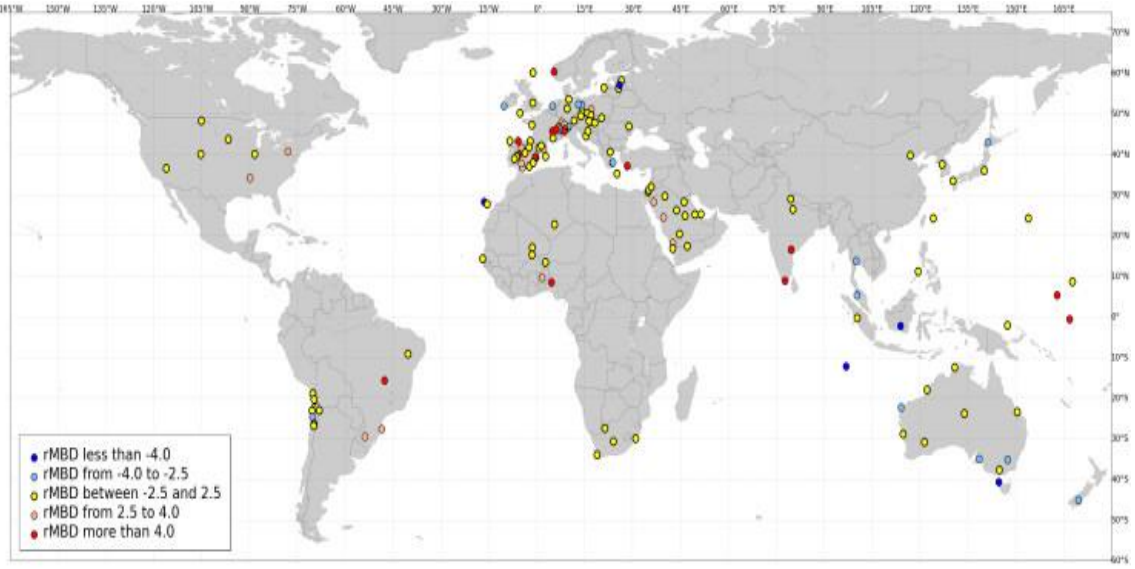


Figure 4.2 SolarGIS GHI Validation Sites

Solar radiation data available from SolarGIS includes GHI, DNI, and DIF components, as well as irradiation for fixed and sun tracking panels. In addition, optimal placement and energy output for locations can be obtained, although this is currently not available for the area of study.

The cost of data from SolarGIS varies based on the service requested and the amount of data needed. Since monthly and annual averages of solar radiation are widely available at no charge, focus has been given to higher temporal resolution, in this case one hour. One-hour solar

data is available through the *ClimData* portal of SolarGIS, which is also their most up-to-date database. The pricing for this service is summarized in tables 4.1 and 4.2 .

Table 4.1 Cost of Multi-Year Solar Data from SolarGIS

| Multi-year data to date | Number of Values (data points) | GHI+GTI+DIF+TEMP+WS | GHI+DNI+TEMP+WS+WD+RH |
|---|---|---|---|
| Monthly sums | 12 | €500 | €1000 |
| Hourly Averages | 8760 | €1000 | €3500 |
| 15 or 30 min | 35040 | €1200 | €4000 |

Table 4.2 Cost of 12 Continuous Months Solar Data from SolarGIS

| Single continuous 12-month period (recent years) | Number of Values (data points/year) | GHI+GTI+DIF+TEMP | GHI+DIF+DNI+TEMP |
|---|---|---|---|
| Monthly sums | 12 | €200 | €400 |
| Daily summaries | 365 | €200 | €400 |
| Hourly Summaries | 8760 | €250 | €600 |
| 15 or 30 min | 35040 | €300 | €800 |

#### 4.2.1.2 Solar Data Warehouse (SDW)

Unlike other data sources reviewed in this report, SDW does not use satellite data to derive solar radiation values. SDW uses publicly available solar radiation data from ground sites in the US and around the world. The United States has over 3500 ground sites [48] from which SDW obtains data and aggregates it into a single database. Most of the equipment used at these stations is medium-quality, with on a few high quality ground measurement sites. The vendor claims that utilizing multiple medium-quality ground measurements provides good or better

accuracy in comparison to some satellite based data from NASA, TMY3 (Typical Meteorological Year), and SUNY (State University of New York) databases.

The vendor also reports an average total error of 9.8% for daily GHI, compared to 21% and 18% from NASA and SUNY satellites respectively [49]. This finding was also reported by the National Renewable Energy Laboratory (NREL) when SDW was tested against the US Climate Reference Network [48]. However, this level of data and accuracy is readily available only for US locations. To obtain data from global locations such as the region of interest, SDW is contracted to perform a search for the data, and provide a detailed report about the available information, and all relevant sites. The timeline for this search and results are not guaranteed, and a fee of $750 is assessed per search making SDW unsuitable for our purpose. However, for similar studies in the U.S., SDW can be a reliable and affordable source.

#### 4.2.1.3 3TIER

3TIER is yet another renewable energy assessment and forecasting service, now owned by the Finnish company *Vaisala*. 3TIER has a database of solar time-series data spanning over a decade. Solar radiation data is available with a temporal and spatial resolutions of one hour and 3km respectively. The data contains the most important aspects when evaluating solar potential and trends, that is, GHI, DNI, and DIF. 3TIER data is derived from satellite images which are translated to radiation values. Satellites covering Africa are Meteosat 5 and Meteosat 7 that have data since 1999. Various databases are used to validate models including the following.

- Surface Radiation Network (SURFRAD)
- National Solar Radiation Database
- MODIS Aerosol Optical Depth and Water Vapor Datasets
- NREL

Data validation by the company indicates a standard error of 5% for GHI and DIF, and 9% for DNI. However, the study shows that for hourly data validation in Africa and the Middle East, root-mean-square error values were 15% and 37% for GHI and DNI respectively and a bias error under 1% for GHI. However, the mean absolute error was only 4.2% and 11.9% for GHI and DNI [50]. Attempts to request a quote were not replied to.

#### 4.2.1.4 SoDa

The SoDa service provides access to information from various sources relating to solar radiation. These services include (in order of number of services).

- MINES ParisTech (France)
- ENTPE (France)
- METEOTEST (Switzerland)
- NASA (U.S.)
- ISAC (Italy)
- NCEP (U.S.)

SoDa manages two families of databases, HelioClim and MACC-RAD.

#### 4.2.1.5 SoDa HelioClim

HelioClim (HC) is a group of databases containing solar radiation data estimated from satellite images of MSG (MeteoSat Second Generation). HelioClim 1 (HC1) and 3 (HC3) both use the HelioSat-2 [51] method to convert the images into radiation values. The more relevant database is HC3, which spans from 2004 to-date with a spatial resolution of 3-5km, and temporal resolution of up to fifteen minutes. A significant advantage is that the dataset provides these values for all orientations of solar panels, a calculation which is not complex but can be tedious if multiple locations are involved.

Data from HC3 includes uncertainty in the data in form of upper and lower bounds to data points. Each data point is given with bounds, which is useful when ascertaining the accuracy

of results obtained using this data. These error estimates are obtained by comparing against data from twenty-nine ground stations. Like other sources, HC3 provides data in the different aspects of solar radiation, that is, GHI, DIF, and DNI for both fixed and sun-tracking panels.

Even though SoDa data was commercialized by Transvalor and MINES ParisTech/ARMINES, a variety of data is still available for free. Two-year data from February 2004 to December 2005 in up to 15-minute time steps and can be downloaded directly from their website using a free account. HC1 data is available for years 1985 to 2005, but with a spatial resolution of 20km. Since the area of study is relatively small with varying weather conditions, this resolution is not very accurate. Solar radiation data from 2004 to date in resolutions up to 1 minute is available for a fee from the SoDa website and price varies based on the amount and type of data required. For more free data, the staff at SoDa suggests an alternate source, MACC-RAD, available through another website.

#### 4.2.1.6 SoDa MACC-RAD

The MACC-II project (Monitoring Atmospheric Composition & Climate) is a service of The European Earth Observation Programme (Copernicus), charged with monitoring atmospheric conditions. Among other things, it monitors and records solar energy resources or solar radiation information. This data is available free of charge through the new SoDa website and provides data on GHI, DIF, DNI on horizontal surfaces in time steps up to 15 minutes. MACC-RAD has Global coverage including Central Africa. Furthermore, SoDa offers to check data obtained from other sources against their models free of charge which is useful to validate data that might be obtained from other sources.

The downside to this source is that a measure of uncertainty in Africa is not given in the data which makes it challenging to establish its accuracy. However, the data does come from

very reliable sources at the renowned MINES ParisTech and ARMINES. The data however was validated against 18 weather stations in different climatic regions around the world, that is, oceanic, Mediterranean, Desertic, and Subtropical. Table 4.3 summarizes the errors obtained from the different test stations for hourly estimates. From this table, it can be observed that maximum bias was 13% and RMSE 34%. This indicates mild accuracy in results from the model

considering the fact that at all stations, correlation coefficients are closer to unity for validated sites.

Table 4.3 Data Validation Bias and Error for MACC-RAD [52]

| Station | Number of samples | Mean observed value W/m² | Bias W/m² (%) | RMSE W/m² (%) | Correlation coefficient |
|---|---|---|---|---|---|
| Lerwick | 11337 | 197 | 15 (7%) | 67 (34%) | 0.938 |
| Toravere | 19293 | 229 | 16 (7%) | 73 (32%) | 0.945 |
| Lindenberg | 10720 | 285 | 17 (6%) | 73 (26%) | 0.953 |
| Cabauw | 18264 | 269 | 36 (13%) | 79 (29%) | 0.956 |
| Camborne | 12690 | 281 | 33 (12%) | 78 (28%) | 0.958 |
| Palaiseau | 6863 | 284 | 30 (11%) | 73 (26%) | 0.962 |
| Payerne | 20119 | 308 | 35 (11%) | 77 (25%) | 0.966 |
| Carpentras | 21493 | 400 | 26 (6%) | 63 (16%) | 0.977 |
| Greoux-les-bains | 4115 | 376 | 32 (8%) | 80 (21%) | 0.963 |
| Nice | 4518 | 383 | 28 (7%) | 70 (18%) | 0.973 |
| Fos-sur-mer | 4512 | 399 | 28 (7%) | 65 (16%) | 0.977 |
| Cener | 3161 | 396 | 18 (5%) | 76 (19%) | 0.963 |
| Plataforma Solar de Almería | 22608 | 457 | 15 (3%) | 83 (18%) | 0.959 |
| Sede Boqer | 18602 | 582 | 3 (1%) | 67 (11%) | 0.973 |
| Tamanrasset | 21338 | 589 | 20 (3%) | 75 (13%) | 0.972 |
| Brasilia | 5635 | 496 | 32 (6%) | 126 (25%) | 0.911 |
| São Martinho da Serra | 6279 | 427 | 14 (3%) | 81 (19%) | 0.964 |
| De Aar | 3204 | 545 | 4 (1%) | 73 (13%) | 0.968 |

#### 4.2.1.7 IrSOLaV

IrSOLaV is a Spain-based company that focuses on assessment and characterization of solar resources. Their data is based on satellite imagery as the previously explored sources. Similar satellites to other sources are used by IrSOLaV and include

- MeteoSat First and Second Generations
- GOES (Geostationary Operational Environmental Satellite system)
- MODIS (Moderate-resolution Imaging Spectroradiometer)
- MIRS (Operational Microwave Integrated Retrieval System)

The vendor sells global solar radiation data including Africa, with a temporal resolution up to 15 minutes dating as far back as 1994 for areas in Africa. Like the other sources, the different aspects of solar radiation are included in the data, that is, GHI, DIF, and DNI. All solar radiation

data from IrSOLaV is available for a fee and downloadable from their vending website (www.solarexplorer.info). Compared to the other sources, data is costlier from this vendor, and samples were not available to ascertain the details of the data, and the uncertainties therein. The cost of data (hourly) is summarized in Table 4.4

Table 4.4 IrSOLaV Pricing for Solar Radiation Data

| **Period** | **Cost** |
|---|---|
| 19 Years (GHI+TEMP) | €1000 |
| 19 Years (GHI+DNI+DIF+TEMP+RHUM+WS+WD) | €3500 |

Data from the vendor is only available as shown in the table above. Requests for fewer number of years for a reduced fee received no response.

#### 4.2.1.8 Summary and Recommendations

This section compares six solar radiation data sources. The major factors considered in choosing a data source included, data availability, time span of data, accuracy, and cost. Table 4.5 is a summarized comparison of data sources and forms the basis for the recommendation. The accuracy listed in the table is subjective since measures of accuracy are given differently for different sources. Instead of values, a subjective term is used (average, good, or excellent). This representation is based on the vendor-based and independent reports on the data, as well as the extent to which errors are reported.

Table 4.5 Comparison of Solar Data Sources

| Data Source | Multiple Years | Single 12 Month Period | Accuracy |
|---|---|---|---|
| SolarGIS | €1000 | €250 | Excellent |
| Solar Data Warehouse | $750 per search | N/A | N/A (for Rwanda) |
| 3Tier | Awaiting Quote | Awaiting quote | Good |
| Soda HelioClim | Free | Free | Average |

| | | | |
|---|---|---|---|
| Soda MACC-RAD | Free | Free | Average |
| IrSOLav | €1000 (GHI only), €3500 | N/A | Good |

Data from SolarGIS showed the most accuracy, and was reported as such in an independent report [47]. A single year's data in any recent year can be obtained for €250 (≈$283), while multiple years can be obtained for €1000. Solar Data Warehouse is significantly more expensive at $750 per search, with no guarantees on results. IrSOLaV only sells data for multiple years at a cost of €1000, and this only includes only the GHI aspect. To obtain other aspects of radiation would cost €3500.The service however is very reportedly reliable.

Based on comparison, the optimal choice would be a combination of HelioClim and MACC-RAD data. Together, the data can be checked for discrepancies. Furthermore, MACC-RAD is completely free, and HelioClim provides up to two years of free data. This choice provides fairly reliable data for this type of study at no charge. As a secondary choice, if higher accuracy and verification is required, a time-series set from SolarGIS spanning 1 year can be obtained for validation purposes, but this was deemed an unnecessary expense. In this study, data

is obtained from Soda MACC-RAD in hourly intervals for multiple years. The annual average radiation is found to be 5.49 kWh/m$^2$/day with monthly averages shown in Figure 4.3.

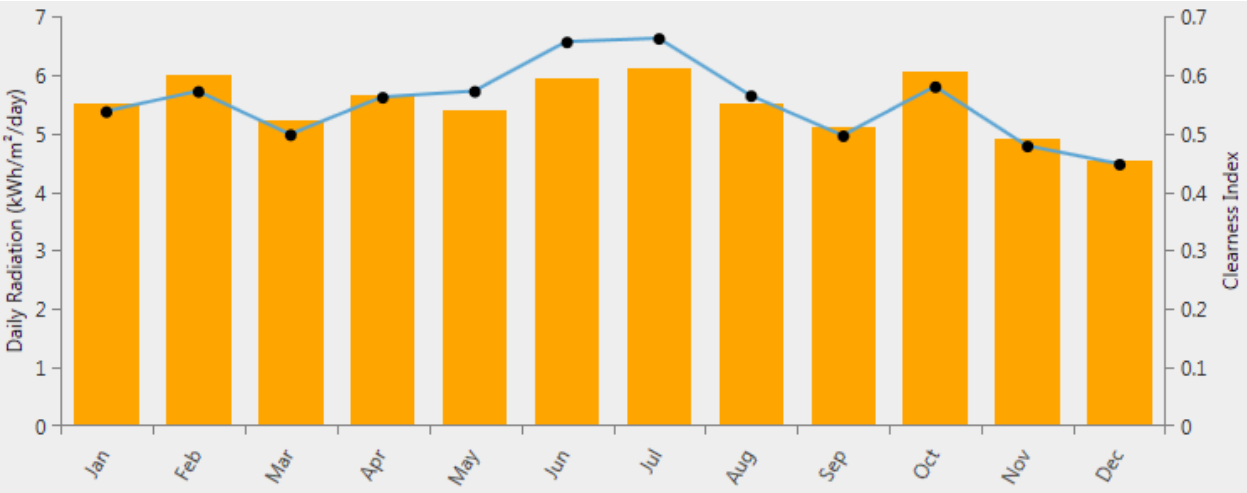


Figure 4.3 Monthly Average Solar Global Horizontal Irradiance (GHI)

### 4.2.2 PV Technology

Photovoltaics commonly referred to as PV, is the direct conversion of radiation into electricity [53]. Even though this technology that sources electricity directly from the sun has been around for decades, it is still in its infancy relative to traditional sources of electricity such as fossil fuels. PV currently accounts for about 0.1% of global energy [53, 54]. While this appears to be an insignificantly small fraction of global energy, it still is a noteworthy milestone when viewed in perspective. The International Energy Agency (IEA) reports that since 2010, the world has added more PV than in the last four decades combined [54], and this is not

insignificant. In fact, the PV market is reported to be growing at a rate estimated between 35% and 60% per year [54-57].

PV technology uses semiconductor material to convert the sun's radiation into electricity. The PV system contains many layers made up of cells. Across these layers, an electric potential is developed when exposed to sunlight, which causes electricity to flow [53]. More radiation on these cells creates a bigger electric field, and hence more electricity flow. This explains why more electricity is produced with more sunlight.

One of the largest hindrances to widespread PV deployment is the cost in comparison to other sources of energy. The high cost of PV is associated with the manufacturing process that is relatively expensive. [54, 56]. However, the cost of PV has dramatically dropped in the last decade, and trends suggest a likely cost parity with other energy sources, which is in turn likely to increase production and deployment.

Figure 4.4 shows this trend and projections till 2020, with the cost of PV modules around US$1/watt for thin film modules and US$2/watt for crystalline silicon modules.

Over the last decade, the most efficient commercial solar panels have been made from crystalline silicon (c-Si) and accounted for about 80% of installed capacity [55]. In addition to cost reduction, PV efficiency is yet another area that needs more development. Commercial flat solar panels current operate between 15% to 25% efficiency [53, 55, 58]. PV efficiency refers to the fraction of radiant sunlight that is converted to electricity by the entire module which is made up of many solar cells, which individually may exhibit higher efficiency as shown in solar cell efficiency tables [58]. Some of the main factors affecting performance of PV are the effects of cell temperature, dust, and humidity, all of which negatively impact performance as they increase [53]. As modules reach their theoretical efficiency limits, attention is being given to thin film

cells, which though cheaper, have lower efficiency than c-Si. It is not certain whether they are better as their lower efficiency could offset whatever benefit is achieved from their lower cost.

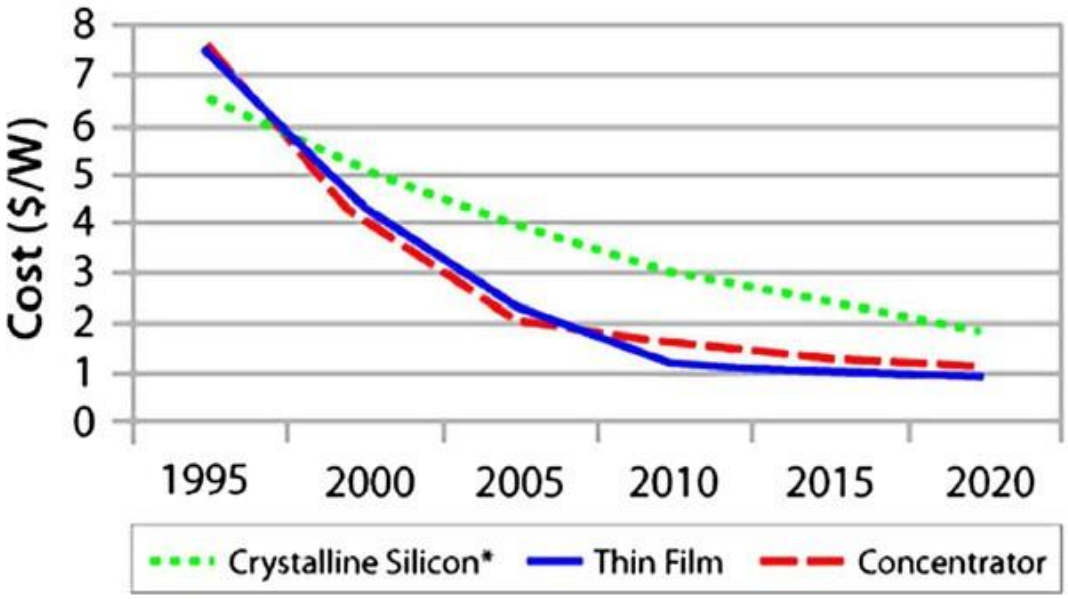


Figure 4.4 Trend in Cost of PV from 1995-2020 [53]

### 4.2.3 PV Model

The PV system is modelled using HOMER, with the ability to model both cost and performance. First, the technical performance of the PV system will be explained, then the cost model will be presented. Solar PV produces electricity by converting light radiation to a direct

current. The equation relating the amount of solar radiation to power output from the PV array (a string set of solar panels) is modelled by in HOMER using equation 4-1.

$$P_{PV} = Y_{PV}\, f_{PV} \left( \frac{\bar{G}}{\bar{G}_{T,STC}} \right) \left[ 1 + \alpha_P \left( T_C - T_{C,STC} \right) \right] \qquad 4\text{-}1$$

Where

$Y_{PV}$ is the rated capacity of the PV array, meaning its power output under standard test conditions (kW)
$f_{PV}$ is the PV derating factor (%)
$\bar{G}_T$ is the solar radiation incident on the PV array in the current time step (kW/m$^2$)
$\bar{G}_{T,STC}$ is the incident radiation at standard test conditions (1 kW/m$^2$)
$\alpha_P$ is the temperature coefficient of power (%/°C)
$T_C$ is the PV cell temperature in the current time step (°C)
$T_{C,STC}$ is the PV cell temperature under standard test conditions (25 °C)

A few of these terms perhaps require elaboration. The derating factor ($f_{PV}$) is a scaling factor used to account for the fact that under normal operating conditions, the PV array's power output will be less than when the module was tested in a controlled laboratory environment. When installed, a PV array might be exposed to shading, or soil particles which reduce the output. In addition, electrical losses in the wiring apparatus coupled with aging might also contribute to lower energy output over its life-time. The temperature coefficient of power ($\alpha_P$) accounts for how sensitive the PV array is to changes in temperature. As indicated before, increased temperature decreases the power output of the PV array, and this is accounted for by this coefficient. Finally, standard test conditions (STC) refer to the controlled conditions used when testing and rating a PV module. STC is a useful standard in that all manufacturers provide ratings for their modules in a way that is easily comparable across brands because they were

tested under similar conditions. Typically, STC is defined as a cell of temperature 25°C, radiation of 1kW/$m^2$, and no wind.

In addition to the above, HOMER models the tracking system for the PV array. Most large scale systems used a fixed tilt, but in some applications, a mechanism is employed to adjust the angle of the panels such that they spend more time directly facing the sun. This tracking can be done in one axis, or two, each time increasing the cost of installation which might offset any benefits in increased output. Furthermore, a maximum power point tracking system, which is a controller that maximizes the PV output by operating the system at a voltage level associated with maximum power, can also be modelled.

The second aspect of modelling the PV system considers the cost. PV system costs are divided among the PV modules, construction and installation, operation and maintenance, and balance of system costs that include interconnection components to electric grid such as inverters and transformers [54, 56]. While the cost of the PV modules has dropped as shown in

Figure 4.4, the so called balance of system (BoS) still remains high and hence a hindrance to large-scale deployment. Therefore, while modelling PV costs, the cost per kilowatt must account for BoS in addition to PV modules prices. An example cost model in HOMER is shown in Figure 4.5. Homer also has the ability to perform sensitivity analysis on these costs to account for uncertainty in estimated PV costs. Sensitivity values can also be added to the

replacement costs of PV, its lifetime, derating factor, operation and maintenance, and other parameters over which the designer has no control or are prone to fluctuation.

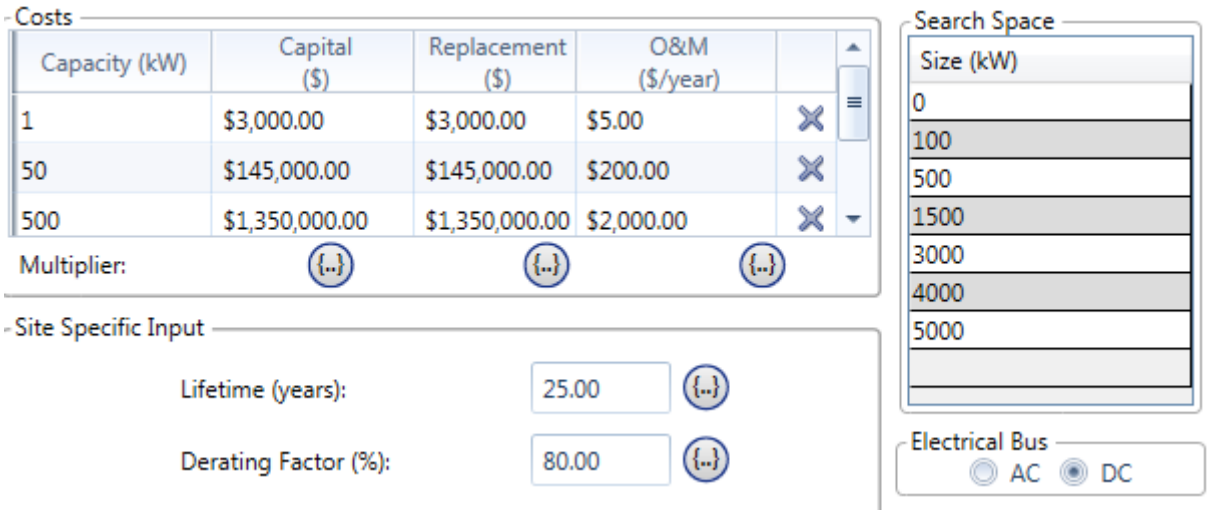


Figure 4.5 Sample PV Cost Model in Homer

## 4.3 Energy Storage Technologies

### 4.3.1 Conventional Vs. New Technologies

Energy storage describes technologies or methods through which it is possible to store energy generated by a system, and retrieve it at a later time when needed [59]. Most large electrical energy storage uses various technologies to convert electrical energy, which is difficult to store in electrical form, to a form that that is easier to store. These forms, as will be detailed, include chemical energy, thermal energy, potential energy, kinetic energy, and so on. Energy storage is prevalent in some modern technologies, but only on a very small scale relative to the energy needs at the utility level. The most common energy storage can be seen in portable electronics, where users are still able to use their devices for significant periods of time without

an electric supply. While that level of storage is not yet a reality for electric utilities, it is a worthwhile goal, and in some applications, imperative.

There are many reasons why energy storage could be useful for utilities, power system operators, planners, and remote communities. One of the main benefits is the ability to store energy from intermittent sources. Underutilized renewable energy sources (RES) such as wind and solar are viewed as some of the solutions needed to meet increasing energy demand as well as increase access to electricity in developing countries [60-63]. RES can also act as an alternative to fossil fuels, which research shows are not only harmful to the environment, but are also depleting in quantity [26, 59, 64]. However, unlike traditional sources such as coal or petroleum, intermittent energy sources cannot be stockpiled. This is the case with wind and solar energy that are only available at certain times of day. Since traditional sources can be stockpiled, increasing or decreasing generation to meet the demand is straightforward, as long as enough fuel is available at the generation station. Intermittent renewables cannot be controlled in this way, and often, their peak availability does not meet the peak demand. Energy storage would fill this gap by storing excess energy from renewables to be dispatched during high demand.

Energy storage can provide other benefits. Many energy systems are over-designed with the aim of serving the load at all times including peaks that last a few hours a year [65]. This makes the system more expensive and less efficient. Using energy storage to meet peak loads can reduce overall cost by eliminating the need for peak generating units, making the system more efficient. *Peak shaving* as it is referred to in power system operation, can benefit consumers if they purchase less from the utility during peak (most expensive) periods [66, 67]. Cost reduction can also be achieved by deferring construction of new transmission lines to feed the growing

demand, and replacing it with storage particularly in areas that receive power across long distances.

Many forms of energy storage exist today, in different application and sizes. By far, the most popular form of large scale storage is pumped hydro storage (PHS) which in 2011, comprised 99% of installed storage worldwide in 2011 [68, 69]. As the name suggest, pumped hydro storage uses excess energy to pump water from a lower water reservoir to one that is higher. The water that is pumped is held in the upper reservoir is then released to run turbines for electricity generation when demand is high. Pumped hydro storage is often done on a large scale because of its potential for storing a lot of energy. Typical ratings range from 100 MW to 3000 MW, but the financial investment required is very large. However, this mode of storage has a relatively high efficiency about 75-80% with a fast response time under a minute [59, 63]. Pumped hydro-storage however is only possible where two large water reservoirs can be created at different elevations. This is of course limited by physical terrain. The size, cost, and geographical constraints make this storage difficult to implement in the Kigali area.

Another popular storage method is compressed air storage (CAS). This technology stores energy by compressing air into a reservoir. The air is stored under high pressure in underground caverns, or storage vessels, which can then later be used by itself or with gas to generate electricity in a gas turbine [63]. Like PHS, CAS is capable of storage in the megawatt range. CAS however suffers from low energy density, long lead times, and geological constraints as a secure underground cavern that can withstand very high pressure is necessary in most cases [63]. On the positive side, both CAS and PHS have a long lifetime in the range of 30-50 years [70].

While traditional storage in CAS and PHS makes up almost all of energy storage, new forms of energy storage are poised to play a big role in the near future. Many of these relatively

new technologies use chemical storage in the form of batteries. Perhaps the most prevalent example is lead-acid batteries which are used in most vehicles today. The lead acid battery consists of a lead anode and lead dioxide cathode in a sulfuric acid electrolyte and is a mature technology with a track record spanning a century [59, 63, 66]. Despite its maturity, wide availability, and low cost, lead acid battery technology suffers from low energy and power density in comparison to other commercial batteries. Lead acid batteries are also considered hazardous, and have a low cycle life. Cycle life refers to the number of times a battery undergoes a charges-discharge cycle before its capacity falls below a certain percentage of its original rating.

Other promising forms of chemical storage include sodium sulfur which has been widely studied and commercialized in recent years, lithium ion which shows the highest efficiency of the chemical lot, and nickel-cadmium among others. Lithium ion and sodium sulfur batteries have high efficiency upward of 90%, and are also energy dense. As expected this comes at significant cost. While CAS and PHS cost about 500-2000 $/kW and 2-100 $/kWh respectively, lithium ion batteries cost about 4000 $/kW and 2500 $/kWh and sodium sulfur costs 1000-3000 $/kW and 300-500 $/kWh [59, 63]. However, these batteries can respond much faster on the order of milliseconds and have a long cycle life and lifetime. They are also capable of supplying power over a wide time span ranging from seconds to hours making them versatile and useful in a myriad of applications ranging from power quality, to grid support and load shifting [68].

The energy density of lithium ion batteries can reach 200 Wh/kg (watt-hours per kilogram) and that of sodium sulfur, 240 Wh/kg [59, 63, 70]. In comparison, PHS offers about 0.5-1.5Wh/kg while CAS provides 30-60 Wh/kg. The implication is that a lot of power and

energy can be stored in a small space such as a room or warehouse using chemical storage, which is a lot easier to secure than landscaping for PHS or creating a cavern for CAS.

There are many other emerging and established energy storage technologies including super capacitors, flywheels, thermal storage, and other chemical based solutions that are not covered in this brief overview of energy storage. In the case of thermal storage, it was found to be more common where the end-use was heat-related and not electric. Direct electrical storage such as capacitors and super-capacitors were not considered because their rated power is relatively low, while those that have higher power ratings can only supply it for seconds which relevant in the realm of power quality and not peak shaving or long term storage. Studies have indicated that flow batteries such as zinc chloride or zinc bromide are promising and possibly perform better than sodium sulfur, but most of these have not been commercialized and are still under research and development or demonstration [68-70].

### 4.3.2 Storage Model

In this study, a chemical storage battery storage is chosen. Battery storage is chosen for its relevance to this application in cost, size, and physical considerations. Other mature technologies such as CAS or PHS are too big for this application, and physical and geological constraints render them unlikely near the city. Battery storage is also readily available with short lead times, and is scalable. This means that increased storage would only require more batteries, an option that is not readily available with other forms of storage. This is particularly useful for

the case of Kigali, and Rwanda general where the system is expected to rapidly grow in coming years.

The battery model, like PV, is modelled on two levels to simulate both performance and cost. On one hand, the physical and electrical properties of the battery are modelled, and on the other the cost associated with storage is computed. Important parameters in battery storage are the amounts of energy that can be absorbed or withdrawn at a given time. HOMER computes these values, the maximum charge and discharge rates, using the Manwell and McGowan model described in [71].

HOMER computes the maximum charge power for the battery at each time step by setting three limitations [72]. Please note terminology in this section. The first limitation relates to the maximum amount of power that can be absorbed by the battery using the kinetic battery model (kbm) as derived by Manwell and McGowan and shown in equation 4-2 [71].

$$P_{batt,cmax,kbm} = \frac{kQ_1e^{-k\Delta t} + Qkc(1 - e^{-k\Delta t})}{1 - e^{-k\Delta t} + c(k\Delta t - 1 + e^{-k\Delta t})} \quad 4\text{-}2$$

Where

$Q_1$ is the available energy (kWh) in the battery at the beginning of the time step,
$Q$ is the total amount of energy (kWh) in the battery at the beginning of the time step,
$c$ is the battery capacity ratio (unitless),
$k$ is the battery rate constant ($h^{-1}$), and
$\Delta_t$ is the length of the time step (h).

The second limitation is based on the maximum charge rate (mcr) specified by the user based on manufacturer specifications. This charge rate has units of A/Ah (amps per amp-hour). HOMER uses this value to derive the corresponding battery charge power using equation 4-3.

$$P_{batt,cmax,mcr} = \frac{(1 - e^{-\alpha_c \Delta t})(Q_{max} - Q)}{\Delta t} \quad \text{4-3}$$

Where

$\alpha_c$ is the battery's maximum charge rate (A/Ah), and
$Q_{max}$ is the total capacity of the battery bank (kWh).

The final limitation imposed on the battery charge power is determined by the maximum charge current (mcc), also specified by the user and given in equation 4-4.

$$P_{batt,cmax,mcc} = \frac{N_{batt} I_{batt} V_{nom}}{1000} \quad \text{4-4}$$

Where

$N_{batt}$ is the number of batteries in the battery bank,
$I_{max}$ is the battery's maximum charge current (Amps), and
$V_{nom}$ is the battery's nominal voltage (Volts).

The minimum of these three limitations is used as the maximum charge and divided by the battery efficiency to exclude the effect of charging losses such that:

$$P_{batt,cmax} = \frac{\min\left(P_{batt,cmax,kbm}, P_{batt,cmax,mcr}, P_{batt,cmax,mcc}\right)}{battery\ charge\ efficiency} \quad \text{4-5}$$

The maximum discharge power is also derived from the kinetic battery model given in equation 4-2. No other limitation is imposed except the assumption that discharging losses occur after the energy leaves the battery bank, such that the maximum discharge power is given by:

$$P_{batt,dmax} = \ batt\ discharge\ efficiency * P_{batt,cmax,kbm} \quad 4\text{-}6$$

The exact battery model used in this study is based on specifications from Aquion Energy for their bulk energy storage systems. Aquion Energy is an America based company specializing in large scale energy storage solutions. This choice is made for a few reasons in addition to those already mentioned for battery storage in general. According to the specifications, these batteries have a very high cycle life, and can be fully discharged unlike lead acid batteries for examples, both parameters used in HOMER simulations. They are also safer with less corrosive and toxic materials. Aquion batteries are already commercialized which means that they are available on the market, and have a low cost. Additionally, they require low maintenance. The complete study on Aquion batteries and the Aqueous Hybrid Ion technology can be found in [73]. Specifications of the battery used can be found in Appendix B.3.

## 4.4 Diesel Generator

Diesel generator technology is based on a diesel engine which has been around for about a century. The other component is the electric generator. In essence, the generator operates by

internal combustion of diesel fuel that is used to run the engine. The mechanical energy from the engine is then converted to electrical energy by means of an electric generator (alternator).

A few aspects in application of diesel generators are important to note. Diesel generators exhibit different fuel efficiency when generating certain amounts of power. Particularly, when operating below a certain fraction of their capacity, their efficiency plummets. For this reason, economic operation of diesel generators ought to apply a lower limit to the generator's operation. This factor is accounted for in the HOMER simulation, and diesel generators are forced to only operate above 40% of their rated capacity.

The cost modeling of the diesel generator in HOMER is expressed as cost per kilowatt. A cost of 500 $/kW is assumed for all generator sizes. Linear fuel consumption is also assumed as long as the generator is operating above the minimum threshold. This means that doubling energy the output requires doubling the fuel input.

## 4.5 : Microgrid Design

The aforementioned technologies form the basis of the microgrid solution. These technologies and all combinations thereof are compared to find the economically optimal composition of the microgrid that can meet the load all year. This optimization is done using the HOMER simulation tool. The problem formulation, design considerations, and results are detailed in this section.

### 4.5.1 Problem Formulation

As noted, the objective here it to design a microgrid that is capable of serving its own load through the year. It was shown in the preceding chapter that disconnection of the airport

microgrid significantly improves security of the system. The disconnection of the microgrid mean that the airport area, which does not have any generation would remain unpowered. What components, and in what quantity are needed to keep this microgrid powered in the most cost effective way? This is the problem addressed in the following sections.

The assumption was made that this area has a similar load curve as the rest of the system. This means that the peak load for this area also occurs at 8pm. The peak load for the airport microgrid is 12.5 megawatts (MW). The daily load curve of Rwanda, peaking at 125 MW was thus scaled down such it peaks at 12.5 MW as shown in Figure 4.6. The objective therefore is to meet this load at all times. The daily load curve for a particular area is usually estimated to be the same for each season, with the only differences usually between weekdays, weekdays, and holidays. It is a safe assumption that seasonal variations do not significantly affect the pattern in Rwanda for two reasons. Rwanda does not experience gross seasonal changes from hot to cold. Seasonal variation is either hot/wet or hot/dry due its location near the equator. Therefore, we can expect that consumption is not greatly affected by seasonal changes. Secondly, the nights and days are close to equal throughout the year and therefore, sunrise and sunset times are roughly the same throughout the year.

HOMER accepts input for the daily load values in hourly increments. This load profile is extrapolated to the whole year. While it was noted that seasonal changes are not extreme near the equator to grossly affect the load curve, slight random variability was added to account for day to day variability, and to make the load more realistic. HOMER allows the user to provide a value for the random variability and this value is used as the standard deviation of a zero mean normal

distribution from which random values are picked to add or subtract from the load of that hour. A conservative value of 2 % was used to account for those small changes.

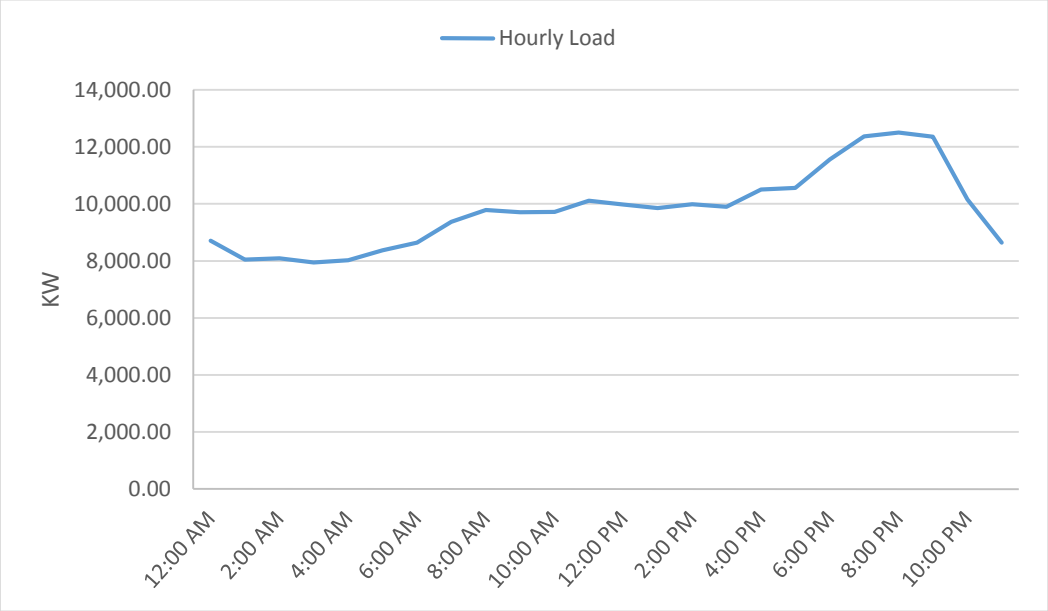


Figure 4.6 Daily Load Profile of Airport Microgrid

Five possible power generation combinations were simulated and compared. These systems were composed of power from either diesel generators alone, diesel with PV, diesel with PV and storage, or PV with storage. PV only or storage only were not considered because they are obviously not feasible. The optimization that compares different technologies to serve the load is visualized in Figure 4.8. Important to note is the particular challenge when considering PV due

to the fact that the peak load occurs at 8pm as shown in the load profile, which is well after sunset. Sunset near the equator occurs at approximately between 6:00-7:00 pm local time. From Figure 4.7, it can be seen that solar energy is completely absent during half of the day, and notably during peak hours.

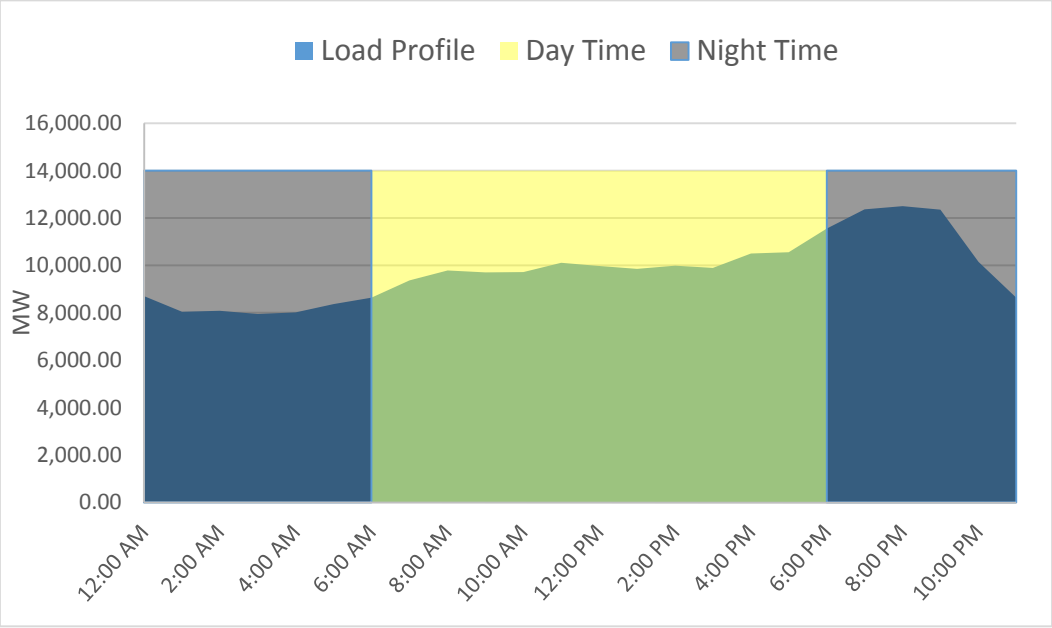


Figure 4.7 Load Profile vs Day and Night

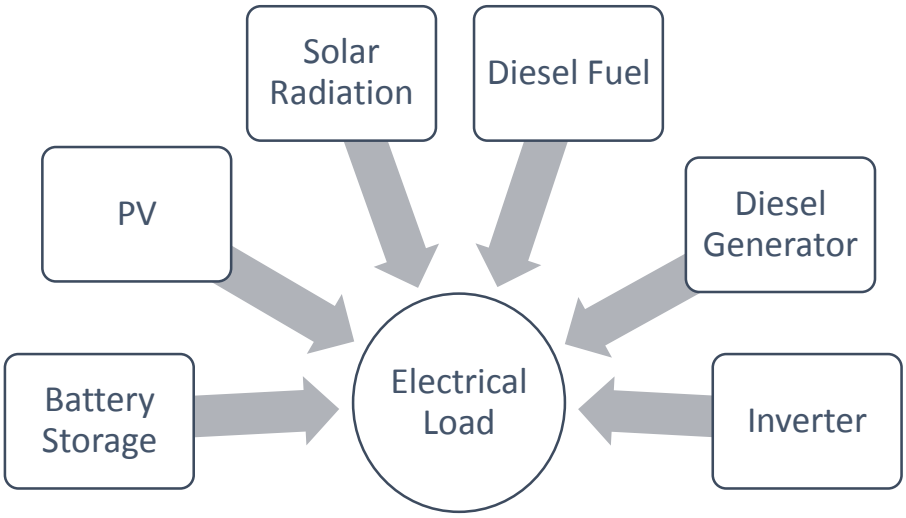


Figure 4.8 Problem Formulation and Optimization Consideration

Additional parameters and constraints are imposed on the system. The project assumes a lifetime of 20 years. Default values are used for interest rate, discount rate, and expected inflation, which are 5.8 percent, 8 percent, and 2 percent respectively. The system was required to operate with a 10 percent reserve of the load at all times and an additional 10 percent reserve if solar power was being used. While is it possible to do so, emission constraints were not imposed.

The 10 percent and 20 percent reserve margins were based on microgrid design experience in previous studies [44, 45, 72]. While traditional power systems insist on the ability of the system to have a margin equal or greater than the largest generator or component, this is not the practice for microgrids in part due to intermittent energy sources such as wind and solar that cannot be

quantified in the same way as dispatchable generation. This issue deserves further studies to obtain metrics for the reserve margins in microgrids.

### 4.5.2 Diesel Only System

The diesel system uses only diesel generators to supply the load. To simulate this system, the daily load curve was added to the model, which was extrapolated to one year, then repeated over the project lifetime of 20 years. Initially, two small diesel generators models were chosen, rated 1.45 MW and the other 545 kW. An array of scaled generator values was provided to HOMER which simulates each combination to find the least cost option that can supply the load subject to all stipulated constraints. The cost of diesel generators which includes the generators, and associated installation costs is obtained from a survey conducted by the Electric Power Research Institute (EPRI) on distributed generators in the range of 1-10 MW owned by utilities [74]. This study reported the average cost to be about 500 $/kW. A 100 kW generator would thus cost $50000. Likewise, operation and maintenance cost were estimated at 0.04 $/hour. As noted before, the additional constraint for diesel generators not run below 40 percent was imposed to

maximize efficiency. Complete specifications for these generators, including sizes considered and fuel consumption can be found in Appendix B.1.

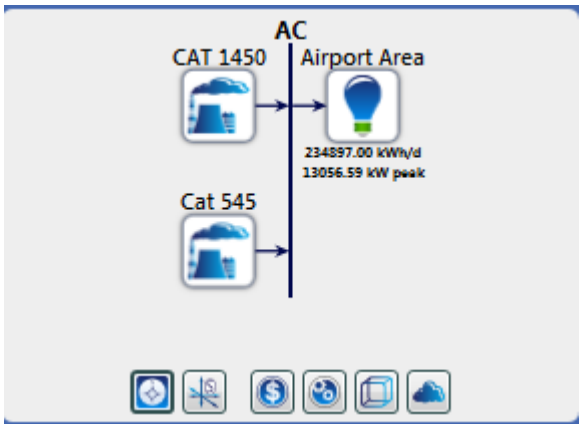


Figure 4.9 Diesel Only System

The cost of diesel in Rwanda averaged 1.4 $/L in 2014 and fluctuated between 1.2 $/L and 1.7 $/L in the last 5 years according to the World Bank [75]. To account for the varying cost of diesel over, a sensitivity analysis was performed to quantify how sensitive this system's cost is to diesel price. The optimal system architecture and associated net present cost and initial capital is shown in Table 4.6.

Table 4.6 Optimal System Design for Diesel Only System (Small Generators)

| Diesel Price ($/L) | CAT 1450 (kW) | Cat 545 (kW) | COE ($) | NPC (Million $) | Operating cost (Million $) | Initial capital ($) |
|---|---|---|---|---|---|---|
| 1.2 | 11600 | 2180 | 0.363 | 360 | 30.5 | 6,890,000 |
| 1.4 | 11600 | 2180 | 0.413 | 411 | 34.9 | 6,890,000 |
| 1.6 | 11600 | 2180 | 0.460 | 461 | 39.2 | 6,890,000 |
| 1.8 | 11600 | 2180 | 0.514 | 511 | 43.6 | 6,890,000 |
| 2.0 | 11600 | 2180 | 0.565 | 562 | 47.9 | 6,890,000 |

A few observations can be made from these results. The system architecture does not change at different diesel costs. Most system are usually dominated by a few system types or

combinations. In this case, one combination is dominant, but it is of interest to know how different combinations would perform against this one. The particular case with diesel at 1.4 $/L is explored further to see how distinct combinations rank. The results are shown in Table 4.7. It was noted that different optimal solutions using different generator combinations does not affect the project cost. For example, having eight of the larger generator and four of the smaller one costs the same as having three of the larger one with eighteen smaller ones[*]. The second observation was that this system is substantially sensitive to changes in diesel price. An increase in diesel price from 1.4 to 1.6 $/L for example increases the net present cost by 50 million US dollars over the projects lifetime, dramatically increasing the cost of electricity.

Table 4.7 Top Ten Least Cost Diesel Only Systems at 1.4 $/L Diesel

| CAT 1450 (KW) | Cat 545 (kW) | COE ($) | NPC ($) | Operating ($) | Initial ($) |
|---|---|---|---|---|---|
| 11600 | 2180 | 0.414 | 410,718,300 | 34,872,080 | 6,890,000 |
| 2900 | 10900 | 0.414 | 411,151,400 | 34,908,620 | 6,900,000 |
| 11600 | 2725 | 0.414 | 411,445,500 | 34,911,350 | 7,162,500 |
| 11600 | 3270 | 0.415 | 412,172,200 | 34,950,570 | 7,435,000 |
| 11600 | 3815 | 0.416 | 412,899,100 | 34,989,810 | 7,707,500 |
| 11600 | 4360 | 0.417 | 413,626,900 | 35,029,120 | 7,980,000 |
| 10150 | 3815 | 0.417 | 413,809,400 | 35,131,020 | 6,982,500 |
| 4350 | 9810 | 0.417 | 414,115,800 | 35,149,060 | 7,080,000 |
| 11600 | 4905 | 0.417 | 414,354,400 | 35,068,420 | 8,252,500 |
| 4350 | 10900 | 0.418 | 414,677,200 | 35,150,480 | 7,625,000 |

It is possible that many smaller generators might be preferred to few large ones for reasons ranging from reliability to maintenance scheduling. Another comparison is made optimizing between the above generators and a much larger one rated for 4.7 MW. The

[*] Economies of scale were not modelled for diesel generators due to lack of consistent data

procedure is similar to the one in the previous step. The optimal systems in this case are shown in Table 4.8. Similar conclusions are reached as in the previous case. The price of diesel significantly affects the cost of this system. Likewise, having a different combination of generator sizes does not affect the overall system cost.

Table 4.8 Optimal System Design for Diesel Only Systems (Small and Large Generators)

| Diesel ($/L) | CAT 1450 (kW) | CAT 545 (kW) | CAT 4700 (kW) | COE | NPC ($) | Operating ($) | Initial capital ($) |
|---|---|---|---|---|---|---|---|
| 1.2 | 2900 | 1635 | 9400 | 0.358 | 355,797,500 | 30,122,770 | 6,967,500 |
| 1.4 | 2900 | 1635 | 9400 | 0.409 | 406,020,800 | 34,459,750 | 6,967,500 |
| 1.6 | 2900 | 1635 | 9400 | 0.460 | 456,244,200 | 38,796,720 | 6,967,500 |
| 1.8 | 2900 | 1635 | 9400 | 0.510 | 506,467,600 | 43,133,700 | 6,967,500 |
| 2.0 | 2900 | 1635 | 9400 | 0.561 | 556,690,900 | 47,470,670 | 6,967,500 |

### 4.5.3 Diesel and PV System

The second design considered included diesel and solar PV. In this design similar diesel generators as in the previous case were used. Differently sized PV arrays were added to the system along with different inverter sizes to convert the direct power (DC) power generated by the PV to alternating current (AC) power that is used by the load. The cost of PV was obtained from a U.S. DOE study conducted through NREL and the Lawrence Berkeley National Laboratory (LBNL) which report an average of $3000/kW with a decreasing trend [57]. PV installations benefit greatly from economies of scale and as such, instead of a single value for PV cost that is extrapolated linearly, a cost curve was specified to account for the fact that the cost per kilowatt of a larger PV array costs significantly less than a smaller one as was reported in the

aforementioned report. The cost curve is shown in Table 4.9. The specifications for these components can be found in Appendix B.2.

Table 4.9 PV Cost Curve

| Capacity (kW) | Capital |
|---|---|
| 1 | $3,000 |
| 50 | $145,000 |
| 500 | $1,350,000 |
| 5000 | $9,750,000 |

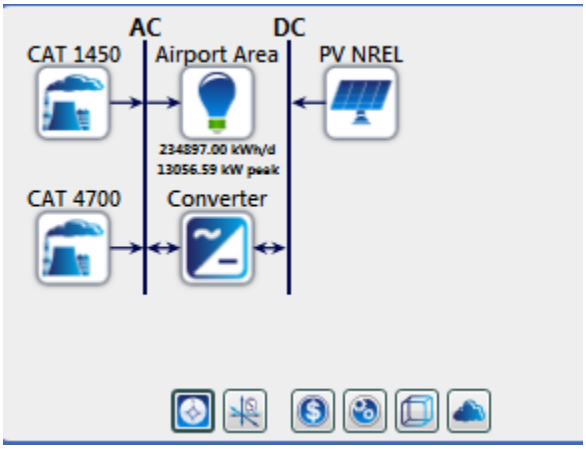


Figure 4.10 Diesel and PV System

The simulation of the diesel and PV system showed in large part a preference for PV as shown in Table 4.10 which shows the optimal system architecture given different diesel prices. The net present cost (NPC) for this design exhibits a slightly lower cost that using diesel alone. This can be attributed to the high cost of diesel in Rwanda which is the biggest cost driver. While

the initial capital investment will be higher due to PV, over the long term, the cost of electricity will be lower due to a reduced operating cost.

Table 4.10 Optimal System Design for Diesel and PV System

| Die $/L | PV (kW) | CAT 1450 (kW) | CAT 4700 (kW) | Converter (kW) | COE ($) | NPC ($) | Operating cost ($) | Initial capital ($) |
|---|---|---|---|---|---|---|---|---|
| 1.2 | 8000 | 4350 | 9400 | 5400 | 0.339 | 336,224,500 | 26,791,210 | 25,975,000 |
| 1.4 | 8000 | 4350 | 9400 | 5500 | 0.382 | 379,519,400 | 30,521,240 | 26,075,000 |
| 1.6 | 8000 | 4350 | 9400 | 5600 | 0.426 | 422,791,400 | 34,249,310 | 26,175,000 |
| 1.8 | 8000 | 4350 | 9400 | 5600 | 0.469 | 466,046,400 | 37,984,540 | 26,175,000 |
| 2.0 | 8000 | 4350 | 9400 | 5600 | 0.513 | 509,301,500 | 41,719,780 | 26,175,000 |

Once again this solution is dominated by one architecture and there is a need to know how varying the architecture would influence the cost. The cost of diesel was fixed at 1.4 $/L and the top ten designs are compared as shown in Table 4.11. What is evident is that the system architecture is mostly unchanging because PV cannot replace diesel capacity because solar energy is only available in the day time, and importantly absent at peak load. Therefore, any feasible design will necessarily require enough diesel generator capacity to meet the peak load. All the energy generated by the PV is not useful towards peak loading at 8:00pm. One way to possibly improve this is to use energy storage such that energy generated by the PV can be stored

to be used later when it is most needed such as at peak loading. This idea is tested in the following section.

Table 4.11 Top Ten Least Cost Diesel & PV System Designs at 1.4 $/L Diesel

| PV (kW) | CAT 1450 (kW) | CAT 4700 (kW) | Converter (kW) | COE () | NPC ($) | Operating cost ($) | Initial capital ($) |
|---|---|---|---|---|---|---|---|
| 8000 | 4350 | 9400 | 5500 | 0.382 | 380,000,000 | 30,500,000 | 26,100,000 |
| 8000 | 4350 | 9400 | 5600 | 0.382 | 380,000,000 | 30,500,000 | 26,200,000 |
| 8000 | 4350 | 9400 | 5200 | 0.382 | 380,000,000 | 30,600,000 | 25,800,000 |
| 8000 | 4350 | 9400 | 5800 | 0.382 | 380,000,000 | 30,500,000 | 26,400,000 |
| 8000 | 4350 | 9400 | 5000 | 0.383 | 380,000,000 | 30,600,000 | 25,600,000 |
| 8000 | 4350 | 9400 | 6200 | 0.383 | 380,000,000 | 30,500,000 | 26,800,000 |
| 8000 | 4350 | 9400 | 6400 | 0.383 | 380,000,000 | 30,500,000 | 27,000,000 |
| 8000 | 5800 | 9400 | 5500 | 0.386 | 383,000,000 | 30,800,000 | 26,600,000 |
| 8000 | 5800 | 9400 | 5400 | 0.386 | 383,000,000 | 30,800,000 | 26,500,000 |
| 8000 | 5800 | 9400 | 5600 | 0.386 | 383,000,000 | 30,800,000 | 26,700,000 |

### 4.5.4 Diesel with PV and Storage

Energy storage is added to the above setup in an attempt to lower the overall system cost, and possibly displace some diesel capacity. The system setup can be seen in Figure 4.12. Simulation results indicated that using energy storage displaced 1.5MW of diesel generation, but the cost benefit was replaced in equal measure and the net present cost remained largely unchanged as seen in Table 4.12. Addition energy storage reduced the net present cost of the system by about three million US dollars over the project lifetime, which in this context is likely within the margins of error. These results suggest little economic justification for the use of energy storage to replace diesel if diesel is still used. A categorized list showing distinct design combinations at a fixed cost of 1.4 $/L is shown in Table 4.13. From Table 4.13, it is evident that designs which incorporate energy storage marginally improve the economic outlook. However,

there are other benefits in the form of emission control and reduction of dependence on imported fuel. A more comprehensive study of the storage with PV is conducted is detailed in the following section.

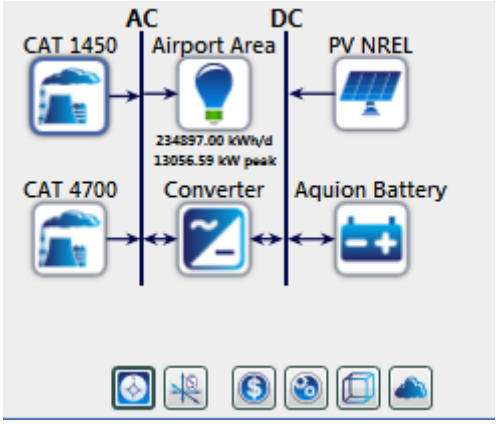


Figure 4.11 Diesel, PV, and Storage System

Table 4.12 Optimal System Design for Diesel, PV, & Storage Systems

| Diesel ($/L) | PV (kW) | CAT 1450 (kW) | CAT 4700 (kW) | Battery 200kW 400kWh | Converter (kW) | COE ($) | NPC (Million $) | Operating (Million $) | Initial Capital (Mil $) |
|---|---|---|---|---|---|---|---|---|---|
| 1.2 | 8000 | 2900 | 9400 | 6 | 5500 | 0.34 | 334 | 26.4 | 28.5 |
| 1.4 | 8000 | 2900 | 9400 | 6 | 5500 | 0.38 | 377 | 30.1 | 28.5 |
| 1.6 | 8000 | 2900 | 9400 | 6 | 5500 | 0.42 | 420 | 33.8 | 28.5 |
| 1.8 | 8000 | 2900 | 9400 | 6 | 5500 | 0.47 | 464 | 37.6 | 28.5 |
| 2.0 | 8000 | 2900 | 9400 | 6 | 5800 | 0.51 | 507 | 41.3 | 28.8 |

Table 4.13 Categorized System Designs of Diesel with PV & Storage at 1.4 $/L Diesel

| PV NREL (kW) | CAT 1450 (kW) | CAT 4700 (kW) | Battery 200 kW 400 kWh | Converter (kW) | COE ($) | NPC ($) | Operating Cost ($) | Initial Capital ($) |
|---|---|---|---|---|---|---|---|---|
| 8000 | 2900 | 9400 | 6 | 5500 | 0.380 | 377,149,200 | 30,107,160 | 28,500,000 |
| 8000 | 4350 | 9400 | 0 | 5500 | 0.384 | 381,195,200 | 30,523,470 | 27,725,000 |
| 8000 | 0 | 14100 | 0 | 5500 | 0.398 | 395,117,600 | 31,710,610 | 27,900,000 |
| 8000 | 0 | 14100 | 1 | 5500 | 0.398 | 395,145,300 | 31,691,420 | 28,150,000 |
| 0 | 2900 | 9400 | 8 | 4500 | 0.415 | 412,375,200 | 34,517,760 | 12,650,000 |
| 0 | 4350 | 9400 | 0 | 0 | 0.416 | 412,906,800 | 35,062,370 | 6,875,000 |

### 4.5.5 PV and Storage

The last design only uses renewable energy in the form of solar PV, with storage to store energy during the day and discharge during the night. It was expected that this design would require a lot more PV and storage for two reasons. One is that enough power must be generated during the day to both supply the day enough and charge the batteries enough to such that they can supply the load throughout the night. The second is that a lot of energy storage would be required to store the energy to supply all the load for approximately 12 hours including peak load at 8pm. On the other hand, while a lot of power is required to supply peak load, the total amount

of energy needed is helped by the fact that the load is significantly lower throughout the rest of the night.

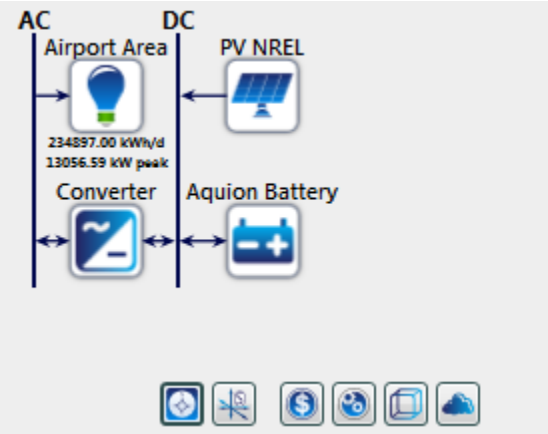


Figure 4.12 PV and Storage Setup

The system was setup in HOMER with only PV and storage, with components whose details can be found in 0. It was noted that the initial capital investment for this type of system is several times higher than all previous systems considered. On the other hand, the operating cost for this system is many times smaller than those that include diesel generation. The total effect of

these variations however is a significantly lower system cost over the project lifetime. The 10 most economic sizing options for this system can be found in Table 4.14.

Table 4.14 Optimal System Designs for PV and Storage System

| PV NREL (kW) | Battery 200 kW 1600 kWh | Converter (kW) | COE ($) | NPC ($) | Operating cost ($) | Initial capital ($) |
|---|---|---|---|---|---|---|
| 72500 | 182 | 14000 | 0.262 | 257,548,500 | 507,634 | 251,670,000 |
| 72500 | 182 | 14000 | 0.262 | 257,548,500 | 507,634 | 251,670,000 |
| 72500 | 182 | 14200 | 0.262 | 257,906,700 | 521,288 | 251,870,000 |
| 72500 | 182 | 14200 | 0.262 | 257,906,700 | 521,288 | 251,870,000 |
| 72100 | 184 | 14000 | 0.262 | 257,952,100 | 510,246 | 252,043,300 |
| 72100 | 184 | 14000 | 0.262 | 257,952,100 | 510,246 | 252,043,300 |
| 72300 | 184 | 13800 | 0.262 | 257,952,800 | 495,332 | 252,216,700 |
| 72300 | 184 | 13800 | 0.262 | 257,952,800 | 495,332 | 252,216,700 |
| 72500 | 182 | 14400 | 0.263 | 258,264,800 | 534,946 | 252,070,000 |
| 72500 | 182 | 14400 | 0.263 | 258,264,800 | 534,946 | 252,070,000 |

Notably, there is a significant reduction in net present cost when diesel is eliminated from the system. The results indicated shown a reduction on the order of over 20 percent in net present cost when compared to other designs. The optimal PV and storage consists of 182 batteries, 72.5 MW of solar PV, a bi-directional converter rated for 14 MW.

### 4.5.6 Comparison of System Architectures

With the results of the different possible system architectures, a cost comparison is done in this section. Diesel has been noted to be one of the major cost drivers and for this reason, the systems are compared at two different prices to ascertain whether the cost of diesel impacts the optimal system architecture. Table 4.15 shows a comparison in net present cost, capital cost,

initial cost, and the cost of electricity for the optimal design in each class with the cost of diesel at 1.2 $/L. Table 4.16 shows the same comparison with the price of diesel at 1.4 $/L.

Table 4.15 Comparison of Optimal Designs (Diesel at 1.2 $/L)

| Case | COE ($/kWh) | NPC ($) | Operating Cost ($) | Initial Capital ($) |
|---|---|---|---|---|
| Diesel Only (1) | 0.363 | 360,451,500 | 30,531,350 | 6,890,000 |
| Diesel Only (2) | 0.358 | 355,797,500 | 30,122,770 | 6,967,500 |
| Diesel and PV | 0.339 | 336,224,500 | 26,791,210 | 25,975,000 |
| Diesel, PV, and Storage | 0.340 | 333,920,600 | 26,374,210 | 28,500,000 |
| PV and Storage | 0.262 | 257,548,500 | 507,634 | $272,390,000 |

Table 4.16 Comparison of Optimal Designs (Diesel at 1.4 $/L)

| Case | COE ($/kWh) | NPC ($) | Operating Cost ($) | Initial Capital ($) |
|---|---|---|---|---|
| Diesel Only (1) | 0.413 | 410,718,300 | 34,872,080 | 6,890,000 |
| Diesel Only (2) | 0.409 | 406,020,800 | 34,459,750 | 6,967,500 |
| Diesel and PV | 0.382 | 379,519,400 | 30,521,240 | 26,075,000 |
| Diesel, PV, and Storage | 0.382 | 379,519,400 | 30,521,240 | 26,075,000 |
| PV and Storage | 0.262 | 257,548,500 | 507,634 | $272,390,000 |

These results suggest that from an economic point of view, a system of solar PV and storage results in the lowest levelized lowest cost of electricity. As expressed before, this system comes at a very high initial cost which might not be suitable for many economies or investors. At about 262 million US dollars, the investment is very pricy. However, this system has some unique benefits. It is a fully independent solution, which for Rwanda is particularly important because it is a landlocked country. Since there is no need for diesel fuel which must be imported and transported through neighboring countries, this system is not only immune to fluctuation in diesel prices, but also operates irrespective of political tension that might exist with neighboring countries. Additionally, once this system is in place, its cost of operation is relatively negligible.

It can almost be guaranteed that the Kigali area will receive power at all times regardless of the situation outside the microgrid.

The second most economical choice is diesel with PV and storage. The storage in this design makes the overall only marginally cheaper than in the design without storage. This system however utilizes better the benefits of solar energy and displaces some of the diesel generation. In some respects, this is a safe choice in that the initial investment is not overwhelming, but considering that PV and storage is 100 million US dollars cheaper, it is the most economical in the long term.

The diesel only design which has the lowest startup cost is the most expensive. This is not all that surprising owing to the very high cost of diesel in Rwanda. For comparison, diesel in Rwanda cost at least twice as much as it does in the United States. Using diesel as a primary source for electricity is therefore not recommended in Rwanda on more than one account, that is, it is the most expensive and also has to be imported across multiple countries due to Rwanda's landlocked disposition.

### 4.5.7 Sensitivity of Storage and PV System

Ever though the cost of the different components were based on previous comprehensive studies, several assumptions were made particularly when applying these costs to Rwanda. Furthermore, certain variables used in this simulation are likely to fluctuate over the years, which is beyond the control of the designer. For example, the solar radiation cannot be expected to

remain constant year after year. For this reason, a sensitivity analysis was performed to establish a range of values that more realistically represent the cost of this system.

First a sensitivity on the average annual solar radiation is simulated. The data obtained averaged 5.47 kWh/$m^2$/day. To establish how the variation in radiation over the years affect the total system cost, a range of values from 5 kWh/$m^2$/day to 5.6 kWh/$m^2$/day is simulated and the results are shown in Table 4.17. It is noted that the levelized cost of electricity varies from $0.258 to $0.274 with the change in solar radiation, representing a 15 million USD increase in total cost over the lifetime of the project. Nonetheless, even with lower solar radiation, this system still has a lower net present cost than the others that use diesel as part of their energy generation.

Table 4.17 Sensitivity of PV and Storage System to Solar Irradiation

| Solar (kWh/ m²/day) | PV NREL (kW) | Battery 200 kW/ 1600kWh | Converter (kW) | COE ($) | NPC ($) | Operating ($) | Initial ($) |
|---|---|---|---|---|---|---|---|
| 5.0 | 80000 | 180 | 14000 | 0.274 | 269,882,100 | 460,448 | 264,550,000 |
| 5.2 | 80000 | 176 | 13600 | 0.271 | 266,923,500 | 432,932 | 261,910,000 |
| 5.4 | 72500 | 182 | 14000 | 0.262 | 257,548,500 | 507,634 | 251,670,000 |
| 5.6 | 72300 | 176 | 14000 | 0.258 | 253,826,300 | 508,590 | 247,936,700 |

Another sensitivity was performed on the cost of solar PV modules. Even though trends indicate a decrease in PV prices, it is possible that these prices could stagnate or increase for unpredictable reasons. It is also possible that the estimates used vary slightly from region to region, and for this reason, we test the system against this variability. To do so, the price of solar PV modules was increased and decreased by 10 percent and 20 percent. Results showed that a change in the cost of PV modules considerably affected the net present cost of the system as shown in Figure 4.13. For example, a 10 percent increase in PV cost resulted in a 5 percent

increase in overall system cost. This is due to the fact that in the PV and storage system, PV modules account for the highest percentage of system cost. Battery costs were also varied in a similar way, and while they affect the overall system cost, they do so to a smaller extent in comparison to PV modules as shown in Figure 4.13.

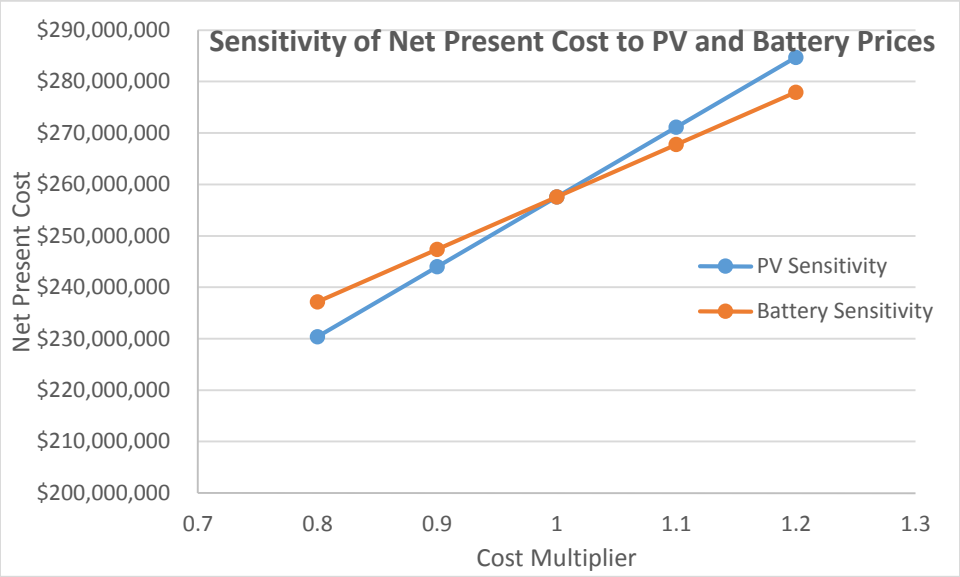


Figure 4.13 Sensitivity of Net Present Cost to PV and Battery Prices

Another interesting fact to note about the PV and storage system is that it not only has the lowest NPC, but is also slightly overdesigned to account for the days in the year when the day is mostly cloudy. As an example, between April 12$^{th}$ and 14$^{th}$, solar radiation is high and over the three days, the battery bank is only discharged to a minimum of 50 percent as shown in Figure 4.14. However, these batteries are designed to be able to fully discharge, such that this might appear to be a waste. In contrast, from March 31$^{st}$ to April 3$^{rd}$, the batteries are discharged to just over 20 percent as shown in Figure 4.15. This explains why the requirements for both PV and storage are quite high and necessary, so as to ensure that the microgrid load can be served even on the cloudiest days. Additionally, the design ensures that the system can maintain this islanded

operation for any extended period. In case an outage on the main transmission line occurred and was not repaired for a long period, this system would allow Kigali to remain powered.

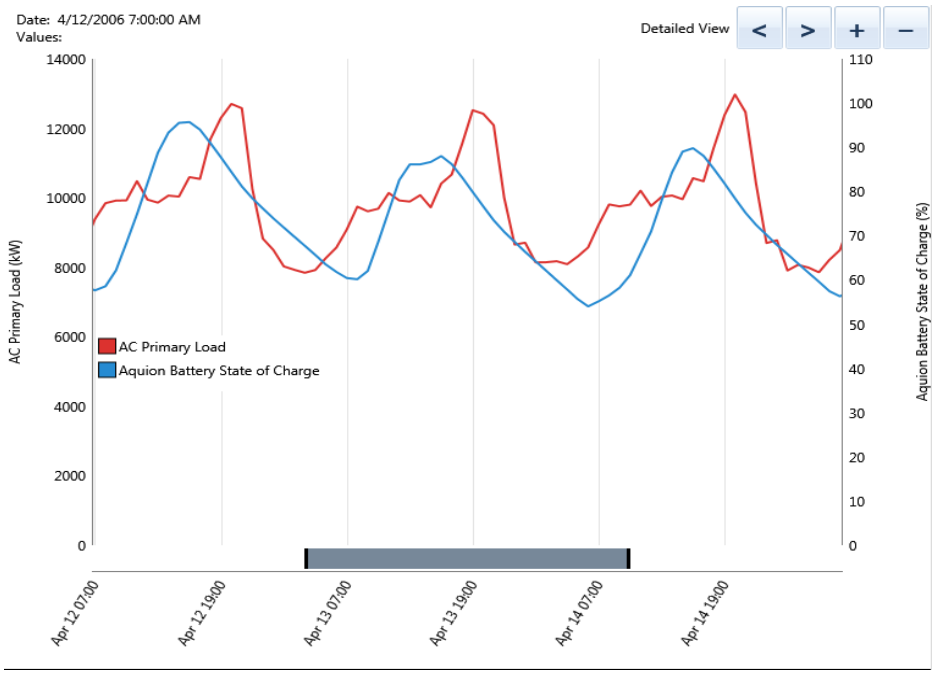


Figure 4.14 Load vs Battery Energy Content April 12th – April 14th

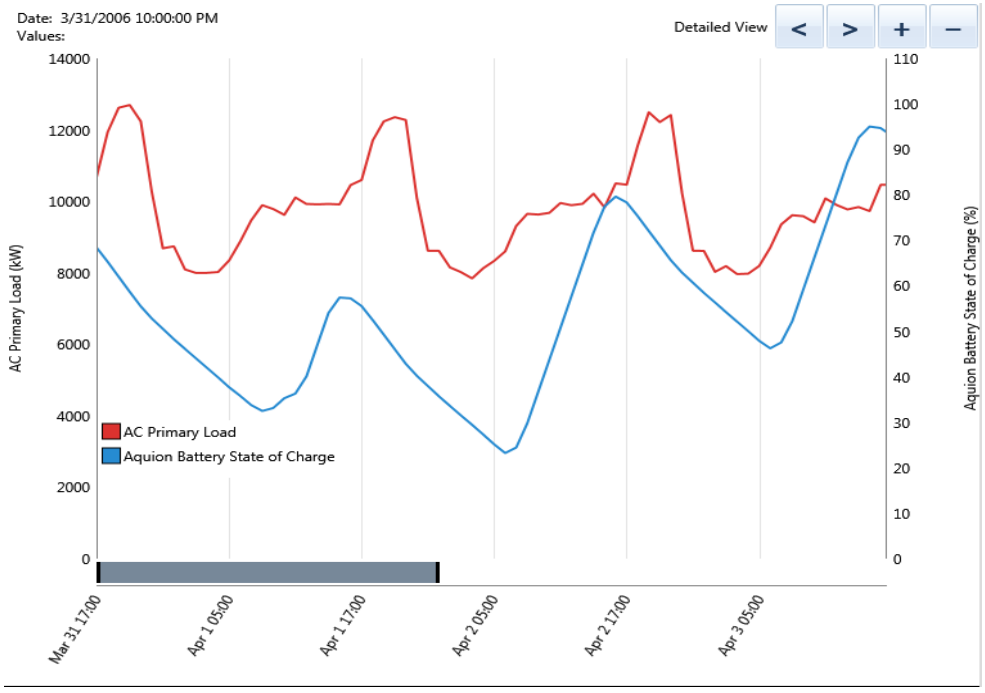


Figure 4.15 Load vs Battery Energy Content March 31st – April 3rd

### 4.5.8 Microgrid Land Requirements

The microgrid with PV and storage has significant land requirements, although they are much smaller than those that would be required for new transmission lines. Additionally, right-of-way requirements are relatively insignificant in comparison to those of new transmission lines. While the battery storage is compact and can be housed in a singular building, the PV land requirements are substantial. It was estimated that the amount of solar PV required 72 megawatts (MW). To approximate the area required for this size installation, data from a previous project in Rwanda were extrapolated. This solar project was recently completed adding 8.5 MW to Eastern Province of Rwanda.

In their feasibility study, Gigawatt Global, a multinational renewable energy company, indicated that the initially planned 10 MW of PV panels would fit on 15.8 hectares (158,000 square meters). Assuming a linear increase in land requirements, 72 MW worth of PV modules would fit on 135 hectares (1.35 square kilometers). This is a substantial land requirement that would be nearly impossible to find in one contiguous piece. Instead of using a single piece of land, areas neighboring each other in the vicinity of the airport were considered. Analysis of the area near the airport area by means of satellite imagery and geographic information system application QGIS, showed that a considerable amount of land is unoccupied and unreserved per the Kigali Master Plan of 2013 [76]. Figure 4.16 is an aerial image with possible candidate areas. Naturally, many factors go into land acquisition which are beyond the capability of the author. This image only serves to show the surrounding areas of the airport. By all standards, it is a

guess at best. The area covered by the different segments, and their proximity to the airport is shown in Table 4.18.

Table 4.18 Area Sizes and Proximity to Airport

| Label | Size ($km^2$) | Distance to Airport (km) |
|---|---|---|
| A | 0.576 | 2.2 |
| B | 0.493 | 1.4 |
| C | 1.08 | 1.3 |
| D | 1.09 | 1.3 |
| E | 3.92 | 5.0 |
| Total | 7.159 | |

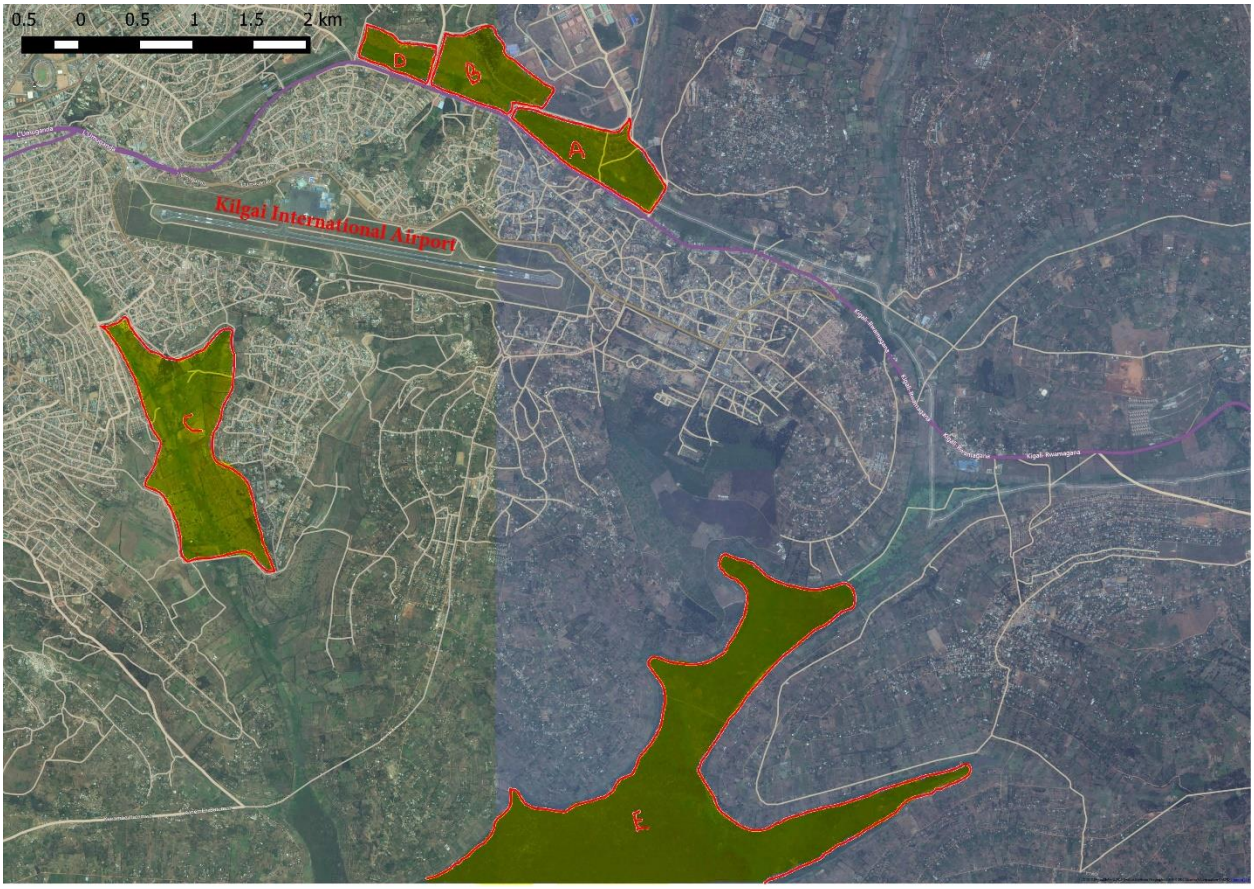


Figure 4.16 “Unoccupied” Land near Kigali International Airport

# Chapter 5 : Conclusions and Future Work

The main goal of this work was to show that a microgrid in Kigali can help mitigate blackouts affecting Kigali. This goal was achieved by simulating a microgrid in the area surrounding the Kigali International Airport with a peak load of 12.5 MW and was shown to alleviate the main causes of blackouts. It was also shown that solar PV and battery storage was not only capable of supplying the energy needs for this area, such a system would have least levelized cost of electricity (LCOE).

This work was performed in two stages, the first stage being a technical examination of the impact of microgrids on mitigating blackout of Kigali during the worst contingencies. The second stage was focused on the economic implications of deploying such a microgrid. In the first stage, it was shown that using a microgrid in Kigali that can disconnect from the rest of the system mitigated most of the issues related to low voltages and overloading in the transmission system. Unsafe low voltages and line overloads are prime candidates in causing system instability and subsequent blackouts. Deploying a microgrid in Kigali was shown to not only protect Kigali, but to also bring the system as a whole back to an operating point within safe limits during the worst contingencies.

The microgrid chosen was located in the neighborhood of the Kigali International Airport, the largest and only international airport in Rwanda. While Kigali peaks at 47 MW, it was shown that a single smaller microgrid covering the peak of 12.5 MW around the airport was capable of minimizing blackouts in Kigali. In addition to the fact that this location was beneficial

for the electric grid's security, it also provides independent power for the airport which was deemed important on grounds of national security.

The second objective of this study was to estimate the cost and feasibility of such a microgrid. While the aim was to provide power to the microgrid by use of solar PV and energy storage, a comparison with generation from diesel was also conducted. Combinations of Diesel generators, solar PV, and energy storage were simulated and optimized to obtain a system that could meet the entire load at all times. Simulations for a twenty-year project indicated that that solar PV and energy storage is the least-cost design with a levelized cost of electricity between $0.258/kWh and $0.274/kWh. Current electricity prices in Rwanda stand around $0.226/kWh according to the African Development Bank [28]. The necessity of energy storage to meet Rwanda's peak load which occurs after dark at 8pm was shown, particularly if solar PV is to be used. Solar PV was indeed shown to be good choice for generation because it is both cheaper and beneficial towards energy independence, in addition to being one of the few resources available within Rwanda. In a sense, this solution simultaneously addresses energy shortage, energy independence, while preventing blackout in Kigali.

The main contribution of this work is first and foremost a microgrid approach that uses solar PV and advanced energy storage to mitigate blackout of Kigali. The use of microgrids and PV with storage has not been considered as a solution in Rwanda. In the course of this work, it was also noted that using a microgrid also alleviates conditions that lead to blackouts across the system as well. The idea that microgrids can be used to secure power within and outside the microgrid electrical boundaries has not received much attention.

This work also provides a sustainable, energy independent strategy for Rwanda. As a landlocked country with meagre energy resources, Rwanda ought to consider the ramifications of

depending on neighboring countries to serve its energy needs. A significant amount of power is generated from diesel fuel which has to be ported and transported through different countries before it makes it to Rwanda, and for this reason, Rwanda is at the mercy of its neighbors in this regard. This work proposes a solution that uses solar power as the primary energy source, which is abundant in Rwanda increasing the countries energy independence.

Finally, this work provides a basis and framework for the evaluation of this solution not only in Kigali, but also in other parts of the country. Subsequent studies can use this work as a reference for various details relevant to the power system needs of Rwanda, as well as data and modeling options. This approach can be tested across the country and well as similar grids in the region to ascertain technical and economic benefits, providing another option for developing electric grids to strengthen their grids.

Future work on this subject is necessary as this is only a preliminary study. Of interest would be the characterization of the impact of large amounts of intermittent energy sources on the rest of the grid. While storage lessens some concerns of energy fluctuations, a more detailed analysis would be required to properly characterize the systems behavior. This area of research is highly active, and some of the major impediments are known, but must be studied on a case by case basis as each electric grid or location provides a unique set of problems.

Additionally, the interaction with the grid in smaller time steps accounting for dynamics of generation, loads, and other components in the power grid is necessary for such an endeavor. This study only focused on steady state analysis, but in fact, dynamic analysis must be conducted on this system to observe the frequency behavior of such a system. This is especially important

in a system that has low system inertia which is usually provided by large synchronous generators.

Finally, care has to be given to designing the reserve margins for microgrids. This study used 10% for dispatchable generation and 20% for solar, but more proven criteria ought to be studied to find optimal reserve margin that balances cost and reliability.

# References


[1] M. Shahidehpour, W. F. Tinney, and F. Yong, "Impact of Security on Power Systems Operation," *Proceedings of the IEEE,* vol. 93, pp. 2013-2025, 2005.

[2] US-Canada Power System Outage Task Force, S. Abraham, H. Dhaliwal, R. J. Efford, L. J. Keen, A. McLellan, *et al.*, *Final report on the August 14, 2003 blackout in the United states and Canada: causes and recommendations*: US-Canada Power System Outage Task Force, 2004.

[3] Federal Energy Regulatory Commission, "The Potential Benefits of Distributed Generation and Rate-Related Issues That May Impede Their Expansion: A study pursuant to Section 1817 of the Energy Policy Act of 2005," *Washington, DC: US Department of Energy,* 2007.

[4] World Bank Group, "Enterprise Surveys: Rwanda," ed, 2012.

[5] R. Lasseter, "Microgrids and Distributed Generation," *Journal of Energy Engineering,* vol. 133, pp. 144-149, 2007/09/01 2007.

[6] J. W. Rosen, "Lake Kivu's Great Gas Gamble," *TECHNOLOGY REVIEW,* vol. 118, pp. 34-46, 2015.

[7] I. Dobson, B. A. Carreras, V. E. Lynch, and D. E. Newman, "Complex systems analysis of series of blackouts: Cascading failure, critical points, and self-organization," *Chaos,* vol. 17, p. 026103, 2007.

[8] G. Andersson, P. Donalek, R. Farmer, N. Hatziargyriou, I. Kamwa, P. Kundur, *et al.*, "Causes of the 2003 major grid blackouts in North America and Europe, and

recommended means to improve system dynamic performance," *Power Systems, IEEE Transactions on,* vol. 20, pp. 1922-1928, 2005.
[9] S. M. Brahma and A. A. Girgis, "Development of adaptive protection scheme for distribution systems with high penetration of distributed generation," *Power Delivery, IEEE Transactions on,* vol. 19, pp. 56-63, 2004.
[10] World Bank, "Rwanda - Urgent Electricity Rehabilitation Project," Washington, DC 2011.
[11] G. Pepermans, J. Driesen, D. Haeseldonckx, R. Belmans, and W. D'haeseleer, "Distributed generation: definition, benefits and issues," *Energy Policy,* vol. 33, pp. 787-798, 4// 2005.
[12] "Technical Analysis of the August 14, 2003, Blackout: What Happened, Why, and What Did We Learn? ," North American Electric Reliability Council, Princeton, New Jersey, 2004.
[13] F. Katiraei and M. R. Iravani, "Power Management Strategies for a Microgrid With Multiple Distributed Generation Units," *Power Systems, IEEE Transactions on,* vol. 21, pp. 1821-1831, 2006.
[14] T. Ackermann, G. Andersson, and L. Söder, "Distributed generation: a definition1," *Electric Power Systems Research,* vol. 57, pp. 195-204, 4/20/ 2001.
[15] R. Lasseter, A. Akhil, C. Marnay, J. Stephens, J. Dagle, R. Guttromson, *et al.*, "Integration of distributed energy resources. The CERTS Microgrid Concept," ed, 2002.
[16] *MICROGRIDS Project*. Available: http://www.microgrids.eu/micro2000/index.php?page=index
[17] P. P. Barker and R. W. de Mello, "Determining the impact of distributed generation on power systems. I. Radial distribution systems," in *Power Engineering Society Summer Meeting, 2000. IEEE*, 2000, pp. 1645-1656 vol. 3.
[18] D. Sharma and R. Bartels, "Distributed Electricity Generation in Competitive Energy Markets: A Case Study in Australia," *The Energy Journal,* vol. 18, pp. 17-39, 1997.
[19] Rwanda Utilities Regulatory Authority, ed, 2015.
[20] N. Hatziargyriou, N. Jenkins, G. Strbac, J. P. Lopes, J. Ruela, A. Engler, *et al.*, "Microgrids–large scale integration of microgeneration to low voltage grids," *CIGRE C6-309*, 2006.
[21] D. Georgakis, S. Papathanassiou, N. Hatziargyriou, A. Engler, and C. Hardt, "Operation of a prototype microgrid system based on micro-sources quipped with fast-acting power electronics interfaces," in *Power Electronics Specialists Conference, 2004. PESC 04. 2004 IEEE 35th Annual*, 2004, pp. 2521-2526 Vol.4.
[22] N. Hatziargyriou, H. Asano, R. Iravani, and C. Marnay, "Microgrids," *Power and Energy Magazine, IEEE,* vol. 5, pp. 78-94, 2007.
[23] S. Van Broekhoven, N. Judson, S. Nguyen, and W. Ross, "Microgrid study: energy security for DoD installations," DTIC Document2012.
[24] A. Yadoo, A. Gormally, and H. Cruickshank, "Low-carbon off-grid electrification for rural areas in the United Kingdom: Lessons from the developing world," *Energy Policy,* vol. 39, pp. 6400-6407, 10// 2011.
[25] S. M. Shaahid and I. El-Amin, "Techno-economic evaluation of off-grid hybrid photovoltaic–diesel–battery power systems for rural electrification in Saudi Arabia—A

way forward for sustainable development," *Renewable and Sustainable Energy Reviews,* vol. 13, pp. 625-633, 4// 2009.
[26] O. Hafez and K. Bhattacharya, "Optimal planning and design of a renewable energy based supply system for microgrids," *Renewable Energy,* vol. 45, pp. 7-15, 9// 2012.
[27] M. Manfren, P. Caputo, and G. Costa, "Paradigm shift in urban energy systems through distributed generation: Methods and models," *Applied Energy,* vol. 88, pp. 1032-1048, 4// 2011.
[28] African Development Bank, "Energy Sector Review and Action Plan - Rwanda," 2013.
[29] SNC Lavalin International Inc. and Parsons Brinckerhoff, "Regional Power System Master Plan and Grid Code Study," Eastern Africa Power Pool and East African Community2011.
[30] B. Safari, "A review of energy in Rwanda," *Renewable and Sustainable Energy Reviews,* vol. 14, pp. 524-529, 2010.
[31] J. Taft and A. Becker-Dippmann, "Grid Architecture," Pacific Northwest National Laboratory2015.
[32] V. Rosato, S. Bologna, and F. Tiriticco, "Topological properties of high-voltage electrical transmission networks," *Electric Power Systems Research,* vol. 77, pp. 99-105, 2// 2007.
[33] E. Cotilla-Sanchez, P. D. Hines, C. Barrows, and S. Blumsack, "Comparing the topological and electrical structure of the North American electric power infrastructure," *Systems Journal, IEEE,* vol. 6, pp. 616-626, 2012.
[34] Merriam-Webster.com, in *Merriam-Webster,* ed, 2015.
[35] O. Alsac and B. Stott, "Optimal Load Flow with Steady-State Security," *Power Apparatus and Systems, IEEE Transactions on,* vol. PAS-93, pp. 745-751, 1974.
[36] T. J. Ypma, "Historical Development of the Newton–Raphson Method," *SIAM Review,* vol. 37, pp. 531-551, 1995.
[37] G. C. Ejebe and B. F. Wollenberg, "Automatic Contingency Selection," *Power Apparatus and Systems, IEEE Transactions on,* vol. PAS-98, pp. 97-109, 1979.
[38] T. Mikolinnas and B. Wollenberg, "An advanced contingency selection algorithm," *Power Apparatus and Systems, IEEE Transactions on,* pp. 608-617, 1981.
[39] G. C. Ejebe, G. D. Irisarri, S. Mokhtari, O. Obadina, P. Ristanovic, and J. Tong, "Methods for contingency screening and ranking for voltage stability analysis of power

systems," in *Power Industry Computer Application Conference, 1995. Conference Proceedings., 1995 IEEE*, 1995, pp. 249-255.
[40] A. Ngarambe. (2013, EWSA struggles to supply electricity. *The EastAfrican*. Available: http://www.theeastafrican.co.ke/Rwanda/News/EWSA-struggles-to-supply-electricity/-/1433218/2075364/-/item/0/-/mgncx/-/index.html
[41] Y. Wang, L. C. P. da Silva, W. Xu, and Y. Zhang, "Analysis of ill-conditioned power-flow problems using voltage stability methodology," *Generation, Transmission and Distribution, IEE Proceedings-*, vol. 148, pp. 384-390, 2001.
[42] J. J. Grainger and W. D. Stevenson, *Power system analysis* vol. 31: McGraw-Hill New York, 1994.
[43] T. J. Overbye, "A power flow measure for unsolvable cases," *Power Systems, IEEE Transactions on,* vol. 9, pp. 1359-1365, 1994.
[44] T. Givler and P. Lilienthal, "Using HOMER software, NREL's micropower optimization model, to explore the role of gen-sets in small solar power systems," *Case Study: Sri Lanka, National Renewable Energy Laboratory, Golden, Colorado,* 2005.
[45] T. Lambert, P. Gilman, and P. Lilienthal, "Micropower System Modeling with Homer," in *Integration of Alternative Sources of Energy*, ed: John Wiley & Sons, Inc., 2006, pp. 379-418.
[46] National Renewable Energy Laboratory. *Glossary of Solar Radiation Resource Terms*. Available: http://rredc.nrel.gov/solar/glossary/
[47] P. Ineichen, "Five satellite products deriving beam and global irradiance validation on data from 23 ground stations," 2011.
[48] T. Stoffel, D. Renné, D. Myers, S. Wilcox, M. Sengupta, R. George, *et al.*, "Concentrating solar power: best practices handbook for the collection and use of solar

resource data (CSP)," National Renewable Energy Laboratory (NREL), Golden, CO.2010.
[49] J. Hall and J. Hall, "Quality Analysis of Global Horizontal Irradiance Data From 3500 U.S. Ground-based Weather Stations," presented at the ASES, Raleigh, 2011.
[50] 3TIER, "3TIER Global Solar Dataset: Methodology and Validation," Oct. 2013.
[51] C. Rigollier, M. Lefèvre, and L. Wald, "The method Heliosat-2 for deriving shortwave solar radiation from satellite images," *Solar Energy*, vol. 77, pp. 159-169, // 2004.
[52] M. Lefevre, A. Oumbe, P. Blanc, B. Espinar, B. ı. Gschwind, Z. Qu, *et al.*, "McClear: a new model estimating downwelling solar radiation at ground level in clear-sky conditions," *Atmospheric Measurement Techniques*, vol. 6, pp. 2403-2418, 2013.
[53] V. V. Tyagi, N. A. A. Rahim, N. A. Rahim, and J. A. L. Selvaraj, "Progress in solar PV technology: Research and achievement," *Renewable and Sustainable Energy Reviews*, vol. 20, pp. 443-461, 4// 2013.
[54] International Energy Agency, "Technology roadmap: solar photovoltaic energy," 2014.
[55] T. M. Razykov, C. S. Ferekides, D. Morel, E. Stefanakos, H. S. Ullal, and H. M. Upadhyaya, "Solar photovoltaic electricity: Current status and future prospects," *Solar Energy*, vol. 85, pp. 1580-1608, 8// 2011.
[56] K. Branker, M. J. M. Pathak, and J. M. Pearce, "A review of solar photovoltaic levelized cost of electricity," *Renewable and Sustainable Energy Reviews*, vol. 15, pp. 4470-4482, 12// 2011.
[57] D. Feldman, G. Barbose, G. Barbose, R. Margolis, T. James, S. Weaver, *et al.*, "Photovoltaic System Pricing Trends: Historical, Recent, and Near-Term Projections," U.S. Department of Energy2014.
[58] M. A. Green, K. Emery, Y. Hishikawa, W. Warta, and E. D. Dunlop, "Solar cell efficiency tables (Version 45)," *Progress in Photovoltaics: Research and Applications*, vol. 23, pp. 1-9, 2015.
[59] T. Kousksou, P. Bruel, A. Jamil, T. El Rhafiki, and Y. Zeraouli, "Energy storage: Applications and challenges," *Solar Energy Materials and Solar Cells*, vol. 120, Part A, pp. 59-80, 1// 2014.
[60] M.-L. Barry, H. Steyn, and A. Brent, "Selection of renewable energy technologies for Africa: Eight case studies in Rwanda, Tanzania and Malawi," *Renewable Energy*, vol. 36, pp. 2845-2852, 2011.
[61] M. S. Adaramola, "Viability of grid-connected solar PV energy system in Jos, Nigeria," *International Journal of Electrical Power and Energy Systems*, vol. 61, pp. 64-69, 2014.
[62] A. Beward, B. Bisselink, K. Bódis, A. Brink, J. Dallemand, A. de Roo, *et al.*, "Renewable Energies in Africa: Current Knowledge," Joint Research Center 1018-5593, 2011.
[63] A. Evans, V. Strezov, and T. J. Evans, "Assessment of utility energy storage options for increased renewable energy penetration," *Renewable and Sustainable Energy Reviews*, vol. 16, pp. 4141-4147, 8// 2012.
[64] S. Shafiee and E. Topal, "When will fossil fuel reserves be diminished?," *Energy Policy*, vol. 37, pp. 181-189, 1// 2009.
[65] H. Chen, T. N. Cong, W. Yang, C. Tan, Y. Li, and Y. Ding, "Progress in electrical energy storage system: A critical review," *Progress in Natural Science*, vol. 19, pp. 291-312, 3/10/ 2009.

[66] C. Chen, J. Wang, F. Qiu, and D. Zhao, "Resilient Distribution System by Microgrids Formation After Natural Disasters," *Smart Grid, IEEE Transactions on*, vol. PP, pp. 1-1, 2015.
[67] E. Hittinger, J. F. Whitacre, and J. Apt, "What properties of grid energy storage are most valuable?," *Journal of Power Sources*, vol. 206, pp. 436-449, 5/15/ 2012.
[68] B. Dunn, H. Kamath, and J.-M. Tarascon, "Electrical energy storage for the grid: a battery of choices," *Science*, vol. 334, pp. 928-935, 2011.
[69] D. Rastler, *Electricity energy storage technology options: a white paper primer on applications, costs and benefits*: Electric Power Research Institute, 2010.
[70] F. Díaz-González, A. Sumper, O. Gomis-Bellmunt, and R. Villafáfila-Robles, "A review of energy storage technologies for wind power applications," *Renewable and Sustainable Energy Reviews*, vol. 16, pp. 2154-2171, 5// 2012.
[71] J. F. Manwell and J. G. McGowan, "Lead acid battery storage model for hybrid energy systems," *Solar Energy*, vol. 50, pp. 399-405, 5// 1993.
[72] HOMER Energy LLC, *HOMER Pro: User Manual*, 2015.
[73] J. F. Whitacre, S. Shanbhag, A. Mohamed, A. Polonsky, K. Carlisle, J. Gulakowski, *et al.*, "A Polyionic, Large-Format Energy Storage Device Using an Aqueous Electrolyte and Thick-Format Composite NaTi2(PO4)3/Activated Carbon Negative Electrodes," *Energy Technology*, vol. 3, pp. 20-31, 2015.
[74] Electric Power Research Institute, "Costs of Utility Distributed Generators, 1-10 MW : Twenty-Four Case Studies," EPRI, Palo Alto2003.
[75] World Bank Group, "Pump Price for Diesel Fuel (US$ per liter) ", ed, 2015.
[76] City of Kigali. (2013). *City of Kigali Master Plan 2013*. Available: http://masterplan2013.kigalicity.gov.rw/

# Appendix A.1 Python Code To Create PSSE Case from Text Files

```
__author__ = 'Marvin K'

import os
import sys
import csv
import numpy

PSSE_PATH = r"c:/Program Files (x86)/PTI/PSSE32/PSSBIN"
sys.path.append(PSSE_PATH)
os.environ['PATH'] += ';' + PSSE_PATH

import psspy
import redirect
redirect.psse2py()

bus_file = open('C:\Users\Marvin K\OneDrive\Virginia
Tech\School\Research\Rwanda Network\\rwanda network bus.csv', 'r')
mach_file = open('C:\Users\Marvin K\OneDrive\Virginia
Tech\School\Research\Rwanda Network\Rwanda Network (psse format).csv', 'r')
xfmr_file = open('C:\Users\Marvin K\OneDrive\Virginia
Tech\School\Research\Rwanda Network\\rwanda network 2windings.csv','r')
load_file = open('C:\Users\Marvin K\OneDrive\Virginia
Tech\School\Research\Rwanda Network\\rwanda network load.csv','r')
branch_file = open('C:\Users\Marvin K\OneDrive\Virginia
Tech\School\Research\Rwanda Network\\rwanda network branch.csv','r')


psspy.psseinit(8000)

# Import Data from csv file
#--------------------------
bus_data = csv.reader(bus_file)
mach_data = csv.reader(mach_file)
xfmr_data = csv.reader(xfmr_file)
load_data = csv.reader(load_file)
branch_data = csv.reader(branch_file)

bus_list = []
mach_list = []
xfmr_list = []
load_list = []
branch_list = []

# create data lists
# -------------------
for row in bus_data:
    bus_list.append(row)
bus_file.close()
for row in mach_data:
    mach_list.append(row)
mach_file.close()
for row in xfmr_data:
```

```
    xfmr_list.append(row)
xfmr_file.close()
for row in load_data:
    load_list.append(row)
load_file.close()
for row in branch_data:
    branch_list.append(row)
branch_file.close()

#list to array
bus_array = numpy.asarray(bus_list)
mach_array = numpy.asarray(mach_list)
xfmr_array = numpy.asarray(xfmr_list)
load_array = numpy.asarray(load_list)
br_array = numpy.asarray(branch_list)

case_rwanda_test = "C:\Users\Marvin K\OneDrive\Virginia
Tech\School\Research\Voltage Stability\Rwanda Network
Files\\rwanda_network_complete.sav"

psspy.case(case_rwanda_test)
num_mach = 50        #number of machines
num_xfmr = 76        #number of transformers
num_load = 244       #number of loads
num_branch = 407     #number of branches
num_bus = 462        #number of buses
_i = psspy.getdefaultint()
_f = psspy.getdefaultreal()
cdef = psspy.getdefaultchar()

#----------------------------
#machine data
for x in range(1,num_mach+1):
    #psspy.newseq()
    b_num = int(mach_array[x,0]) #bus number
    plant_inf1 = float(mach_array[x,6]) #remote bus number
    plant_inf2 = [float(mach_array[x,4]),100]  #scheduled, percent var
    bus_id = (mach_array[x,2])

    ierr = psspy.plant_data(b_num,plant_inf1,plant_inf2)

    mach_stat = int(mach_array[x,34])
    owner1 = int(mach_array[x,18])
    mach_inf = [mach_stat,owner1,_i,_i,_i,_i]
    PG = float(mach_array[x,6])
    QG = float(mach_array[x,9])
    QT = float(mach_array[x,10])
    QB = float(mach_array[x,11])
    PT = float(mach_array[x,7])
    PB = float(mach_array[x,8])
    Mbase = float(mach_array[x,12])
    ZR = float(mach_array[x,13])
    ZX = float(mach_array[x,14])
    RT = float(mach_array[x,15])
    XT = float(mach_array[x,16])
    GTAP = float(mach_array[x,17])
```

```
    ierr = psspy.machine_data_2(b_num, bus_id, mach_inf,

[PG,QG,QT,QB,PT,PB,Mbase,ZR,ZX,RT,XT,_i,_i,_i,_i,_i])
    psspy.machine_data_2
    #machine sequence data
    zrpos = float(mach_array[x,26])
    zxpos = float(mach_array[x,27])
    zrneg = float(mach_array[x,28])
    zxneg = float(mach_array[x,29])
    rzero = float(mach_array[x,30])
    xzero = float(mach_array[x,31])

    ierr =
psspy.seq_machine_data(b_num,bus_id,[zrpos,zxpos,zrneg,zxneg,rzero,xzero])

psspy.save(case_rwanda_test)


#------------------------------------------------------
#transformer data
for y in range(1,num_xfmr+1):
    #psspy.newseq()

    b_numfr = int(xfmr_array[y,0])
    b_numto = int(xfmr_array[y,2])
    ckt_id = (xfmr_array[y,4])
    stat = int(xfmr_array[y,6])
    metbus = int(xfmr_array[y,7])  #metered bus
    #----------------------
    w1side = int(xfmr_array[y,8])  #winding 1 side: 0=tobus 1=frombus


    #----------------------
    ntp1 = int(xfmr_array[y,11])   #num tap positions
    tab1 = int(xfmr_array[y,45])   #impedance correction table

    cont1 = int(xfmr_array[y,9])
    #sicod1 =
    #cod1 =
    #xfmr inf1 = []

    r12 = float(xfmr_array[y,17])     #nominal resistance
    x12 = float(xfmr_array[y,18])     #nominal reactance
    sbs12 = float(xfmr_array[y,32])   #winding base
    windv1 = float(xfmr_array[y,33])  #winding 1 ratio (pu or kV)
    #temp
#     if w1side == 0:
    nomv1 = float(xfmr_array[y,34])   #winding 1 nominal kV
    nomv2 = float(xfmr_array[y,37])   #winding 2 nominal kV
#     else:
#         nomv1 = float(xfmr_array[y,37])   #winding 1 nominal kV
#         nomv2 = float(xfmr_array[y,34])   #winding 2 nominal kV
    if w1side == 0:
        w1_side = b_numto
    else:
        w1_side = b_numfr
```

```
    #----
    ang1 = float(xfmr_array[y,35])     #winding 1 phase shift
    windv2 = float(xfmr_array[y,36])   #winding 2 ratio (pu or kV)
    rata1 = float(xfmr_array[y,19])    #A line rating
    ratb1 = float(xfmr_array[y,20])    #B line rating
    ratc1 = float(xfmr_array[y,21])    #C line rating
    xfmr_f1 = float(xfmr_array[y,24]) #owner 1 fraction
    mag1 = float(xfmr_array[y,22])     #conductance or no load losses
    mag2 = float(xfmr_array[y,23])     #susceptance or exciting current
    rma1 = float(xfmr_array[y,38])     #winding 1 max (ratio/angle)
    rmi1 = float(xfmr_array[y,39])     #winding 1 min
    vma1 = float(xfmr_array[y,40])     #voltage/flow max limit
    vmi1 = float(xfmr_array[y,41])     #voltage/flow min limit
    #xfmr sequence data
    xfmr_cc_list = (xfmr_array[y,50])    #connection code list
    xfmr_cc = int(xfmr_cc_list[0])       #connection code first character
    xfmr_rg = float(xfmr_array[y,54])    #groungding resistance
    xfmr_xg = float(xfmr_array[y,55])    #grounding reactance
    xfmr_r1 = float(xfmr_array[y,56])    #zero sequence resistance
    xfmr_x1 = float(xfmr_array[y,57])    #zero sequence reactance
    xfmr_rg2 = float(xfmr_array[y,58])   #winding 2 side resistance to gnd
    xfmr_xg2 = float(xfmr_array[y,59])   #winding 2 side reactance to gnd



    ierr =
psspy.two_winding_data_3(b_numfr,b_numto,ckt_id,[stat,metbus,_i,_i,_i,_i,ntp1
,tab1,w1_side,cont1,_i,_i,_i,_i,_i],

[r12,x12,sbs12,windv1,nomv1,ang1,windv2,nomv2,rata1,

ratb1,ratc1,xfmr_f1,_f,_f,_f,mag1,mag2,rma1,rmi1,vma1,vmi1,_f,_f,_f],cdef)
    ierr =
psspy.seq_two_winding_data(b_numfr,b_numto,ckt_id,[xfmr_cc],[xfmr_rg,xfmr_xg,
xfmr_r1,xfmr_x1,xfmr_rg2,xfmr_xg2])


#---------------------------------
#load data
for z in range(1,num_load+1):
    bnum_ld = int(load_array[z,0])  #bus number
    ld_id = (load_array[z,2])    #identifier
    ld_stat = int(load_array[z,10]) #status
    ld_area = int(load_array[z,4])  #load area
    ld_zone = int(load_array[z,6])  #zone
    ld_owner = int(load_array[z,8])
    ld_skl = int(load_array[z,11])  #scalable
    ld_pl = float(load_array[z,13])
    ld_ql = float(load_array[z,14])
    ld_ip = float(load_array[z,15])
    ld_iq = float(load_array[z,16])
    ld_yp = float(load_array[z,17])
    ld_yq = float(load_array[z,18])

    ierr = psspy.load_data_3(bnum_ld,ld_id, [ld_stat,ld_area,ld_zone,
                          ld_owner,ld_skl],[ld_pl,ld_ql,ld_ip,ld_iq,
```

```
                                        ld_yp,ld_yq])

#------------------------------------------------
#branch data

for w in range(1,num_branch+1):
    br_bnumfr = int(br_array[w,0])  #from bus
    br_bnumto = int(br_array[w,2])  #to bus
    br_ckt = br_array[w,4]          #circuit id
    br_stat = int(br_array[w,8])    #branch status
    #br_metbus = edit later
    br_own1 = int(br_array[w,18])
    #     used default for other owners
    br_r = float(br_array[w,5])      #nominal branch resistance
    br_x = float(br_array[w,6])      #nominal branch reactance
    br_chrg = float(br_array[w,7])   #charging resistance
    br_rata = float(br_array[w,10])
    br_ratb = float(br_array[w,11])
    br_ratc = float(br_array[w,12])
    br_len = float(br_array[w,17])   #line length
    #br_fr1 = float(br_array[w,19])  #owner 1 fraction
    #sequence data
    br_rlinz = float(br_array[w,26]) #zero seq resistance
    br_xlinz = float(br_array[w,27]) #zero sequence reactance
    br_bchz = float(br_array[w,28])  #zero sequence total line charging


    ierr =
psspy.branch_data(br_bnumfr,br_bnumto,br_ckt,[br_stat,_i,br_own1,_i,_i,_i],[b
r_r,br_x,br_chrg,br_rata,br_ratb,br_ratc,_f,_f,_f,_f,br_len,_f,_f,_f,_f])
    ierr =
psspy.seq_branch_data(br_bnumfr,br_bnumto,br_ckt,[br_rlinz,br_xlinz,
                                br_bchz,_f,_f,_f,_f])


    psspy.save(case_rwanda_test)
```

# Appendix B Microgrid Parameters, Economics, and Control

## Project Location

| | |
|---|---|
| Location | Kigali International Airport, Kigali, Rwanda |
| Latitude | 1 degrees 57.78 minutes South |
| Longitude | 30 degrees 8.10 minutes East |
| Time zone | Africa/Kigali |

## Load

| | |
|---|---|
| Data source | Synthetic |
| Daily noise | 1% |
| Hourly noise | 1% |
| Scaled annual average | 234,897.000 kWh/d |
| Scaled peak load | 14,483.9151 kW |
| Load factor | 0.6757 |

## Economics

| | |
|---|---|
| Annual real interest rate | 6% |
| Project lifetime | 20 yr |
| Capacity shortage penalty | $0/kWh |
| System fixed capital cost | 0 |
| System fixed O&M cost | 0 |

## System control

| | |
|---|---|
| Check load following | Yes |
| Check cycle charging | Yes |
| Setpoint state of charge | 80 |
| Allow systems with multiple generators | Yes |
| Allow multiple generators to operate simultaneously | Yes |
| Allow systems with generator capacity less than peak load | Yes |

# Appendix B.1 Diesel Generators

### Caterpillar 3516 TA Diesel Generator Set. Full Specs at

http://www.cat.com/en_US/power-systems/electric-power-generation/diesel-generator-sets/18316873.html

Generator: Cat 3516A

| Size | Capital | Replacement | O&M |
|---|---|---|---|
| 1.00 | $500.00 | $500.00 | $0.04 |

| | |
|---|---|
| Sizes to consider | 0,1450,2900,4350,5800,7250,8700,10150,11600,13050,14500 |
| Lifetime | 87,600 hrs |
| Min. load ratio | 30% |
| Heat recovery ratio | 0% |
| Fuel used | Diesel |
| Fuel curve intercept | 0.0032 L/hr/kW |
| Fuel curve slope | 0.2492 L/hr/kW |

### Caterpillar XQ600 Diesel Generator

Full specs at: http://www.cat.com/en_US/power-systems/electric-power-generation/rental-generator-sets/18504460.html

Generator: Cat XQ600

| Size | Capital | Replacement | O&M |
|---|---|---|---|
| 1.00 | $500.00 | $500.00 | $0.04 |

| | |
|---|---|
| Sizes to consider | 0,545,1090,1635,2180,2725,3270,3815,4360,4905,5450,5995,6540,7085,7630,8175,8720,9265,9810,10355,10900 |
| Lifetime | 87,600 hrs |
| Min. load ratio | 30% |
| Heat recovery ratio | 0% |
| Fuel used | Diesel |
| Fuel curve intercept | 0.0032 L/hr/kW |
| Fuel curve slope | 0.2492 L/hr/kW |

**Caterpillar 3616**

http://www.cat.com/en_US/products/new/power-systems/electric-power-generation/diesel-generator-sets/18492095.html

Generator: Cat 4700 ekW

| Size | Capital | Replacement | O&M |
|---|---|---|---|
| 1.00 | $500.00 | $500.00 | $0.04 |

| | |
|---|---|
| Sizes to consider | 0,4700,9400,14100 |
| Lifetime | 120,000 hrs |
| Min. load ratio | 30% |
| Heat recovery ratio | 0% |
| Fuel used | Diesel |
| Fuel curve intercept | 0.0032 L/hr/kW |
| Fuel curve slope | 0.2492 L/hr/kW |

# Appendix B.2 Solar PV

PV:PV NREL

| Size | Capital | Replacement | O&M |
|---|---|---|---|
| 1.00 | $3,000.00 | $3,000.00 | $5.00 |
| 50.00 | $145,000.00 | $145,000.00 | $200.00 |
| 500.00 | $1,350,000.00 | $1,350,000.00 | $2,000.00 |
| 5,000.00 | $9,750,000.00 | $9,750,000.00 | $20,000.00 |

| | |
|---|---|
| Sizes to consider | 0,5000,6000,7000,8000 |
| Lifetime | 25 yr |
| Derating factor | 80% |
| Tracking system | No Tracking |
| Slope | 1.963 deg |
| Azimuth | 180.000 deg |
| Ground reflectance | 20.0% |

# Appendix B.3 Battery Storage

Name: **Aquion 200-400**

Abbreviation:

Manufacturer: **Aquion**

Nominal Voltage (V): **700**

Maximum Capacity (Ah): **822**

Round Trip Efficiency (%): **92.0**

Float Life (years): **20.0**

Suggested Life Throughput (kWh): **17,520,000**

Electrolyte replacement interval (yrs): **125**

Capacity Ratio, c: **0.281**

Rate Constant, k: **8.74**

Max. Charge Current (A): **230**

Max. Discharge Current (A): **354**

Website: www.aquionenergy.com

Notes:
**200kW-400kWh Aquion Aqueous Hybrid Ion**

The battery used in the PV storage only is rated for 200kW-1600kWh